Profiling of the Secondary Metabolites and the Characterization Two Novel Antilisterial Peptides, Xenopep and Rhabdin, Produced by *Xenorhabdus khoisanae*

by
Elzaan Booysen

Dissertation presented for the degree of Doctor of Science in the Faculty of Science at Stellenbosch University

Supervisor: Prof. Leon M.T. Dicks

Co-supervisor: Prof Marina Rautenbach

April 2022

Declaration

By submitting this dissertation electronically, I declare that the entirety of the work contained therein is my own, original work, that I am the sole author thereof (save to the extent explicitly otherwise stated), that the reproduction and publication thereof by Stellenbosch University will not infringe any third party rights and that I have not previously in its entirety or in part submitted it for obtaining any qualification.

April 2022

Elzaan Booysen

Summary

In the early 1900's the discovery of sulfonamides and penicillin paved the way for antibiotics and led to a boom in the discovery of other antibiotics. Unfortunately, this boom was short lived and soon the discovery and approval of novel antibiotics by the food and drug association and other similar associations dwindled. With the ever-increasing prevalence of antibiotic resistant pathogens this soon became a problem that was not foreseen.

Most antibiotics currently on the market have been isolated from a select few genera. With nearly all the antibiotics from such few sources, bacteria were able to acquire resistance at an enhanced pace. This study focused on a relatively unexplored niche for novel antibiotics, from the genus *Xenorhabdus*. Species of this genus is mutually associated with *Steinernema* nematodes and have a unique life cycle. *Xenorhabdus* spp. are known to produce various secondary metabolites (SMs) that have antimicrobial, insecticidal, antiviral, immunosuppressant and proteolytic properties. Species from this genus use different synthesis machineries to produce these compounds, although the majority are produced via the non-ribosomal peptide synthesis. The ability of non-ribosomal peptides to incorporate non-proteogenic amino acids, D-amino acids, fatty chains, or polyketide chains result in unique resistance to proteinases and environmental stressors.

Xenorhabdus khoisanae J194 is mutually associated with *Steinernema jeffreyense* J194, a nematode that was isolated from soil in the Eastern Cape. Culture conditions, especially oxygen, greatly affected SM production of *X. khoisanae* J194. PAX peptides, xenocoumacins and xenoamicins were identified in the cell-free crude extract of *X. khoisanae* J194 cultures. Two novel antilisterial peptides, xenopep and rhabdin, were also detected in the cell-free crude extract of. Xenopep has a narrow spectrum of activity and inhibited the growth of only, *Listeria monocytogenes* and *Staphylococcus epidermidis*, while rhabdin is active against both Gram-positive and Gram-negative bacteria. Xenopep and rhabdin share numerous characteristics and both contain a tetra-peptide in their structure including a tetra-peptide in their structure. Both peptides share the same amphipathic characteristic and behave similar suspension. Membrane potential and ATP release assays have shown that xenopep formed pores/lesions in the cell membrane of *L. monocytogenes* within minutes, followed by a rapid decrease in cell numbers over 3 hours. Scanning electron microscopy (SEM) images of *L.*

monocytogenes treated with xenopep became elongated and formed filaments. This suggests that xenopep may inhibit penicillin binding protein three.

This is the first study reporting on SMs produced by *X. khoisanae* when cultured under different conditions and is the first detailed description of antilisterial peptides produced by the species.

Opsomming

In die vroeë 1900's het die ontdekking van sulfonamiede en penisillien die weg gebaan vir antibiotika en gelei tot 'n oplewing in die ontdekking van ander antibiotika. Ongelukkig was hierdie oplewing van kort duur en gou het die ondekking en goedkeuring van nuwe antibiotikums deur die kos en dwelm vereniging (KDV) en ander soortgelyke verenigings afgeneem. Met die toename in antibiotika-weerstandige patogene het dit vinnig 'n probleem geword wat nie voorsien is nie.

Die meeste antibiotika wat tans op die mark is, is uit 'n paar uitegesoekte genera geïsoleer. Met byne al die antibiotika uit so min bronne kon bakterieë weerstand teen 'n groter tempo ontwikkel. Hierdie studie het gefokus op 'n relatiewe onontginde nis vir nuwe antibiotika, bakterieë van die genus *Xenorhabdus*. Spesies van hierdie genus is wedersyds geassosieer met *Steinernema* nematodes en het 'n unieke lewens siklus. *Xenorhabdus* spp. produceer verskeie sekondêre metaboliete (SMe) met antimikrobiese, insekdodende, antivirale, immuunonderdrukkende en proteolitiese eienskappe. Spesies van hierdie genus gebruik ook verskeie sintese-masjinerie om hierdie verbindings te produseer, alhoewel die meederheid deur die nie-ribosomale peptiedsintese geproduseer word. Die vermoë van nie-ribosomale peptiede om nie-proteogeniese aminosure, D-aminosure, vetkettings of polieketiedkettings te inkorporeer, het hulle 'n unieke weerstand teen proteïenase en omgewings stres faktore.

Xenorhabdus khoisanae J194 is wedersyds met *Steinernema jeffreyense* J194 geassosieer wat uit grond in die Oos-kaap geïsoleer is. Kultuurtoestande, veral suurstof, het 'n groot invloed op SM produksie van *X. khoisanae* J194. PAX-peptiede, xenocoumasiene en xenoamisiene is in sel-vry kru-ekstrak van *X. khoisanae* J194 kulture geïdentifiseer. Twee unieke antilisteriale peptiede, xenopep en rhabdin, is ook in die sel-vry kru-ekstrak van *X. khoisanae* J194 geïdentifiseer. Xenopep het 'n nou spektrum van aktiwiteit en het slegs die groei van *Listeria monocytogenes* en *Staphylococcus epidermidis* geïnhibeer, terwyl rhabdin aktief is teen beide Gram-postiewe en Gram-negatiewe bacterieë. Xenopep en rhabdin dell verskeie eienskappe en beide besit 'n tetra-peptied in hul struktuur. Beide peptiede deel dieselfde amfipatiese eienskappe en reageer soortgelyke gedrag in suspensie. Membraan potensiaal en ATP vrystellings toetse het getoon dat xenopep porieë of letsels in die selmembraan van behandelde *L. monocytogenes* binne minute na blootstelling vorm, gevolg deur 'n vinnige afname in selgetalle binne drie ure. Skandeer elektronmikroskopie (SEM) beelde van *L.*

Monocytogenes wat met xenopep behandel is, het getoon dat selle verleng en filamente vorm. Dit mag dus wees dat xenopep penisillien bindede proteïen drie inhibeer.

Hierdie is die eerste bekendmaking van SMe wat deur *X. Khoisanae,* blootgestel aan verskillende kultuur toestande, geproduseer word en is die eerste gedetailleerde beskrywing van antilisteriale peptiede geprodusser deur die spesie.

Biographical sketch

Elzaan Booysen was born in Cape Town, South Africa on the 21st of December 1992. She matriculated at Paarl Girls' High, South Africa, in 2011. In 2012 she enrolled as a B.Sc. student in Molecular Biology and Biotechnology at the University of Stellenbosch and obtained the degree in 2014. In 2015 she obtained her B.Sc (Hons) in microbiology at the University of Stellenbosch. In January 2016 she enrolled as M.Sc student in Microbiology at the University of Stellenbosch, receiving her M. Sc (Cum Laude) in 2018. In 2018 she enrolled as a Ph.D student in Microbiology at the University of Stellenbosch.

Preface

This dissertation is presented as a compilation of 5 chapters. Each chapter is introduced separately. Chapter 1, 2 and 5 is written according to the style of Probiotic and Antimicrobial proteins. Chapter 3 is written according to the style of Frontiers in Chemistry. Chapter 4 is written according to the style of Journal of Antimicrobial Chemotherapy

Chapter 1: General Introduction

Chapter 2: Does the Future of Antibiotics Lie in Secondary Metabolites Produced by *Xenorhabdus* spp.? A Review

Chapter 3: Profiling the Production of Antimicrobial Secondary Metabolites by Xenorhabdus khoisanae J194 Under Different Culturing Conditions

Chapter 4: Characterisation of Xenopep and Rhabdin, novel antilisterial peptides produces by *Xenorhabdus khoisanae*

Chapter 5: General Discussion and Conclusions

Acknowledgements

I would like to sincerely thank the following people and organizations:

My **family** and **friends** for their unrelenting support and encouragement

Prof. L.M.T. Dicks (Department of Microbiology, Stellenbosch University) for granting me this opportunity and all his support and guidance

Prof Marina Rautenbach (Department of Biochemistry, Stellenbosch University) for her valuable insight, assistance with experiments and critical reading of the manuscript

Dr. Marietjie Stander and **Mr. Malcolm Taylor** (LCMS Central Analytical Facility, Stellenbosch University) for their assistance with MS analysis

All my **co-workers** in the Department of Microbiology for their insight and support

The **Nation Research Foundation (NRF) of South Africa** for financial support and funding of the research

This dissertation is dedicated to my parents, Philip and Nicolette Booysen

Table of Contents

Chapter 1

Chapter 2

Does the future of antibiotics lie in secondary metabolites produced by *Xenorhabdus* spp.?

Chapter 3

Profiling the production of antimicrobial secondary metabolites by *Xenorhabdus khoisanae* J194 under different culturing conditions

Chapter 4

Characterisation of Xenopep and Rhabdin, novel antilisterial peptides produces by *Xenorhabdus khoisanae*

Chapter 5

STELLENBOSCH UNIVERSITY

Chapter 1

General Introduction

General Introduction and Rational

The antimicrobial revolution started in the late 1920's with the discovery and eventual commercialization of penicillin [1]. The discovery of novel antibiotics and widespread approval by the Food and Drug Administration (FDA) of the USA led to many experts believing that we have finally conquered infectious diseases, especially those caused by bacteria [2]. Since the discovery of antibiotics, 64% of the antibiotics on the market today were naturally derived from Actinomycetes, while the rest were naturally derived from *Bacillus* spp., and a select few fungal species [4]. Antibiotics not only play a big role in the prevention and treatment of bacterial infections but is also used in combination with immunosuppressants used in organ transplants, to prevent rejection. Patients undergoing chemotherapy and treated with anticancer drugs are prone to developing bacterial infections and also benefit from treatment with antibiotics. Rinsing of dissected areas with antibiotics during surgery makes extremely complicated operative procedures possible [3, 4].

Over the last 30 years only a few new antibiotics have been registered [4–6]. This, and the increase in bacterial resistance led to a drastic increase in microbial diseases, with bacterial infections amongst the top 10 causes of death world-wide [7]. Many bacteria develop resistance to commonly used antibiotics and the rate at which multi-drug resistant strains develop is increasing [5, 6, 8, 9]. Part of the problem is the misuse and reckless abuse of antibiotics not only in the medical and veterinary fields, but also as growth stimulants in animal feed [10].

Most bacterial infections are caused by biofilms [11]. Biofilms form when planktonic cells adhere to a surface and produce insoluble gelatinous exopolymers to form three-dimensional structures [12]. The polymers protect bacterial cells from external factors. In general biofilms are difficult to treat. Cells are more resistant to antibiotics and may lead to recurrent and chronic infections [13]. Biofilms form on almost any surface, including medical devices, living tissue and water pipes. Biofilms is also a major problem in ready-to-eat food, as shown with the 2017 *Listeria* outbreak in South Africa [14]. In some cases the removal of biofilms requires a combination of mechanical and antimicrobial treatment [11]. Bacteriophages may offer an alternative option, especially when cells developed resistance to antibiotics [11].

In recent years the search for alternatives to antibiotics increased dramatically, especially with changes in culturing methods and more information becoming available from DNA sequencing [15, 16]. *Xenorhabdus* bacteria, endosymbionts of *Steinernema* nematodes, is an excellent example [17]. Species of this genus live within the reciprocal of the nematodes. Once the

nematodes enter the insect haemocoel through natural openings, they regurgitate the bacteria. The bacteria then start to multiply and produce various secondary metabolites (SM), including insecticides, proteases, immune suppressors, and antimicrobial compounds. Once the nutrients in the dyeing insect are depleted, the bacteria are reabsorbed by the nematodes and the latter leave the insect in search of a new prey [18, 19]. The unique lifestyle of *Xenorhabdus* renders the genus a perfect source for the discovery of novel antibiotics [19]. To date 23 different antimicrobial compounds have been isolated from *Xenorhabdus*. Unfortunately none of these compounds have been put through clinical trials [20]. Of these compounds the majority are peptides, with a wide range of antimicrobial activities.

Antimicrobial peptides (AMP) are either synthesised via non-ribosomal peptide (NRP) synthesis or ribosomal peptide (RP) synthesis. Although RP have enjoyed a renewed interest, NRP are also great candidates for novel antibiotics [21]. The ability of NRP synthesis machinery to incorporate polyketide chains, non-proteomic amino acids and D-amino acids, renders the peptides more resistant to temperature, pH and other environmental stressors [22]. These unique characteristics of NRP also makes them more resistant to proteases employed by target bacteria.

The majority of antimicrobial peptides are cationic and targets the cell membrane of bacteria [23-25]. These peptides utilise various models to target and ultimately destabilise the cell membrane. The most well-known are the toroidal, barrel-stave, and carpet models, although numerous other less known models have also been described [26]. Little is known about the mode of action of *Xenorhabdus* compounds, apart from those described for PAX peptides [27] and nematophin [28]. In the first part of this study, the effect of culture conditions on the SM produced by *X. khoisanae* J194 were evaluated. Ultraperformance-liquid chromatography linked to mass spectrometry (UPLC-MS) was used to identify known and novel compounds produced by *X. khoisanae* J194. Two novel antilisterial peptides were identified. The second part of this study focussed on characterising these two peptides. The structure of the peptides was elucidated with high resolution collision induced dissociation (CID) analysis in the tandem mass spectrometry (MS) mode and nuclear magnetic resonance (NMR). The stability of the peptides in different conditions were also analysed. Lastly the effect of the peptides on the cell membrane of *Listeria monocytogenes* were studied using various fluorescent dyes and scanning electron microscopy (SEM).

References

1. Abraham E, Chain E (1940) An enzyme from bacteria able to destroy penicillin. Nature 146:677–678
2. Power E (2006) Impact of antibiotic restrictions: The pharmaceutical perspective. Clin Microbiol Infect 12:25–34
3. Martínez JL, Baquero F (2014) Emergence and spread of antibiotic resistance: Setting a parameter space. Ups J Med Sci 119:68–77
4. Hutchings M, Truman AE, Wilkinson B (2019) Antibiotics: past, present and future. Curr Opin Microbiol 51:72–80
5. Conly JM, Johnston BL (2005) Where are all the new antibiotics? The new antibiotic paradox. Can J Infect Dis Med Microbiol 16:159–160
6. Katz ML, Mueller LV, Polyakov M, Weinstock SF (2006) Where have all the antibiotic patents gone? Nat Biotechnol 24:1529–1531
7. (2018) Global Health Estimates 2016: Disease burden by cause, age, sex by country and by region, 2000-2016. In: Geneva, World Heal. Organ.
8. Shlaes DM (2010) Antibiotics: the perfect storm, 1st ed. Springer, The Neverlands
9. Charles PGP, Grayson ML (2004) The death of new antibiotic development: Why we should be worried and what we can do about it. Med J Aust 181:549–553
10. Cantas L, Shah SQA, Cavaco LM, Manaia CM, Walsh F, Popwska M, Garelick H, Bürgmann H, Sørum H (2013) A brief multi-disciplinary review on antimicrobial resistance in medicine and its linkage to the global environmental microbiota. Front Microbiol 4:1–14
11. Bryers JD (2008) Medical biofilms. Biotechnol Bioeng 100:1-18
12. Donlan RM (2002) Biofilms: Microbial life on surfaces. Emerg Infect Dis 8:881-890
13. Ghigo JM (2001) Natural conjucative plasmid induce bacterial biofilm development. Nature 412:442-445
14. Pidot SJ, Coyne S, Kloss F, Hertweck C (2014) Antibiotics from neglected bacterial sources. Int J Med Microbiol 304:14–22

15. Challinor VL, Bode HB (2015) Bioactive natural products from novel microbial sources. Ann N Y Acad Sci 1354:82–97

16. Dreyer J, Malan AP, Dicks LMT (2017) Three novel *Xenorhabdus* – *Steinernema* associations and evidence of strains of *X. khoisanae* switching between different clades. Curr Microbiol 74:938–942

17. Gotz P, Boman A, Boman HG (1981) Interactions between insect immunity and an insect-pathogenic nematode with symbiotic bacteria. Proc R Soc B Biol Sci 212:333–350

18. Dreyer J, Malan AP, Dicks LMT (2018) Bacteria of the genus *Xenorhabdus*, a novel source of bioactive compounds. Front Microbiol 9:1–14

19. Booysen E, Dicks LMT (2020) Does the future of antibiotics lie in secondary metabolites produced by *Xenorhabdus* spp.? A Review. Probiotics Antimicrob. Proteins 12:1310–1320

20. Huan Y, Kong Q, Mou H, Yi H (2020) Antimicrobial Peptides: classification, design, application and research progress in multiple fields. Front Microbiol 11:1–21

21. Inoue M (2011) Total synthesis and functional analysis of non-ribosomal peptides. Chem Rec 11:284–294

22. Zou R, Zhu X, Tu Y, Wu J, Landry MP (2018) Activity of antimicrobial peptide aggregates decreases with increased cell membrane embedding free energy cost. Biochemistry 57:2606–2610

23. Remington JM, Liao C, Sharafi M, Ste.Marie EJ, Ferrell JB, Hondal RJ, Wargo MJ, Schneebeli ST, Li J (2020) Aggregation state of synergistic antimicrobial peptides. J Phys Chem Lett 9501–9506

24. Zhong C, Zhu N, Zhu Y, Liu T, Gou S, Xie J, Yao J, Ni J (2020) Antimicrobial peptides conjugated with fatty acids on the side chain of D-amino acid promises antimicrobial potency against multidrug-resistant bacteria. Eur J Pharm Sci 141:105123.

25. Clark S, Jowitt TA, Harris LK, Knight CG, Dobson CB (2021) The lexicon of antimicrobial peptides: a complete set of arginine and tryptophan sequences. Commun Biol 4:1–14.

26. Nguyen LT, Haney EF, Vogel HJ (2011) The expanding scope of antimicrobial peptide structures and their modes of action. Trends Biotechnol 29:464–472

27. Duy Vo T (2020) Target identification of peptides from Xenorhabdus and Photorhabdus

28. Zhang S, Liu Q, Han Y, Han J, Yan Z, Wang Y, Zhang X (2019) Nematophin, an antimicrobial dipeptide compound from *Xenorhabdus nematophila* YL001 as a potent biopesticide for *Rhizoctonia solani* control. Front Microbiol 10:1–15

Chapter 2

Does the future of antibiotics lie in secondary metabolites produced by *Xenorhabdus* spp.?

(Published in Probiotics and antimicrobial Proteins)

Does the future of antibiotics lie in secondary metabolites produced by *Xenorhabdus* spp.? A review

E. Booysen and L.M.T. Dicks

Department of Microbiology, Stellenbosch University, Stellenbosch 7600, South Africa

Running Head: Bioactive secondary metabolites of *Xenorhabdus* spp.

Abstract The over-prescription of antibiotics for treatment of infections is primarily to blame for the increase in bacterial resistance. Added to the problem is the slow rate at which novel antibiotics are discovered and the many processes that need to be followed to classify antimicrobials safe for medical use. *Xenorhabdus* spp. of the family Enterobacteriaceae, mutualistically associated with entomopathogenic nematodes of the genus *Steinernema*, produce a variety of antibacterial peptides, including bacteriocins, depsipeptides, xenocoumacins and PAX (peptide antimicrobial-*Xenorhabdus*) peptides, plus additional secondary metabolites with antibacterial and antifungal activity. The secondary metabolites of some strains are active against protozoa and a few have anti-carcinogenic properties. It is thus not surprising that nematodes invaded by a single strain of a *Xenorhabdus* species are not infected by other microorganisms. In this review, the antimicrobial compounds produced by *Xenorhabdus* spp. are listed and the gene clusters involved in synthesis of these secondary metabolites are discussed. We also review growth conditions required for increased production of antimicrobial compounds.

Keywords: *Xenorhabdus*, Secondary metabolites, Antimicrobial Peptides, Infection Control

Introduction

Bacteria live in confined spaces and have to compete for nutrients, electron acceptors, adhesion to substrates and physical space. In nutrient-rich niches that supports the growth of millions of species, competition becomes fierce and calls for the developing of unique survival strategies. These may include the production of secondary metabolites such as organic acids, fatty acids, hydrogen peroxide, ethanol and carbon dioxide, or the secretion of antibiotics, toxins and

antimicrobial peptides. Antagonistic compounds of low molecular weight diffuse through biofilms, destroy communities and create zones inhospitable to competitors [1].

Since resources and growth conditions in microenvironments often changes rapidly, microbial communities have to adapt metabolically and structurally to survive [2]. Not all species adapt equally well to changes and communities may consist of individual micro communities, each with unique characteristics and growth requirements. Perhaps the most evident form of community changes and cell re-orientation is observed amongst aerobic bacteria. Obligate aerobes such as *Pseudomonas fluorescens* compete for oxygen-rich areas by increasing the production of extracellular polysaccharides (EPS) to "force" cells to the surface [3]. In the case of *Bacillus subtilis,* EPS-producing cells undergo controlled cell death, which decreases lateral pressure between cells in the micro community. The lowering in pressure causes the cells to buckle and force adjacent cells to the surface [4]. Another example of cells undergoing structural repositioning is observed in dental plague. *Streptococcus sanguinis*, normally present in oral cavities, oxidizes pyruvate and produces hydrogen peroxide (H_2O_2) that inhibits the growth of *Streptococcus mutans* [5]. To prevent cell death, glutathione-producing cells of *S. mutans* detoxifies H_2O_2 [6] and, at the same time, protect *Escherichia coli* from H_2O_2 [7]. Control of microbial environments is clearly a complex process and involves many forms of biochemical interchanges and cellular interactions, referred to as metabolicsyntrophism [8]. Only cells genetically streamlined to a specific environment survive. Cells that are not genetically programmed to cope with drastic changes are forced to take part in syntrophic interactions [9]. An excellent example of the latter is *Synechococcus* that detoxifies H_2O_2, using the enzyme complex catalase-peroxidase (KatG). Detoxification of H_2O_2 allows *Prochlorococcus* void of the *katG* gene to grow and form a symbiotic relationship with *Synechococcus*. Should cells from both genera lose the *katG* gene, the whole community is destroyed. Metabolic pressure inflicted by *Prochlorococcus* onto *Synechococcus* to maintain the *katG* gene is a good example of selection due to competitive pressure [10]. In syntrophic communities, selection may enhance genetic adaption and the fitness of cells [11]. The adoption of new survival strategies may thus affect how cells interact with each other in a microenvironment.

Almost all bacteria produce antimicrobial compounds, either as a survival strategy, or a defence mechanism. Of these, polyketides have been best studied. The cellular components they target vary and may be cell walls, cell membranes, energy cycles (ATP production), or pathways involved in protein and nucleic acid biosynthesis [12]. The rate at which cells become resistant to antibiotics differ. Resistance to rifampicin, for example, develops relatively fast, as

cells have the ability to rapidly change their DNA-dependent RNA polymerases [13]. Some pathogens have developed active inactivation methods to destroy antibiotics [14, 15], e.g. β-lactamase acting on the β-lactam ring in penicillins and cephalosporins [16, 17]. Other pathogens opted for a longer, but perhaps more effective, way of resistance, such as changing the permeability of their cell membranes to prevent the uptake of antibiotics [15, 18, 19], or by changing efflux pumps to ensure antibiotics that do enter cells are immediately excreted [14, 20, 21]. Cells that do not have up-front mechanisms of protection need to rely on mechanisms to bypass damaged cell components [15, 22, 23]. A more drastic form of resisting the onslaught of antibiotics is altering the target site on the surface of the cell, thereby preventing adhesion of the antibiotic [13, 24, 25]. The ease at which bacteria develop resistance to antibiotics has to do with the rapid rate at which cells divide and their access to resistance genes through conjugation, transduction and transformation [15, 26].

Bioactive secondary metabolites produced by bacteria living in symbiosis with nematodes may hold the answer to the discovery of novel antimicrobial compounds. One genus that deserves special attention is *Xenorhabdus*, a member of the family Enterobacteriaceae. The strains live in close association with entomopathogenic nematodes of the family Steinernematidae. Once a nematode is invaded, biologically active compounds with a broad spectrum of antimicrobial activity inhibits the growth of bacteria, fungi and protozoa [27]. The invaded nematode then elicits and intense immune response [28] leading to overproduction of quinones and the killing of the insect larvae. The insecticidal mode of activity used by *Xenorhabdus* spp. varies, as reviewed by Dreyer *et al.* [29].

In this review, the antimicrobial compounds produced by *Xenorhabdus* spp. are listed, the gene clusters involved in synthesis of these secondary metabolites, biosynthetic pathways and growth requirements needed for increased production are discussed.

Antimicrobial compounds produced by *Xenorhabdus* spp.

Xenorhabdus spp. produce of a broad range of antibacterial, antifungal and antiprotozoal compounds that may differ between strains of the same species. These include depsipeptides such as xenematides, xenomacins, szentiamide and xenobactin, lipodepsipeptides, xenocoumacins, fabclavines, pristinamycin, xenortides, rhabdopeptides, bicornitun, PAX peptides, cabanillasin, nemaucin, dithiolopyrrolone derivates, indole-containing compounds, benzylideneacetone, rhabdicin, bacteriocins and a few unnamed peptides. Unfortunately, a

number of antimicrobial compounds produced by *Xenorhabdus* spp. are cytotoxic, e.g. xenoamicin, taxlllaids, szentiamide, xenortides, rhabdopeptides, fabclavins, and cabanillasin (Table 1). One compound in particular, xenortides, has strong anticancer properties and is significantly less toxic to normal cell lines. For a compilation of the molecular structures of these compounds, the reader is referred to the review of Dreyer *et al.* [29]. The ability of *Xenorhabdus* spp. to produce so many broad spectrum bioactive compounds is ascribed to the large variation in gene clusters (as many as 23) described for the genus [30]. None of these bioactive compounds have been produced in large scale and commercialized. It is not the intention of this review to summarise the antimicrobial compounds produced by *Xenorhabdus* spp. For further information the reader is referred to the review by Dreyer *et al.* [29].

Table 1: Biosynthetic pathways in the production of antimicrobial compounds produced by *Xenorhabdus* spp.

Compounds	**Biosynthetic pathway**	**Bioactivity**	**Cytotoxicity**	**References**
Xenoamicin	NRPS	Antiprotozoal	L-6[a]	Zhou *et al.* **[96]**
Taxlllaids	NRPS	Antiprotozoal Cytotoxic	L-6[a], U937[b] and Hela[c]	Kronenwerth *et al.***[97]**
Xenematides	NRPS	Antibacterial Insecticial	Unknown	Crawford *et al.* **[98]**
Xenobactin	NRPS	Antibacterial Antiprotozoal	No cytotoxicity reported for L-6	Grundmann *et al.* **[99]**
Szentiamide	NRPS	Antibacterial Antifungal Cytotoxic	L-6[a], Hela[b]	Ohlendorf *et al.* **[100]** Nollmann *et al.* **[101]**
Xenortides	NRPS	Antiprotozoal Cytotoxic	HCT-116[d], H460[e], OV-2008[f], MDA-MB-231[g], DU145[h], CRL-1459[i], CHO[j]	Reimer *et al.* **[102]** Esmati *et al.* ***[103]***
Rhabdopeptides	NRPS	Antiprotozoal Insecticidal Cytotoxic	L-6[a]	Hacker *et al.* **[104]** Zhao *et al.* **[105]**
Bicornitun	NRPS	Antibacterial Anti-oomycete	Unknown	Fuchs *et al.* **[106]**
PAX Peptides	NRPS	Antibacterial Antifungal	No cytotoxicity reported for CHO[j]	Fuchs *et al.* **[107]** Gualtieri *et al.* **[108]**
Nematophin	NRPS	Antibacterial Antifungal	Unknown	Cai *et al.* **[109]**
Xenocin	RPS	Antibacterial	Unknown	Singh and Banerjee **[110]**
Xenorhabdicin	RPS	Antibacterial	Unknown	Thaler, Baghdiguian and Boemare **[111]**
Xenocyloins	PKS Type III	Insecticidal	Unknown	Proschak *et al.* **[112]**

Table 1 continued

Xenocoumacins	Hybrid NRPS/PKS	Antibacterial Antifungal Antiulcer	Unknown	Guo *et al.* **[113]**
Fabclavins	Hybrid NRPS/PKS	Antibacterial Antifungal Antiprotozoal Cytotoxic	L-6[a]	Fuchs *et al.* **[114]**
Pristinamycin	Hybrid NRPS/PKS	Antibacterial	No cytotoxicity reported	Brachmann *et al.* **[115]**
Xenorhabdins	Hybrid NRPS/PKS	Antibacterial	Unknown	Qin *et al.* **[116]**; Li *et al.* **[117]**
Xenorxides	Hybrid NRPS/PKS	Antibacterial Antifungal	Unknown	Qin *et al.* **[116]**; Li *et al.* **[117]**
Cabanillasin	Hybrid NRPS/PKS	Antifungal	PC-3[k], hTERT HME-1[l]	Houard *et al.* **[118]**
Nemaucin	Hybrid NRPS/PKS	Antibacterial	Unknown	Masschelein, Jenner and Challis **[119]**
Rhabducin	Isonitrile biosynthesis	Insecticidal	Unknown	Crawford *et al.* **[120]**
Benzylidene-acetone	Unknown	Antibacterial Immuno-suppressant Insecticidal	Unknown	Ji *et al.* **[121]**
GP-19	Unknown	Antibacterial Antifungal	Unknown	Xiao *et al.* **[122]**
EP-20	Unknown	Antifungal	Unknown	Xiao *et al.* **[122]**

[a]L-6: Rat skeletal myoblasts, [b]U937: Human leukaemic monocyte cells, [c]Hela: Human carcinoma cells, [d]HCT-116: Colon carcinoma, [e]H460: Human lung carcinoma, [f]OV-2008: Human ovarian carcinoma, [g]MDA-MB-231: Human breast adenocarcinoma, [h]DU145: Human prostate adenocarcinoma, [i]CRL-1459: Human epithelial colon, [j]CHO: Chinese hamster ovary cells, [k]PC-3: Human prostatic carcinoma, [l]hTERT HME-1: Human normal mammary epithelial cells

Genetic clusters and biosynthetic pathways involved in production of antimicrobial compounds

The majority of *Xenorhabdus* antimicrobial compounds are produced via non-ribosomal peptide synthesis (NRPS) and a combination of polyketide synthesis (PKS) and NRPS (NRPS/PKS). Although not that common, some peptides are also produced via ribosomal peptide synthesis (RPS) (Table 1). Ribosomal peptide synthesis (Fig. 1), also known as nucleic acid dependent synthesis, relies on post-translation modification for incorporation of various rings and non-proteinogenic substances [31]. Non-ribosomal peptide synthesis is more complicated than RPS and relies on a minimum of three proteins. In contrast to RPS, NRPS is nucleic acid-independent and relies on multienzyme complexes to identify and determine the

sequence of amino acid residues [32, 33]. The NRPS proteins are collectively referred to as modules [34]. Mega-multifunctional enzymes synthesize a broad range of biologically active peptides, including antibiotics, immunosuppressants, antitumor agents, biosurfactants, siderophores and antiviral compounds [34, 35]. This is possible due to the ability of these enzymes to incorporate D and L forms of proteinogenic- and non-proteinogenic amino acids, hydroxy acids and fatty acid building blocks [36]. Peptides released by these multifunctional enzymes have various tertiary structures and may be cyclic, branched-cyclic or linear [37].

Although true NRPS is only observed in bacteria and fungi, similar systems have been described for higher eukaryotes. One example is amino adipic acid semi-aldehyde dehydrogenase U26 that catabolizes lysin in mice [38]. Three categories of NRPS have been identified, i.e. linear (type 1), iterative (type 2) and nonlinear (type 3), shown in Figure 2. During linear synthesis (type 1), each module encodes a single amino acid and the module order determines the sequence of the incorporated amino acids. In type 2 NRPS, a single module may be reused to incorporate multiple copies of the same amino acid, as in the case of gramicidin S [39, 40]. Type 2 NRPS usually consists of repeated sequences. Amino acid sequences formed via nonlinear synthesis (type 3) does not correlate to the arrangement of modules [38–40].

A module may be composed of a combination of six proteins, referred to as domains. A minimal module has a condensation (C) domain, adenylation (A) domain and peptidyl carrier protein (PCP) [41-45], shown in Figure 3. The domains are identified by the presence of consensus sequences (Table 2). The C-domain is responsible for peptide bond formation and is a member of the chloramphenicol acetyltransferase family [46, 47]. It is also the first domain in a module, except for the first module of a synthetase [41]. In hybrid NRPS-PKS, the C-domain acts as a bridge between NRPS and PKS [48]. The A-domain is responsible for monomer (amino acid) selection and activation [43]. Monomer selection is based on a binding pocket within the N-terminal and consists of approximately 10 amino acid residues [41, 44, 49]. The PCP-domain acts as a transporter and is the smallest of all the domains, consisting of 80 to 100 amino acids [33, 50, 51]. The PCP domain contains one conserved sequence or motif with a highly conserved serine that links a phosphopantetheine cofactor derived from coenzyme A (Table 2). In addition to the three core domains, a module may also contain one of various modification domains, of which the epimerization (E) domain and the methyltransferase (M) domain are the most common [32]. The E-domain is responsible for the incorporation of D-amino acids in non-ribosomal peptides [33, 47, 52, 53], whilst the M-domain is responsible for methylating the monomers [41, 54-56]. Some of the lesser known

modification domains include a cyclization (Cy), reduction (R), oxidation (Ox) and α-hydroxylation (Ox') domain [57]. The sixth, a thioesterase (TE) domain, is only present in the last module [32]. The TE-domain is responsible for the release or cyclization of the intermediate peptide product [34]. Due to the vast variety of NRP structures, the sequence similarity among TE domains is extremely low (10% - 15%), with only one core motif. For further reading on NRPS, the reader is referred to Marahiel *et al.*[33], Finking and Marahiel [38], Hur *et al.* [41], Payne *et al.* [43] and Süssmuth and Mainz [47].

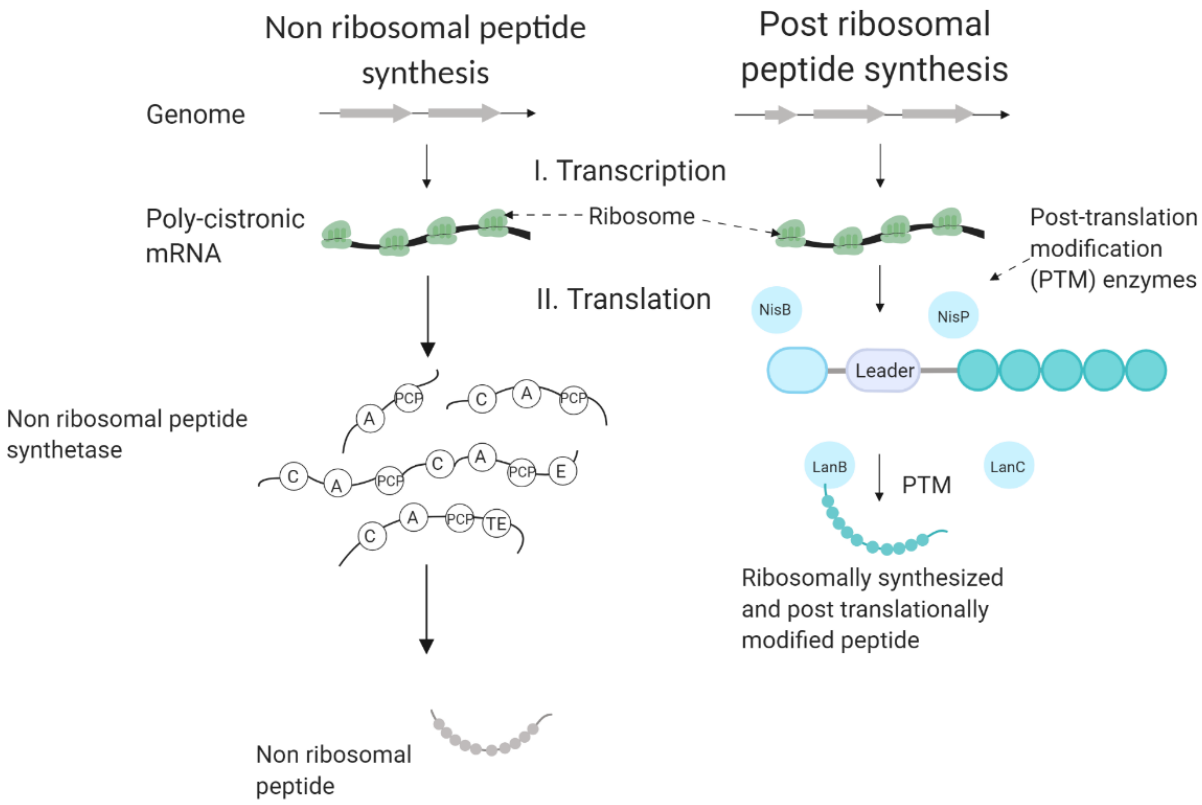

Figure 1: A graphical overview of the differences and similarities between ribosomal peptide synthesis (RPS) and non-ribosomal peptide synthesis (NRPS). The transcription process for RPS and NRPS is similar but differ during translation. RPS – Ribosomes decode mRNA to synthesise active peptide. NRPS – ribosomes decode mRNA, resulting in the synthesis of non-ribosomal peptide synthetase that synthesizes the active peptide.

Polyketide antimicrobial compounds are synthesized from acetyl/malonyl coenzyme A (CoA) precursors and their biosynthesis depends on multifunctional polyketide synthases. The structure of these synthases was extrapolated from fatty acid synthases (FAS's) since they share various similarities in terms of overall extension mechanisms, precursors and architectural and structural design [58-60].

A classic polyketide synthetase is composed of an initiation module, followed by elongation and termination modules (Fig. 4). Initiation and elongation modules consist of an acyltransferase (AT), β-ketoacyl synthase (KS) and acyl carrier protein (ACP) domain. The AT domain recruits and catalyses the binding of the monomers and the KS domain catalyses a chain-elongation reaction via a decarboxylative Claisen thioester condensation reaction. The ACP domain acts as an arm and transfers the monomer to a domain located on the elongation module. Additional auxiliary domains are also found in the initiation/elongation modules, namely methyl transferase (MT), dehydratase (DH), cyclase (CYC), aromatase (ARO), enoylreductase (ER) and β-ketoreductase (KR). These additional domains contributes to structural complexity of PKS [58-60].

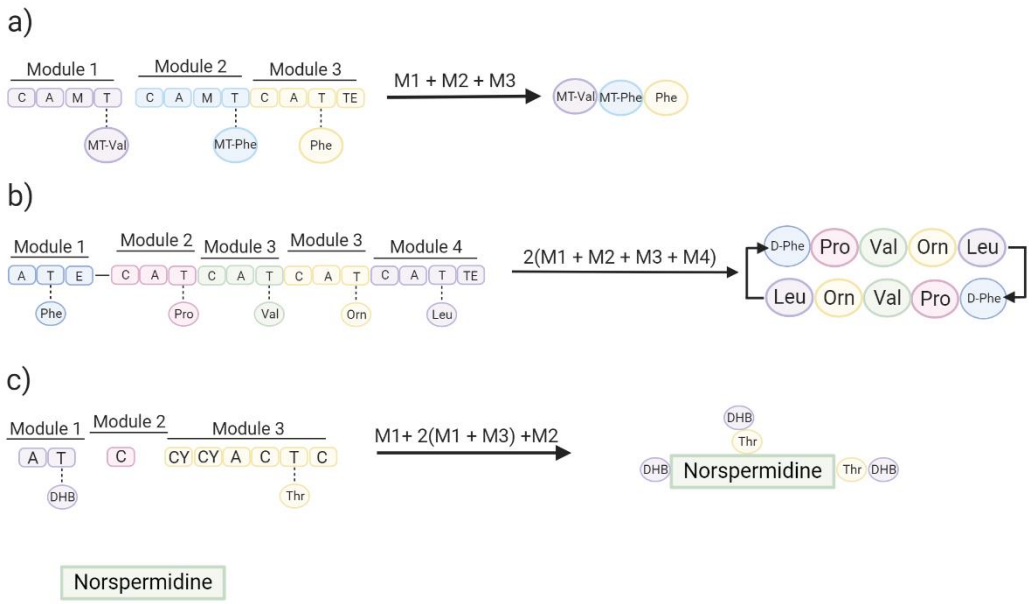

Figure 2: The biosynthetic strategies employed by organisms for the assembly of non-ribosomal peptides. (a) Linear (type I) non-ribosomal peptide synthesis (NRPS). In linear NRPS each module encodes for a single amino acid to produce xenortide A, (b) while in iterative (type II) NRPS the modules are reused to incorporate multiples of the same amino acids as seen in the biosynthesis of gramicidin S. (c) Non-linear (type III) NRPS is unique as the order of the modules do not correlate to the structure of the peptide as can be seen for the synthesis of vibriobactin.

Polyketides are divided into three classes, i.e. type I, II and III [48, 59, 61]. The multifunctional polyketide synthetase domain of type I PKS is linearly arranged and covalently fused in cis and are divided into subclasses as iterative or non-iterative. Iterative type I PKS is mainly found in the fungal domain, although some examples do exists in bacteria [62, 63].

Iterative type I fungal PKS is classified as highly reducing (HR), partially reducing (PR) or non-reducing (NR), depending on the presence or absence of KR processing domains. Bacterial iterative type I PKS is mostly monomodular and is involved in the formation of small polyenes, or aromatic compounds [64]. Non-iterative type I PKS is mainly produced by bacteria, although they have been found in protozoans. In non-iterative type I PKS, each module is responsible for incorporating a single CoA unit. The number of modules thus directly correlate with the number of decarboxylative Claisen thioester condensation reactions executed by PKS. This allows easy manipulation and rational reprogramming of the synthetases to further enrich the diversity of polyketides [65].

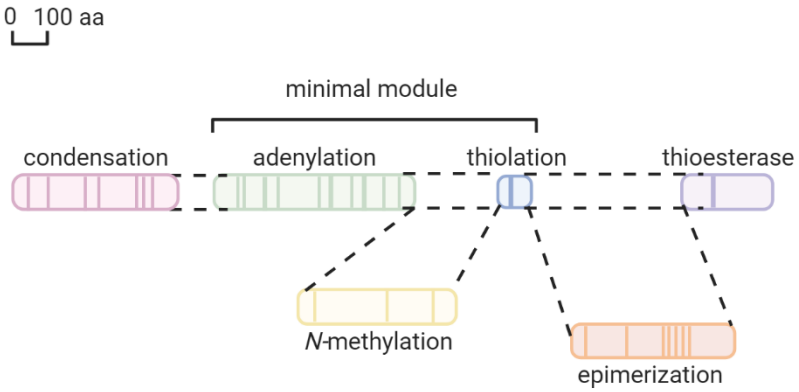

Figure 3: Overview of a non-ribosomal peptide synthetase. The condensation domain (pink) is always the first domain in the module followed by the adenylation domain (green) and thiolation domain (blue), except for except for a minimal module also known as the first module in the synthetase. The *N*-methylation domain (yellow) and epimerization domain (orange) is the most common modification domains in NRPS. The thioesterase domain (purple) is in the last module of the operon. The domains are identified by the presence of consensus sequences, as indicated in Table 2. Adapted from Marahiel *et al.* (1997)[40]

Type II PKS is mainly present in actinomycetes, with only two examples described for Gram-negative bacteria. In contrast to type I PKS, the domains are organised on freestanding monofunctional enzymes in an iterative manner [48, 58-60]. The freestanding monofunctional enzymes are each encoded by a single gene within an operon. A minimal type II PKS consists of an ACP and two β-ketosynthase units (KS_α and KS_β). The KR, CYC and ARO auxiliary domains converts the poly-β-keto chain into an aromatic polyketide [66, 67].

Type III PKS is a self-contained chalcone synthase-like PKS that forms homodimers and utilizes the CoA thioesters directly without ACP. The homodimers catalyse a number of reactions in a single catalytic centre [68]. Aromatic metabolites formed from these reactions are mostly found in the plants, but occasionally also in bacteria [64, 69, 70]. Another distinguishing factor of type III PKS is the use of an malonyl-CoA as a substrate [48], although it was recently discovered that bacterial type III PKS can also utilize branched fatty acids as a extender unit.

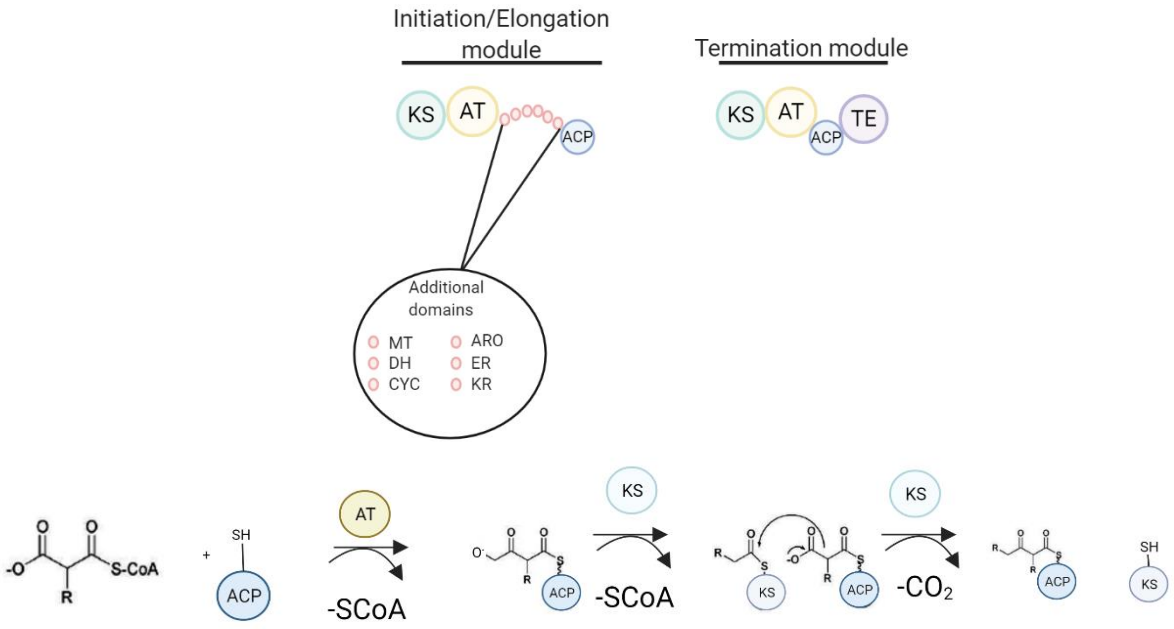

Figure 4: Modular polyketide biosynthesis. The initiation and elongation modules consist out of three core domains, a β-ketoacyl synthetase (KS), an acyltransferase (AT) and an acyl carrier protein (ACP). Additional domains can also be present contributing to the complexity of polyketide structures. The additional auxiliary domain is a methyl transferase (MT), dehydratase (DH), cyclase (CYC), aromatase (ARO), enoylreductase (ER) and β-ketoreductase (KR). The termination domain also contains the KS, AT, and ACP domains, and one additional domain the termination (TE) domain.

Second to NRPS is hybrid NRPS/PKS, the most common biosynthetic pathway used by *Xenorhabdus* spp. for the production of secondary metabolites (Table 1). The similarities (modular organization and carrier proteins) between the biosynthetic pathways of NRPS and type I PKS have allowed the development of a hybrid synthetase [60]. Hybrid NRPS/PKS are extremely variable. The fabclavin biosynthetic gene cluster, for example, consists of six NRPSs (non-ribosomal peptide synthetases) and three PKSs (polyketide synthetases) [52], whilst the

biosynthetic gene cluster of xenocoumacins consists of five PKSs and three NRPSs [71]. Hybrid PKS/NRPS is subdivided into two classes. Class I, has a hybrid PKS/NRPS system that hybridises the PKS-bound polyketide intermediate to NRPS peptidyl intermediate, or *vice versa*. Class II has an external enzyme that hybridises NRPS and PKS intermediates. One such example is coronatine, where a ligase is responsible for hybridising NRP and PKS. Direct functional hybridization is much more common and examples in nature include the biosynthesis of bleomycin, xenocoumacins, fabclavins, streptogramin A, epothilones and myxothiazol [57].

Table 2: The conserved core motifs of the different catalytic domains of non-ribosomal peptide synthetases.

Domain	Motif	Consensus sequence
Adenylation	A1	L(TS)YxEL
	A2	LK(AS)GxAY(VL)P(LI)D
	A3	LAYxxYTSG(ST)TGxPKG
	A4	FDxS
	A5	NxYGPTE
	A6	GELxIxGxG(VL)ARGYL
	A7	Y(RK)TGDL
	A8	GRxDxQVKIRGxRIELGEIE
	A9	LPxYM(IV)P
	A10	NGK(VL)DR
Peptidyl carrier protein	T	DxFFxLGG(HD)S(LI)
Condensation	C1	SxAQxR(LM)(WY)xl
	C2	RHExLRTxF
	C3	MHHxISDG(WV)S
	C4	YxD(FY)AVW
	C5	(IV)GxFVNT(QL)(CA)xR
	C6	(HN)QD(YV)PFE
	C7	RDxSRNPL
Thioesterase	TE	G(HY)SxG
Epimerization	E1	PIQxWF
	E2	HHxISDG(WV)S
	E3	DxLLxAxG
	E4	EGHGRE
	E5	RTVHWFTxxYP(YV)PFE
	E6	PxxGxGYG
	E7	FNYLG(QR)
N-methylation	M1	VL(DE)GxGXG
	M2	NELSxYRYxAV
	M3	VExSxARQxGxLD

Growth requirements

Before a novel antibiotic can be commercialized, it has to be produced in large quantities. Various methods have been employed to increase the production of secondary metabolites produced by *Xenorhabdus* spp. These include optimizing growth conditions [72-74], homologous gene expression [75], exchanging promotors in gene clusters [76] and induction, or deletion, of regulatory proteins that play an important role in the expression of secondary metabolites [77].

Various studies have shown that altering of growth conditions (e.g. pH, incubation temperature, agitation, aeration and nutrients) affects the way in which *Xenorhabdus* spp. produce secondary metabolites [72-74]. Production of antibiotics by *X. nematophilia* can be enhanced by manipulating the pH of growth media [78]. The same authors showed that changing of pH during mid-exponential growth from 6.5 to, pH 7.5 enhanced the production of antibiotics by as much as 185%. Wang *et al.* [73] reported an increase in production of antibiotics when strains of *X. nematophila* were incubated at 28.5 °C and in the presence of elevated levels of dissolved oxygen.

In another study, Wang *et al.* [57] reported an increase in the production of antibiotics when *X. bovienii* was grown in the presence of high levels of NaCl. Similar results were published by Crawford *et al.* [79]. Sorbitol added to growth media resulted in decreased antibiotic production [79]. Carbon and nitrogen levels are equally important. *X. bovienii* produced highest levels of antibiotic when cultured in the presence of glycerol and soytone [80]. In the case of *X. nematophilia*, antibiotic production increased when strains were grown in the presence of glucose and peptone [81]. Sa-uth *et al.* [74] reported an increase in antibiotic production when strains of *X. stockiae* were cultured in the presence of sucrose and yeast extract. It is thus clear that species are fastidious regarding the source, and concentration, of carbon and nitrogen.

Advanced sequencing technology to improve secondary metabolite production by *Xenorhabdus* spp.

The size of gene clusters involved in encoding secondary antimicrobial compounds reported for *Xenorhabdus* spp. are in excess of 100kb. The number of repeats in restriction enzyme recognition sites made cloning of DNA fragments, using classical methods, extremely difficult. Advancements in sequencing, such as sequencing and ligation independent cloning (SLIC)

[82], ligation independent cloning (LIC) [83], RED/ET recombination kits [84] and Gibson cloning [85] changed all of this. These methods are expensive, time consuming and requires more skill than general cloning. However, overlap extension PCR-yeast homologous recombination (ExRec) [86, 87] is done with smaller DNA fragments and requires only 15 to 40 homologous nucleotides. The technique was used by Schimming *et al.* [75] to clone three biosynthetic gene clusters (GameXpeptide, ambactin and xenolindicins) of *Xenorhabdus* spp. into *E. coli*. Xenoamicins could, however, not be expressed using the same method due to a lack of certain building blocks and genetic elements only available in the native host. A solution to the latter came with a study reported by Bode *et al*. [76]. The authors enhanced the expression of secondary metabolites in *Xenorhabdus* spp. by exchanging the native promotor for P_{BAD}, an inducible promotor. This also showed that tightly regulated inducible promotors, such as P_{BAD}, may be used instead of heterologous gene expression.

It is widely known that regulatory proteins play an important role in gene expression [88]. Although the role between regulatory proteins and pathogenicity of *Xenorhabdus* spp. have been studied extensively [89-92], reports on the effect regulatory proteins have on secondary metabolites biosynthesis and function are lacking. To date, only one report on regulatory proteins involved in the production of secondary metabolites of *Xenorhabdus* spp. have been published [55]. The authors focused on two global regulators, Lrp (Leucine responsive protein) and LeuO. Another study have shown that Lrp plays and important role in the association of *X. nematophilia* with nematodes and thus insect pathogenicity [69]. Upon further investigation, Engel *et al*. [77] discovered that overexpression of Lrp increased the expression levels of xenematide A, xenocoumacin 1, xenortide A and rhabdopeptide 1. Under the same conditions, lower expression of the genes encoding nematophin and xenotetrapeptides was observed. This is in accordance with Cowles *et al.* [91], who described a *X. nematohila* Lrp mutant with attenuated virulence towards tobacco hornworm larvae. These studies indicated that Lrp is a positive regulator of secondary metabolite biosynthesis [77] and plays a role in the virulence of xenematides, xenortides and rhabdopeptides [92]. Overexpression of the LeuO global regulator had an overall negative effect on secondary metabolite production, but increased the biosynthesis of xenematide A and xenotetrapeptides [77]. These findings are in agreement with results reported for *S. enterica* [93], *Vibrio cholerae* [94] and *Vibrio parahaemolyticus* [95], i.e. overexpression of LeuO attenuated virulence. LeuO from *X. nematophilia* was heterologously expressed in *X. szentirmaii* [77], indicating that this method can be used to improve expression of secondary metabolites without the knowledge of the relevant biological

pathways. The overexpression of global regulators may thus lead to the discovery of previously non-detected antimicrobial metabolites.

Conclusions

The rate at which new antibiotics are discovered and approved needs to be increased to allow successful treatment of microbial infections, especially caused by multi-drug resistant bacteria. To date, more than 20 antimicrobial compounds produced by *Xenorhabdus* spp. have been described, indicating that the genus may be a unique source of novel antibiotics. The biosynthetic machinery used to produce these compounds are complex and the genes encoding production are dispersed into separate clusters. However, with the latest sequencing and cloning techniques, overproduction of these compounds is possible. More fermentation and purification studies need to be done to allow upscaling to industrial levels.

Acknowledgement

This work was funded by a South African National Research Foundation grant.

Conflict of interest

The authors declare that they have no competing interests.

References

1. Stubbendieck RM, Straight PD (2016) Multifaceted interfaces of bacterial competition. J Bacteriol 198:2145–2155.
2. Hibbing ME, Fuqua C, Parsek MR, Peterson BS (2010) Bacterial competition: Surviving and thriving in the microbial jungle. Nat Rev Micro 8:15–25.
3. Kim W, Racimo F, Schluter J, Levy SB, Foster, KR (2014) Importance of positioning for microbial evolution. Proc Natl Acad Sci USA 111: E1639-E1647.
4. Asally M, Kittisopikul M, Rué P, Du Y, Hu Z, Çağatay T, Robison AB, Lu H, Garcia-Ojalvo J, Süel GM (2012) Localized cell death focuses mechanical forces during 3D patterning in a biofilm. Proc Natl Acad Sci USA 109: 18891–18896.
5. Kreth J, Zhang Y, Herzberg MC (2008) Streptococcal antagonism in oral biofilms: *Streptococcus sanguinis* and *Streptococcus gordonii* interference with *Streptococcus mutans*. J Bacteriol 2008 190: 4632–4640.
6. Zheng X, Zhang K, Zhou X, Liu C, Li M, Li Y, Wang R, Li Y, Li J, Shi W, Xu X (2013) Involvement of gshAB in the interspecies competition within oral biofilm. J Dent Res 92: 819–824.
7. Chen J, Lee SM, Mao Y. (2004) Protective effect of exopolysaccharide colanic acid of *Escherichia coli* O157:H7 to osmotic and oxidative stress. Int J Food Microbiol 93: 281–286.
8. Prokopenko MG, Hirst MB, De Brabandere L, Lawrence DJP, Berelson,, WM, Granger J, Chang BX, Dawson S, Crane EJ, Chong L, Thamdrup B, Townsend-Small A, Sigman DM (2013) Nitrogen losses in anoxic marine sediments driven by Thioploca-anammox bacterial consortia. Nature 500: 194–198.
9. Koskiniemi S, Sun S, Berg OG, Andersson DI (2012) Selection-driven gene loss in bacteria. PLoS Genet 8: 1–8.
10. Morris JJ (2015) Black Queen evolution: The role of leakiness in structuring microbial communities. Trends Genet 31: 475–482.
11. Johnson DR, Goldschmidt F, Lilja EE, Achermann (2012) Metabolic specialization and the assembly of microbial communities. ISME J 6: 1985–1991.
12. Kaufman G (2011) Antibiotics: Mode of action and mechanisms of resistance. Nurs Stand 24: 49–55.
13. Lambert PA (2005) Bacterial resistance to antibiotics: Modified target sites. Adv Drug Deliv Rev 57: 1471–1485.

14. Peterson E, Kaur P (2018) Antibiotic resistance mechanisms in bacteria: Relationships between resistance determinants of antibiotic producers, environmental bacteria, and clinical pathogens. Front Microbiol 9. http://www.ncbi.nlm.nih.gov/pubmed/27227291.
15. Munita JM, Arias CA (2016) Mechanisms of antibiotic resistance. Microbiol Spectr 4. http://www.ncbi.nlm.nih.gov/pubmed/27227291.
16. Jacoby GA (2009) AmpC B-Lactamases. Clin Microbiol Rev 22: 161–182.
17. Abraham E, Chain E (1940). An enzyme from bacteria able to destroy penicillin. Nature 146: 677–678.
18. Hancock REW, Brinkman FSL (2002) Function of *Pseudomonas* porins in uptake and efflux. Annu Rev Microbiol 56: 17–38.
19. Quinn JP, Dudek EJ, Divincenzo CA, Lucks DA, Lerner SA (1986) Emergence of resistance to imipenem during therapy for *Pseudomonas aeruginosa* infections. J Infect Dis 154: 289–294.
20. Poole K (2005) Efflux-mediated antimicrobial resistance. J Antimicrob Chemother 56: 20–51.
21. Nikaido H (2003) Molecular basis of bacterial outer membrane permeability revisited. Microbiol Mol Biol Rev 67: 593–656.
22. Enright MC, Robinson AD, Randle G, Feil EJ, Grundmann H, Spratt BG (2002) The evolutionary history of methicillin-resistant *Staphylococcus aureus* (MRSA). Proc Natl Acad Sci USA 99: 7687–7692.
23. Grebe T, Hakenbeck R (1996) Penicillin-binding proteins 2b and 2x of *Streptococcus pneumoniae* are primary resistance determinants for different classes of β-lactam antibiotics. Antimicrob Agents Chemother 40: 829–834.
24. Ropp PA, Hu M, Olesky M, Nicholas RA (2002) Mutations in *ponA*, the gene encoding penicillin-binding protein 1, and a novel locus, *penC*, are required for high-level chromosomally mediated penicillin resistance in *Neisseria gonorrhoeae*. Antimicrob Agents Chemother 46: 769–777.
25. Neu HC (1992) The crisis in antibiotic resistance. Science 257: 1064–1073.
26. Colavecchio A, Cadieux B, Lo A, Goodridge LD (2017) Bacteriophages contribute to the spread of antibiotic resistance genes among foodborne pathogens of the Enterobacteriaceae family - A review. Front Microbiol 8: 1–13.
27. Dunphy GB, Webster JM (1991). Antihemocytic surface components of *Xenorhabdus nematophilus* var. *dutki* and their modification by serum nonimmune larvae of *Galleria mellonella*. J Invertebr Pathol 58: 40–51.

28. Yang J, Zeng H-M, Lin H-F, Yang X-F, Liu Z, Guo L-H, Yuan J-J, Qiu, D-W (2012) An insecticidal protein from *Xenorhabdus budapestensis* that results in prophenoloxidase activation in the wax moth, *Galleria mellonella*. J Invertebr Pathol 110: 60–67.
29. Dreyer J, Malan AP, Dicks LMT (2018) Bacteria of the Genus *Xenorhabdus,* a novel source of bioactive compounds. Front Microbiol 9: 1–14.
30. Reimer D, Nollmann FI, Schultz K, Kaiser M, Bode HB (2014) Xenortide biosynthesis by entomopathogenic *Xenorhabdus nematophila*. J Nat Prod 77: 1976–80.
31. Van Staden ADP, Faure LM, Vermeulen RR, Dicks LMT, Smith C (2019) Functional expression of GFP-fused Class I lanthipeptides in *Escherichia coli*. ACS Synth Biol 8: 2220–2227.
32. Belshaw PJ, Walsh CT, Stachelhaus T (1999) Aminoacyl-CoAs as probes of condensation domain selectivity in nonribosomal peptide synthesis. Science 284: 486–489.
33. Marahiel MA, Stachelhaus T, Mootz HD (1997) Modular peptide synthetases involved in nonribosomal peptide synthesis. Chem Rev 97: 2651–2674.
34. Roongsawang N, Siew PL, Washio K, Takano K, Kanaya S, Morikawa M (2005) Phylogenetic analysis of condensation domains in the nonribosomal peptide synthetases. FEMS Microbiol Lett 252: 143–151.
35. Ackerley DF (2016) Cracking the nonribosomal code. Cell Chem Biol 23: 535–537.
36. Inoue M (2011) Total synthesis and functional analysis of non-ribosomal peptides. Chem Rec 11: 284–294.
37. Martínez-Núñez MA, López VEL (2016) Nonribosomal peptides synthetases and their applications in industry. Sustain Chem Process 4: 13–20.
38. Finking R, Marahiel MA (2004) Biosynthesis of nonribosomal peptides. Annu Rev Microbiol 58: 4530–488.
39. Steiniger C, Hoffmann S, Süssmuth RD (2019) Desymmetrization of cyclodepsipeptides by assembly mode switching of iterative nonribosomal peptide synthetases. ACS Synth Biol 8: 661–667.
40. Juguet M, Lautru S, Francou FX, Nezbedovà S, Leblond P, Gondry M, Pernodet J-L (2009) An iterative nonribosomal peptide synthetase assembles the pyrrole-amide antibiotic congocidine in *Streptomyces ambofaciens*. Chem Biol 16: 421–431.
41. Hur GH, Vickery CR, Burkart MD (2012) Explorations of catalytic domains in non-ribosomal peptide synthetase enzymology. Nat Prod Rep 29: 1074–1098.

42. Luo C, Liu X, Zhou X, Guo J, Truong J, Wang X, Xhou H, Li X, Chen Z (2015) Unusual biosynthesis and structure of locillomycins from *Bacillus subtilis* 916. Appl Environ Microbiol 81: 6601–6609.
43. Payne JAE, Schoppet M, Hansen MH, Cryle MJ (2017) Diversity of nature's assembly lines-recent discoveries in non-ribosomal peptide synthesis. Mol Biosyst 13: 9–22.
44. Challis GL, Ravel J, Townsend CA (2000) Predictive, structure-based model of amino acid recognition by nonribosomal peptide synthetase adenylation domains. *Che*m Biol 7: 211–224.
45. Hancock REW, Chapple DS (1999) Peptide antibiotics. Antimicrob Agents Chemother 43: 1317–1323.
46. Challis GL, Naismith JH (2004) Structural aspects of non-ribosomal peptide biosynthesis. Curr Opin Struct Biol 14: 748–756.
47. Süssmuth RD, Mainz A (2017) Nonribosomal peptide synthesis — principles and prospects. Angew Chemie - Int Ed 56: 3770–3821.
48. Fischbach MA, Walsh CT (2006) Assembly-line enzymology for polyketide and nonribosomal peptide antibiotics: logic, machinery and mechanisms. Chem Rev 106: 3468–3496.
49. Baranašić D, Zucko J, Diminic J, Gacesa R, Long PF, Cullum J, Hranueli D, Starcevic A (2014) Predicting substrate specificity of adenylation domains of nonribosomal peptide synthetases and other protein properties by latent semantic indexing. J Ind Microbiol Biotechnol 41: 461–467.
50. Crosby J, Crump MP (2012) The structural role of the carrier protein - Active controller or passive carrier. Nat Prod Rep 29: 1111–1137.
51. Miller BR, Gulick AM (2016) Structural biology of non-ribosomal peptide synthetases. Methods Mol Biol 1401: 3–29.
52. Hoffmanns K, Schneider-scherzers E, Kleinkauf H, Rainer Z (1994) Purification and characterization of eucaryotic alanine racemase acting as key enzyme in cyclosporin biosynthesis. J Biol Chem 269: 12710–12714.
53. Stein T, Kluge B, Vater J, Franke P, Otto A, Wittmann-Liebold B (1995) Gramicidin S synthetase 1 (phenylalanine racemase), a prototype of amino acid racemases containing the cofactor 4'-phosphopantetheinet. Biochem 34: 4633–4642.
54. Chatterjee J, Rechenmacher F, Kessler H (2013) N-Methylation of peptides and proteins: An important element for modulating biological functions. Angew Chem Int Ed Engl 52: 254–269.

55. Mori S, Pang AH, Lundy TA, Garzan A, Tsodikov OV, Garneau-Tsodikova S (2018) Structural basis for backbone N-methylation by an interrupted adenylation domain. Nat Chem Biol 14: 428–30.
56. Stachelhaus T, Marahiel MA (1995) Modular structure of genes encoding multifuctional peptide synthetases required for non-ribosomal peptide synthesis. FEMS Microbiol Lett 125: 3–14.
57. Du L, Sánchez C, Shen B (2001) Hybrid peptide-polyketide natural products: Biosynthesis and prospects toward engineering novel molecules. Metab Eng 3: 78–95.
58. Smith S, Tsai SC (2007) The type I fatty acid and polyketide synthases: A tale of two megasynthases. Nat Prod Rep 24: 1041–1072.
59. Caulier S, Nannan C, Gillis A, Licciardi F, Bragard C, Mahillon J (2019) Overview of the antimicrobial compounds produced by members of the *Bacillus subtilis* group. Front Microbiol 10: 1–19.
60. Hertweck C (2009) The biosynthetic logic of polyketide diversity. Angew Chemie - Int Ed 48: 4688–4716.
61. Rawlings BJ (19997) Biosynthesis of polyketides. Nat Prod Rep 14: 523–556.
62. Cox RJ (2007) Polyketides, proteins and genes in fungi: Programmed nano-machines begin to reveal their secrets. Org Biomol Chem 5: 2010–2026.
63. Schümann J, Hertweck C (2006) Advances in cloning, functional analysis and heterologous expression of fungal polyketide synthase genes. J Biotechnol 124: 690–703.
64. Chen H, Du L (2016) Iterative polyketide biosynthesis by modular polyketide synthases in bacteria. Appl Microbiol Biotechnol 100: 541–557.
65. Cane DE, Walsh CT, Khosla C (1998) Harnessing the biosynthetic code: Combinations, permutations, and mutations. Science 282: 63–68.
66. Tang GL, Zhang Z, Pan HX (2017) New insights into bacterial type II polyketide biosynthesis. F1000Research 6: 1–12.
67. Staunton J, Weissman KJ (2001) Polyketide biosynthesis: A millennium review. Nat Prod Rep 18: 380–416.
68. Katsuyama Y, Ohnishi Y (2012) Type III polyketide synthases in microorganisms. 1st ed. Elsevier Inc.
69. Sierra JM, Fusté E, Rabanal F, Vinuesa T, Viñas M (2017) An overview of antimicrobial peptides and the latest advances in their development. Expert Opin Biol Ther 17: 663–676.

70. Nakano C, Ozawa H, Akanuma G, Funa N, Hornouchi S (2009) Biosynthesis of aliphatic polyketides by type III Polyketide synthase and methyltransferase in *Bacillus subtilis*. J Bacteriol 191: 4916–4923.
71. Reimer D, Luxenberger E, Brachmann AO, Bode HB (2009) A new type of pyrrolidine biosynthesis is involved in the late steps of xenocoumacin production in *Xenorhabdus nematophila*. ChemBioChem 10: 1997–2001.
72. Chen G, Maxwell P, Dunphy GB, Webster JM (1996) Culture conditions for *Xenorhabdus* and *Photorhabdus* symbionts of entomopathogenic nematodes. Nematologica 42: 127–130.
73. Wang YH, Feng JT, Zhang Q, Zhang X (2008) Optimization of fermentation condition for antibiotic production by *Xenorhabdus nematophila* with response surface methodology. J Appl Microbiol 104: 735–744.
74. Sa-uth C, Rattanasena P, Chandrapatya A, Bussaman P (2018) Modification of medium composition for enhancing the production of antifungal activity from *Xenorhabdus stockiae* PB09 by using response surface methodology. Int J Microbiol 2018: 1–10. https://www.hindawi.com/journals/ijmicro/2018/3965851/.
75. Schimming O, Fleischhacker F, Nollmann FI, Bode HB (2014) Yeast homologous recombination cloning leading to the novel peptides ambactin and xenolindicin. ChemBioChem 15: 1290–1294.
76. Bode E, Brachmann AO, Kegler C, Simsek R, Dauth C, Zhou Q, Kaiser M, Klemmt P, Bode HB (2015) Simple 'on-demand' production of bioactive natural products. ChemBioChem 16: 1115–1119.
77. Engel Y, Windhorst C, Lu X, Goodrich-Blair H, Bode HB (2017) The global regulators Lrp, LeuO, and HexA control secondary metabolism in entomopathogenic bacteria. Front Microbiol 8: 1–13.
78. Wang Y, Fang X, Cheng Y, Zhang X (2011) Manipulation of pH shift to enhance the growth and antibiotic activity of *Xenorhabdus nematophila*. J Biomed Biotechnol 2011: 1–9.
79. Crawford JM, Kontnik R, Clardy J (2010) Regulating alternative lifestyles in entomopathogenic bacteria. Curr Biol 20: 69–74.
80. Wang Y, Fang X, An F, Wang G, Zhang X (2011) Improvement of antibiotic activity of *Xenorhabdus bovienii* by medium optimization using response surface methodology. Microb Cell Fact 10: 1-15.

81. Wang YH, Li YP, Zhang Q, Zhang X (2008) Enhanced antibiotic activity of *Xenorhabdus nematophila* by medium optimization. Bioresour Technol 99: 1708–1715.
82. Zhang Y, Werling U, Edelmann W (2012) SLiCE: A novel bacterial cell extract-based DNA cloning method. Nucleic Acids Res 40: 1–10.
83. Aslanidis C, de Jong PJ (1990) Ligation-independent cloning of PCR products (LIC-PCR). Nucleic Acids Res 18: 6069–6074.
84. Wenzel SC, Gross F, Zhang Y, Fu J, Stewart F, Müller R (2005) Heterologous expression of a myxobacterial natural products assembly line in *Pseudomonas* via Red/ET recombineering. Chem Biol 12: 349–356.
85. Gibson DG, Young L, Chuang RY, Venter JC, Hutchison CA, Smith H (2009) Enzymatic assembly of DNA molecules up to several hundred kilobases. Nat Methods 6: 343–345.
86. Ramjee MK, Petithory JR, McElver J, Weber SC, Kirsch JF (1996) A novel yeast expression/secretion system for the recombinant plant thiol endoprotease propapain. Protein Eng 9: 1055–1061.
87. Oldenburg KR, Vo KT, Michaelis S, Paddon C (1997) Recombination-mediated PCR-directed plasmid construction *in vivo* in yeast. Nucleic Acids Res 25: 451–452.
88. Yilmaz A, Grotewold E (2010) Components and mechanisms of regulation of gene expression. In: Ladunga I (ed) Computational biology of transcription factor binding, methods in molecular biology,1st ed. Humana Press, Totowa, NJ, pp 23–32.
89. Heungens K, Cowles CE, Goodrich-Blair H (2002) Identification of *Xenorhabdus nematophila* genes required for mutualistic colonization of *Steinernema carpocapsae* nematodes. Mol Microbiol 45: 1337–1353.
90. Jubelin G, Lanois A, Severac D, Rialle S, Longin C, Gaudriault S, Givaudan A (2013) FliZ is a global regulatory protein affecting the expression of flagellar and virulence genes in individual *Xenorhabdus nematophila* bacterial Cells. PLoS Genet 9:1-15.
91. Cowles KN, Cowles CE, Richards GR, Martens EC, Goodrich-Blair H (2007) The global regulator Lrp contributes to mutualism, pathogenesis and phenotypic variation in the bacterium *Xenorhabdus nematophila*. Cell Microbiol 9: 1311–1323.
92. Hinchliffe SJ (2013) Insecticidal toxins from the *Photorhabdus* and *Xenorhabdus* bacteria. Open Toxinology J 3: 101–118.
93. Espinosa E, Casadesús J (2014) Regulation of *Salmonella enterica* pathogenicity island 1 (SPI-1) by the LysR-type regulator LeuO. Mol Microbiol 91: 1057–1069.
94. Bina XR, Taylor DL, Vikram A, Ante VM, Bine JE (2013) *Vibrio cholerae* ToxR downregulates virulence factor production in response to cyclo(Phe-Pro). MBio 4:1-9.

95. Whitaker WB, Parent MA, Boyd A, Richards GP, Boyd F (2012) The *Vibrio parahaemolyticus* ToxRS regulator is required for stress tolerance and colonization in a novel orogastric streptomycin-induced adult murine model. Infect Immun 80: 1834–45.
96. Zhou Q, Grundmann F, Kaiser M, Schiell M, Gaudriault S, Batzer A, Kurz M, Bode HB (2013) Structure and biosynthesis of xenoamicins from entomopathogenic *Xenorhabdus*. Chem Eur J 19: 16772–16779.
97. Kronenwerth M, Bozhüyük KAJ, Kahnt AS, Steinhilber D, Gaudriault S, Kaiser M, Bode HB (2014) Characterisation of taxlllaids A-G; natural products from *Xenorhabdus indica*. Chem - A Eur J 20: 17478–17487.
98. Crawford JM, Portmann C, Kontnik R, Walsh CT, Clardy J (2011) NRPS substrate promiscuity diversifies the xenematides. Org Lett 13: 5144–5147.
99. Grundmann F, Kaiser M, Kurz M, Schiell M, Batzer A, Bode HB (2013) Structure determination of the bioactive depsipeptide xenobactin from *Xenorhabdus* sp. PB30.3. RSC Adv 3: 22072–22077.
100. Ohlendorf B, Simon S, Wiese J, Imhoff JF (2011) Szentiamide, an N-formylated cyclic depsipeptide from *Xenorhabdus szentirmaii* DSM 16338 T. Nat Prod Commun 6: 1247–1250.
101. Nollmann FI, Dowling A, Kaiser M, Deckmann K, Grösch S, French-Constant R, Bode H (2012) Synthesis of szentiamide, a depsipeptide from entomopathogenic *Xenorhabdus szentirmaii* with activity against *Plasmodium falciparum.* Beilstein J Org Chem 8: 528–533.
102. Reimer D, Nollmann FI, Schultz K, Kaiser M, Bode HB (2014) Xenortide biosynthesis by entomopathogenic *Xenorhabdus nematophila*. J Nat Prod 77: 1976-1980
103. Esmati N, Maddirala AR, Hussein N, Amawi H, Tiwari AK, Andreana PR (2018) Efficient syntheses and anti-cancer activity of xenortides A-D including ent/epi-stereoisomers. Org Biomol Chem 16: 5332–5342.
104. Hacker C, Cai X, Kegler C, Zhao L, Weickmann K, Wurm JP, Bode HB, Wöhnert J (2018) Structure-based redesign of docking domain interactions modulates the product spectrum of a rhabdopeptide-synthesizing NRPS. Nat Commun 9: 4366-4377.
105. Zhao L, Kaiser M, Bode HB (2018) Rhabdopeptide/xenortide-like peptides from *Xenorhabdus innexi* with terminal amines showing potent antiprotozoal activity. Org Lett 20: 5116–5120.
106. Fuchs SW, Sachs CC, Kegler C, Nollmann FI, Karas M, Bode HB (2012) Neutral loss

fragmentation pattern based screening for arginine-rich natural products in *Xenorhabdus* and *Photorhabdus*. Anal Chem 84: 6948–9655.

107. Fuchs SW, Proschak A, Jaskolla TW, Karas M, Bode HB (2011) Structure elucidation and biosynthesis of lysine-rich cyclic peptides in *Xenorhabdus namtophila*. Org Biomol Chem 9: 3130–3132.
108. Gualtieri M, Aumelas A, Thaler J-O (2009) Identification of a new antimicrobial lysine-rich cyclolipopeptide family from *Xenorhabdus nematophila*. J Antibiot (Tokyo) 62:295–302.
109. Cai X, Challinor VL, Zhao L, Reimer D, Adihou H, Grün P, Kaiser M, Bode HB (2017) Biosynthesis of the antibiotic nematophin and its elongated derivatives in entomopathogenic bacteria. Org Lett 19: 806–809.
110. Singh J, Banerjee N (2008) Transcriptional analysis and functional characterization of a gene pair encoding iron-regulated xenocin and immunity proteins of *Xenorhabdus nematophila*. J Bacteriol 190: 3877–3885.
111. Thaler JO, Baghdiguian S, Boemare N (1995) Purification and characterization of xenorhabdicin, a phage tail-like bacteriocin, from the lysogenic strain F1 of *Xenorhabdus nematophilus*. Appl Environ Microbiol 61: 2049–2052.
112. Proschak A, Zhou Q, Schöner T, Thanwisai A, Kresovic D, Dowling A, Ffrench-constant R, Proschak E, Bode HB (2014) Biosynthesis of the insecticidal xenocyloins in *Xenorhabdus bovienii*. ChemBioChem 15: 369–372.
113. Guo S, Zhang S, Fang X, Liu Q, Gao J, Bilal M, Wang Y, Zhang X (2017) Regulation of antimicrobial activity and xenocoumacins biosynthesis by pH in *Xenorhabdus nematophila*. Microb Cell Fact 16: 1–14.
114. Fuchs SW, Grundmann F, Kurz M, Kaiser M, Bode HB (2014) Fabclavines: Bioactive peptide – polyketide-polyamino hybrids from *Xenorhabdus*. ChemBioChem15: 512–516.
115. Brachmann AO, Reimer D, Lorenzen W, Alonso EA, Kopp Y, Piel J, Bode HB (2012) Reciprocal cross talk between fatty acid and antibiotic biosynthesis in a nematode symbiont. Angew Chemie - Int Ed 51: 12086–12089.
116. Qin Z, Huang S, Yu Y, Deng H (2013) Dithiolopyrrolone natural products: Isolation, synthesis and biosynthesis. Mar Drugs 11: 3970–3997.
117. Li B, Wever WJ, Walsh CT, Bowers AA (2014) Dithiolopyrrolones: Biosynthesis, synthesis and activity of a unique class of disulfide containing antibiotics. Nat Prod Rep 31: 905–923.

118. Houard J, Aumelas A, Noël T, Pages S, Givaudan A, Fitton-Ouhabi V, Villain-Guillot P, Gaultieri M (2013) Cabanillasin, a new antifungal metabolite, produced by entomopathogenic *Xenorhabdus cabanillasii* JM26. J Antibiot 66: 617–620.
119. Masschelein J, Jenner M, Challis GL (2017) Antibiotics from Gram-negative bacteria: A comprehensive overview and selected biosynthetic highlights. Nat Prod Rep 34: 712–783.
120. Crawford JM, Portmann C, Zhang X, Roeffaers MBJ, Clardy J (2012) Small molecule perimeter defense in entomopathogenic bacteria. Proc Natl Acad Sci USA 109: 10821–10826.
121. Ji D, Yi Y, Kang GH, Choi Y-H, Kim P, Baek N-I, Kim Y (2004) Identification of an antibacterial compound, benzylideneacetone, from *Xenorhabdus nematophila* against major plant-pathogenic bacteria. FEMS Microbiol Lett 239: 241–248.
122. Xiao Y, Meng F, Qiu D, Yang X (2012) Two novel antimicrobial peptides purified from the symbiotic bacteria *Xenorhabdus budapestensis* NMC-10. Peptides35: 253–60.

STELLENBOSCH UNIVERSITY

Chapter 3

Profiling the production of antimicrobial secondary metabolites by *Xenorhabdus khoisanae* J194 under different culturing conditions

Booysen E, Rautenbach M, Stander MA, Dicks LMT. (2021) Profiling the production of antimicrobial secondary metabolites by *Xenorhabdus khoisanae* J194 under different culturing conditions. *Front Chem* 9, 1–15

Profiling the production of antimicrobial secondary metabolites by *Xenorhabdus khoisanae* J194 under different culturing conditions

Elzaan Booysen[1], Marina Rautenbach[2], Marietjie A Stander[2,3], Leon MT Dicks[1]*.

[1]Department of Microbiology, [2]Department of Biochemistry, [3]LCMS Central Analytical Facility, Stellenbosch University, Stellenbosch, South Africa

ABSTRACT

Species from the genus *Xenorhabdus,* endosymbiotic bacteria of *Steinernema* nematodes, produce several antibacterial and antifungal compounds, some of which are anti-parasitic. In this study, we report on the effect growth conditions have on the production of antimicrobial compounds produced by *Xenorhabdus khoisanae* J194. The strain was cultured in aerated and non-aerated broth, respectively, and on solid media. Production of antimicrobial compounds was detected after 24 h of growth in liquid media, with highest levels recorded after 96 h. Highest antimicrobial activity (350 mm^2/mg) was obtained from cells cultured on solid media. By using ultraperformance liquid chromatography linked to mass spectrometry (UPLC-MS) and HPLC, a plethora of known *Xenorhabdus* compounds were identified. These compounds are the PAX lipopeptides (PAX 1', PAX 3', PAX 5 and PAX 7E), xenocoumacins and xenoamicins. Differences observed in the MS-MS fractionation patterns collected in this study, when compared to previous studies indicated that this strain produces novel xenoamicins. Three novel antimicrobial compounds, khoicin, xenopep and rhabdin, were identified and structurally characterised based on MS-MS fractionation patterns, amino acid analysis and whole genome analysis. The various compounds produced under the three different conditions indicates that the secondary metabolism of *X. khoisanae* J194 may be regulated by oxygen, water activity or both. Based on these findings *X. khoisanae* J194 produce a variety of antimicrobial compounds that may have application in disease control.

Keywords: *Xenorhabdus khoisanae,* secondary metabolites, antimicrobial peptides, UPLC-MS, culture conditions

INTRODUCTION

Careless and frequent use of antibiotics have led to an increase in resistance (D'Costa et al., 2011; Fair and Tor, 2014; Ventola, 2015). With only a handful novel classes of antibiotics approved during the last three decades (Spellberg et al., 2008), many researchers are of the opinion that we have entered a post-antibiotic era (Lee Ventola, 2015). Novel antimicrobial compounds with modes of activity different to traditional antibiotics may be the answer. This is, however, a challenge, as many newly discovered antimicrobial compounds do not pass stringent safety tests, or production costs are too high.

Approval of daptomycin, an antimicrobial lipopeptide from *Streptomyces roseosporus*, by the Food and Drug Administration (FDA) in 2003(Arbeit et al., 2004) and the re-approval of polymyxin B, produced by *Bacillus polymyxa* (Zavascki et al., 2007), led to renewed interest in antimicrobial peptides. Most bacteria produce antimicrobial compounds, either for survival, or as a defence mechanism. Many of these compounds target cellular structures such as cell walls and membranes, pathways involved in energy (ATP)-production, or protein- and, nucleic acid synthesis (Kaufman, 2011).

Bacteria living in symbiosis with soil dwelling nematodes produce several antimicrobial compounds. *Xenorhabdus*, a member of the family Enterobacteriaceae, is closely associated with *Steinernema* entomopathogenic nematodes that infect the larvae of *Galleria mellonella* Linnaeus (Dunphy and Webster, 1991). A single, or at the most only a few strains, of a *Xenorhabdus* sp. develops a symbiotic relationship with the nematode and keeps the host free from other bacteria. This suggests that the invading strain(s) produce either a single broad spectrum antimicrobial compound, or several compounds. As soon as the nematode invades the insect, *Xenorhabdus* elicits the production of a plethora of secondary metabolites, including antimicrobial peptides, polyketides, proteases and hydrolytic exo-enzymes (Dreyer et al., 2018). In the case of *Xenorhabdus budapestensis*, production of the immune suppressor prophenoloxidase leads to an increase in quinones, killing the insect host (Yang et al., 2012).

A total of 23 antimicrobial compounds produced by *Xenorhabdus* spp. have been described, of which the majority have bactericidal and fungicidal activity (reviewed by Dreyer et al., 2019). These include xenocoumacins (Park et al., 2009; Reimer et al., 2009), bicornitun (Böszörményi et al., 2009), PAX peptides (Gualtieri et al., 2009; Dreyer et al., 2019), xenorhabdins (McInerney et al., 1991a, b), xenorxides (Webster et al., 1996) and benzylideneacetone (Ji et al., 2004). A few antimicrobial compounds are also insecticidal and anti-parasitic (Ji et al., 2004; Crawford et al., 2011, 2012; Zhou et al., 2013; Grundmann et al., 2013; Fuchs et al., 2014; Kronenwerth et al., 2014; Proschak et al., 2014; Reimer et al., 2014;

Laurent et al., 2017; Hacker et al., 2018). Also refer to review by Booysen and Dicks (2020) that focusses on the potential of *Xenorhabdus* for antibiotic production.

Xenocoumacins are one of the major antimicrobial compounds produced by *Xenorhabdus* spp. and was first described by McInerney et al. (1991a, b). These compounds are known as benzopyran-1-one derivates encoded by the *xcnA-N* gene cassette on the genome of *Xenorhabdus nematophilia* (Park et al., 2009). A total of six xenocoumacins were identified, although xenocoumacins I and II are the two mainly expressed by the *xcnA-N* gene cassette (Reimer et al., 2009). Both xenocoumacins I and II show antimicrobial activity, although xenocoumacin I is more active and kills bacteria and fungi (McInerney et al., 1991b).

Bicornitun is an arginine-rich non-ribosomal antifungal peptide produced by *X. budapestensis,* first described by Böszörményi et al. Four different bicornitun compounds have been described, i.e. bicornitun A1, A2, B and C. Lysine-rich cyclic lipopeptides, the PAX peptides, were first reported by Gualtieri et al. An additional eight PAX peptides were later described by Fuchs et al. (2011). Genes encoding the PAX peptides are located in the *paxABC* gene cassette (Fuchs et al., 2011). PAX 5 is active against *Pseudomonas aeruginosa* and *Escherichia coli,* while PAX 3, PAX 4 and PAX 5 are active against *Streptococcus epidermidis.* All PAX peptides are active against *Fusarium oxysprum.*(Gualtieri et al., 2009) No cytotoxic activity was recorded against Chinese Hamster Ovary cells (Gualtieri et al., 2009).

Xenorhabdins and xenorxides are dithiolopyrrolones derivatives, first described by McInerney et al. (1991 a, b) and Webster et al. (1996), respectively. These compounds are known for their wide-spread antibacterial, antifungal and insecticidal activity (McInerney et al., 1991a, 1991b; Li et al., 2014). Benzylideneacetone, produced by *X. nematophilia,* is used as a flavouring additive in cigarettes, food products, detergents and cosmetics (Dreyer et al., 2018). Although this compound have been used in industry for decades, the antibacterial activity of benzylideneacetone was only discovered in 2004 (Ji et al., 2004). For a more in-depth review of *Xenorhabdus* compounds refer to (Dreyer et al., 2018)

Most of the *Xenorhabdus* antimicrobial compounds are produced by non-ribosomal peptide synthesis (NRPS) (Fuchs et al., 2011; Zhou et al., 2013; Kronenwerth et al., 2014; Hacker et al., 2018), or a combination of polyketide synthesis (PKS) and NRPS (NRPS/ PKS) (Qin et al., 2013; Fuchs et al., 2014; Guo et al., 2017). Although not that common, some antimicrobial peptides are also produced by ribosomal peptide synthesis (RPS) (Singh and Banerjee, 2008). Examples of antimicrobial compounds produced by NRPS are xenoamicins (Zhou et al., 2013), PAX peptides (Fuchs et al., 2011) and nematophin (Cai et al., 2017), while xenocoumacins and fabclavins are produced by NRPS/PK synthesis (Guo et al., 2017).

Xenocin (Singh and Banerjee, 2008) and xenorhabdicin (Thaler et al., 1995) are the only two RPS peptides described to date. For a more extensive review on antimicrobial compound synthesis by *Xenorhabdus* spp., the reader is referred to Booysen and Dicks (2020). *Xenorhabdus* peptides are usually synthesised by the non-ribosomal synthetases, hybrid non-ribosomal/polyketide synthetases or ribosomes and can include fatty acid or polyketide chains (Gualtieri et al., 2009; Reimer et al., 2011; Zhou et al., 2013), while non-peptide compounds like benyzlideacetone does not contain any amino groups (Dreyer et al., 2018).

Only a few reports have been published on growth conditions affecting the production of antimicrobial compounds, and only those produced by *X. nematophilia* and *Xenorhabdus bovienii*. These included the effect of pH (Wang et al., 2011b), incubation temperature (Chen et al., 1996; Wang et al., 2008a), agitation, aeration (Wang et al., 2008a) and nutrients(Chen et al., 1996; Wang et al., 2008b, 2011a; Crawford et al., 2010). In this study, we report on secondary metabolites and antimicrobial compounds produced by *X. khoisanae* J194, a bacterium indigenous to South Africa identified by Ferreira et al. in 2013,and the production of these compounds when cells were cultured in aerated broth, non-aerated broth, and on the surface of solid media.

RESULTS

Influence of culturing and extract procedure on antimicrobial activity

Various studies have shown that culturing conditions have an effect on bacterial metabolism and production of secondary metabolites. This study showed that the pH of non-aerated cultures (method A) increased from 6.0 to 8.5 over 96 h, while the pH of cells grown under aerated conditions (method B) decreased from 6.0 to 5.5 over the same period (**Figure 1**). Compared to the aerated cultures (method B) a rapid increase in OD (biomass) was observed for the non-aerated cultures (method A) of strain J194 (**Figure 1**). Cells of J194 cultured under oxygen-limiting conditions always produced a yellow pigment, that was not observed to the same extent when J194 was cultured under oxygen rich conditions.

During 96 h of growth under non-aerated conditions, 4196 mg freeze-dried material was collected from CFSs. Of this, 2863 mg was from the oily bottom fraction (NAO, oily fraction from a non-aerated broth culture) and the rest from the acetonitrile upper fraction (NAA, acetonitrile fraction of a non-aerated broth culture). Over the same period, 1010 mg freeze-dried material was isolated from the CFSs of aerated cultures (AB, fraction from an aerated culture). Cells grown on the surface of TSA plates produced 5504 mg of hydrophobic/amphipathic material (SM, extract from a culture grown on the surface of solid

media). Less than 100 mg of intracellular material was extracted from aerated and non-aerated cultures.

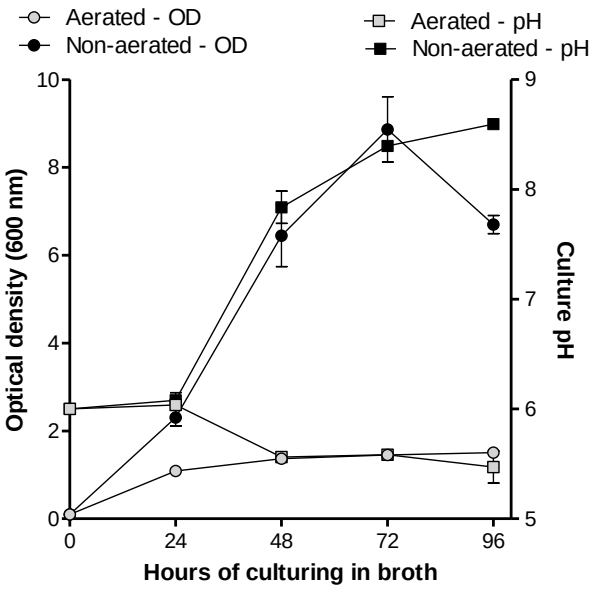

FIGURE 1. Changes in growth (optical density) and culture pH of *X. khoisanae* J194 under non-aerated (method A) and aerated (method B) culturing in broth over 4 days. Data depicts the mean of the three independent cultures. Error bars show standard deviation.

The antimicrobial activity of material collected from the CFSs of non-aerated and aerated cultures, and from surface-grown cells after treatment with XAD beads, varied considerably. After 24 h of incubation, antimicrobial activity was recorded in CFSs collected from non-aerated cultures and cultures grown on the surface of TSA (**Figure 2**). However, after 48 h of incubation in liquid media, all samples, except for the biomass extract, inhibited the growth of *Staphylococcus aureus* ATCC 25923, *Listeria monocytogenes* EDGe, *Escherichia coli* Xen 14 and *Pseudomonas aeruginosa* ATCC 27853. Highest levels of activity were recorded after 96 h of incubation in non-aerated broth and on the agar surface (**Figure 2**). NAA material collected using method A showed highest activity against *E. coli* Xen 14, while AB material collected using method B and hydrophobic material collected using method C showed the highest activity against *P. aeruginosa* ATCC 27853 (**Table 1**). Overall, hydrophobic compounds isolated with method C (SM fractions) displayed the highest specific activity against *P. aeruginosa* ATCC 27853 (350 mm^2/mg), *E. coli* Xen 14 (263 mm^2/mg), *S. aureus* Xen 31 (275 mm^2/mg) and *L. monocytogenes* EDGe (263 mm^2/mg) (**Table 1**). NAA material collected from

of non-aerated cultures were not active against *S. aureus* ATCC 25923, *S. aureus* Xen 31 and *Streptococcus epidermidis* SE1 (**Table 1**).

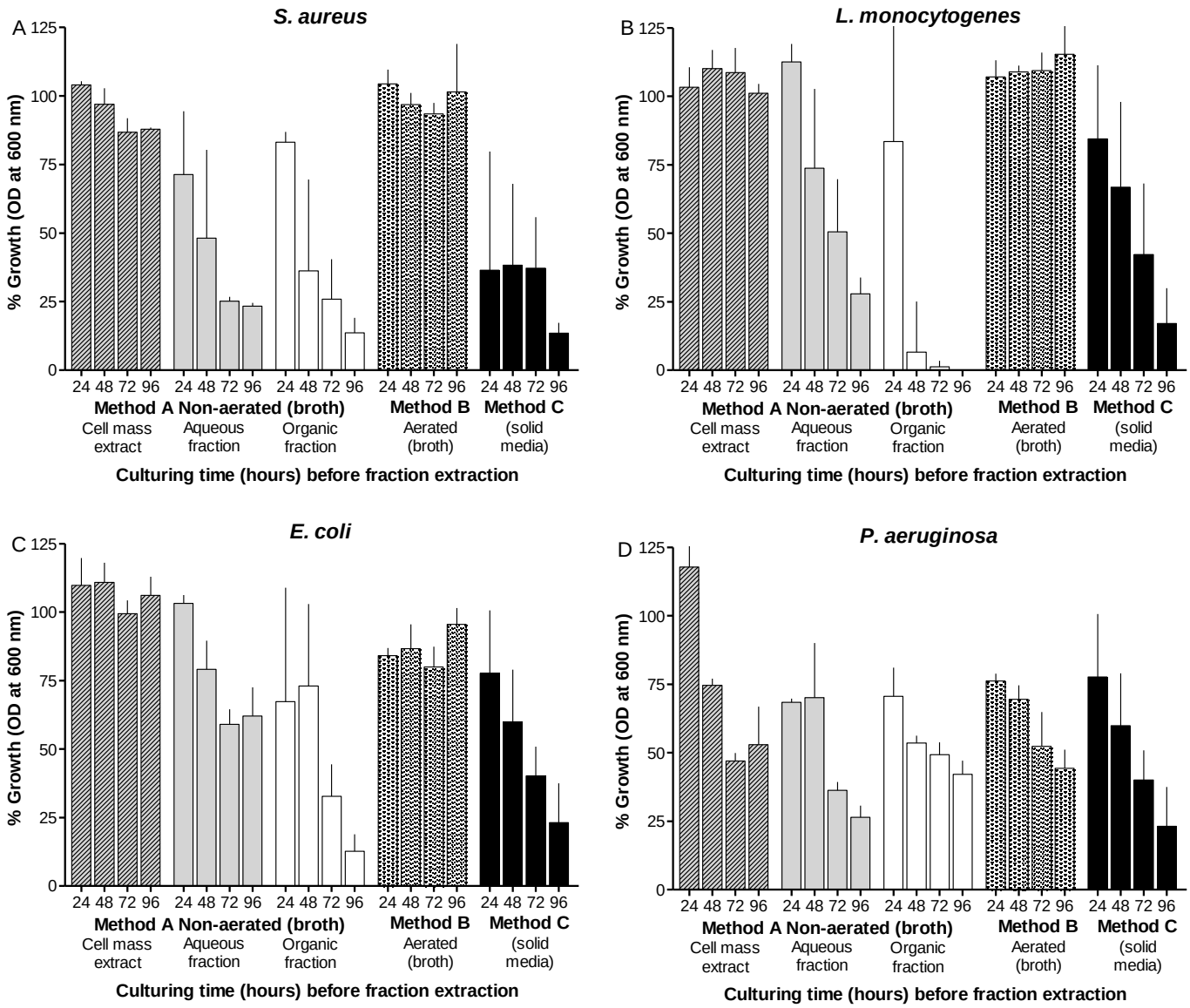

FIGURE 2. Growth inhibition (%) of different target bacteria as observed by changes in OD at 595 nm, compared to control cultures, after exposure to the five different *X. khoisanae* J194 culture extracts. The response (OD at 595 nm) of the selected target bacteria *S. aureus* ATCC 25923, *L. monocytogenes* EDGe, *E. coli* Xen 14 and *P. aeruginosa* ATCC 27853, are shown after 24 h exposure to extracts and incubation at 37 °C. Three cultures of each target organism were treated with cell-free supernatants (CFS) of *X. khoisanae* J194 cultured in non-aerated broth, aerated broth and on the surface of solid media, respectively. CFSs of non-aerated culture were separated into the acetonitrile (NAA) and organic fractions (NAO) . The hours indicated in the graphs refer to the time at which CFSs were collected and freeze-dried.

TABLE 1. Antibacterial activity of extracts collected from *Xenorhabdus* cultures grown under different conditions. Activity is indicated by clear zone area (mm^2/mg) in the agar well diffusion assay

Bacterial target	Non-aerated, acetonitrile phase extract (NAA)	Non-aerated, oily phase extract (NAO)	Aerated broth extract (AB)	Solid media extract (SM)
P. aeruginosa ATCC 27853	100	175	300	350
E. coli Xen 14	175	150	150	263
S. aureus ATCC 25923	0	100	163	113
S. aureus Xen 31	0	138	250	275
S. epidermidis SE1	0	163	175	150
L. monocytogenes EDGe	63	113	213	263

UPLC-MS fingerprinting of culture extracts

By performing UPLC-MS, we characterised the compounds from the antibiotic/antimicrobial complex based on elution from the C_{18} matrix, signal intensity and accurate Mr. The compounds were grouped into early eluting compounds (0 to 6 min), representing polar/hydrophilic and amphipathic compounds (**Figure 3**) and the mid- to late gradient eluting compounds (6 to 17 min), representing amphipathic and hydrophobic compounds (**Figure 4**).

A complex mixture of 44 novel metabolites were selected on the grounds of ion intensity and confirmation of an elution peak in the UPLC-MS analysis (**Table 2, Figures 3 and 4, supplementary data Figures S1-S5**). From these analyses we generated a heatmap (**Table 2**) to fingerprint and compare the culture conditions and extract fraction. From the fingerprinting we observed that the more polar and amphipathic compounds (Rt 0-6 minutes) were found in the broth culture extracts (NAA, NAO and AB) (**Figure 3, Table 2**). The more amphipathic and hydrophobic compounds eluting from 7-16 minutes were observed primarily in the sold media extract (SM) with some in the oily fraction of the non-aerated broth culture extract (NAO) (**Figure 4, Table 2**)

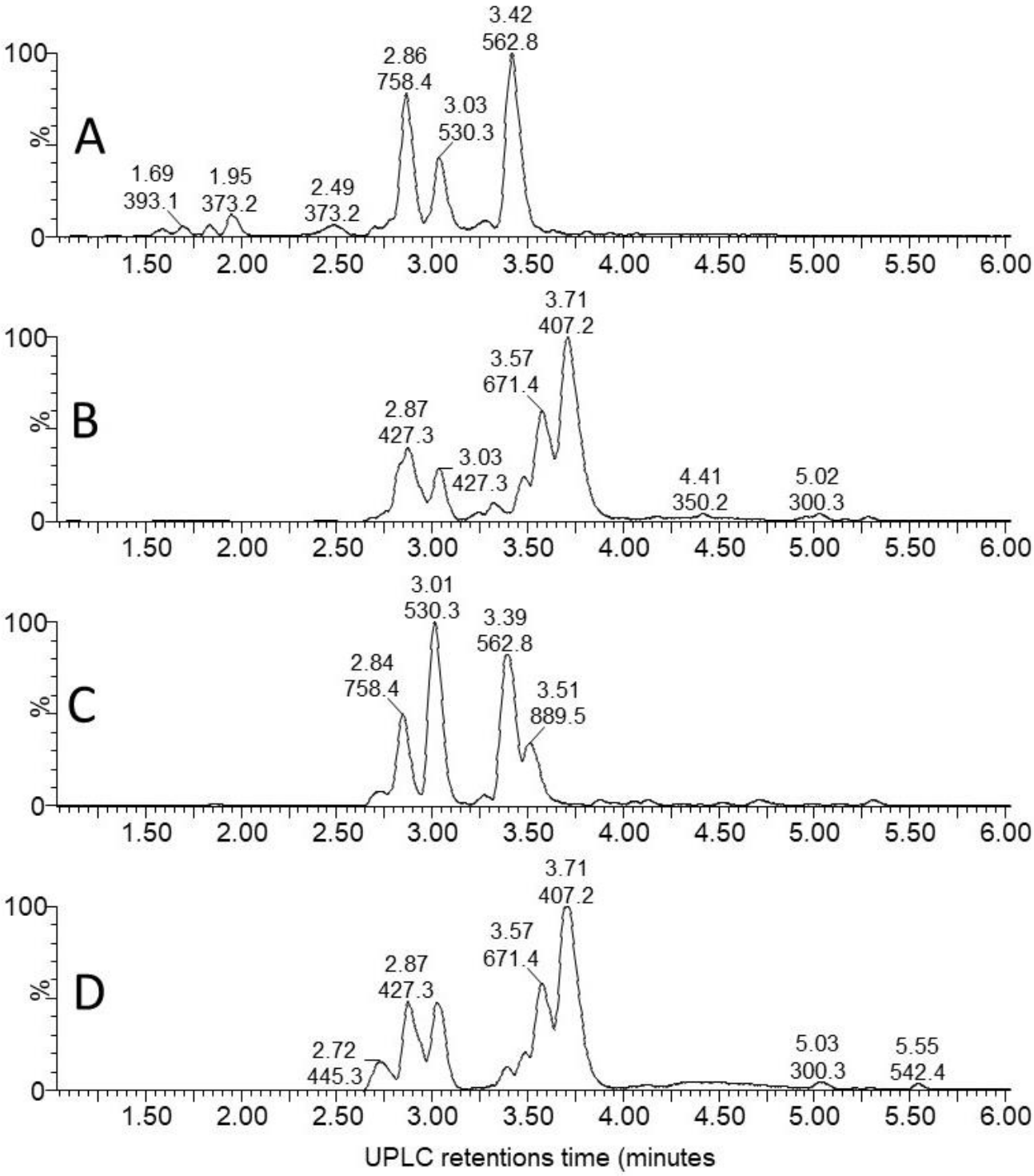

FIGURE 3. UPLC-MS of the early eluting components (0 to 6 min) from the four *X. khoisanae* J194 extracts that showed antibacterial activity: (A) aqueous fraction of non-aerated broth culture, (B) NAO fraction of non-aerated broth culture, (C) fraction from aerated broth culture and (D) extract from culture grown on surface of solid medium. The masses in the spectra are protonated masses of the most prominent detected compounds.

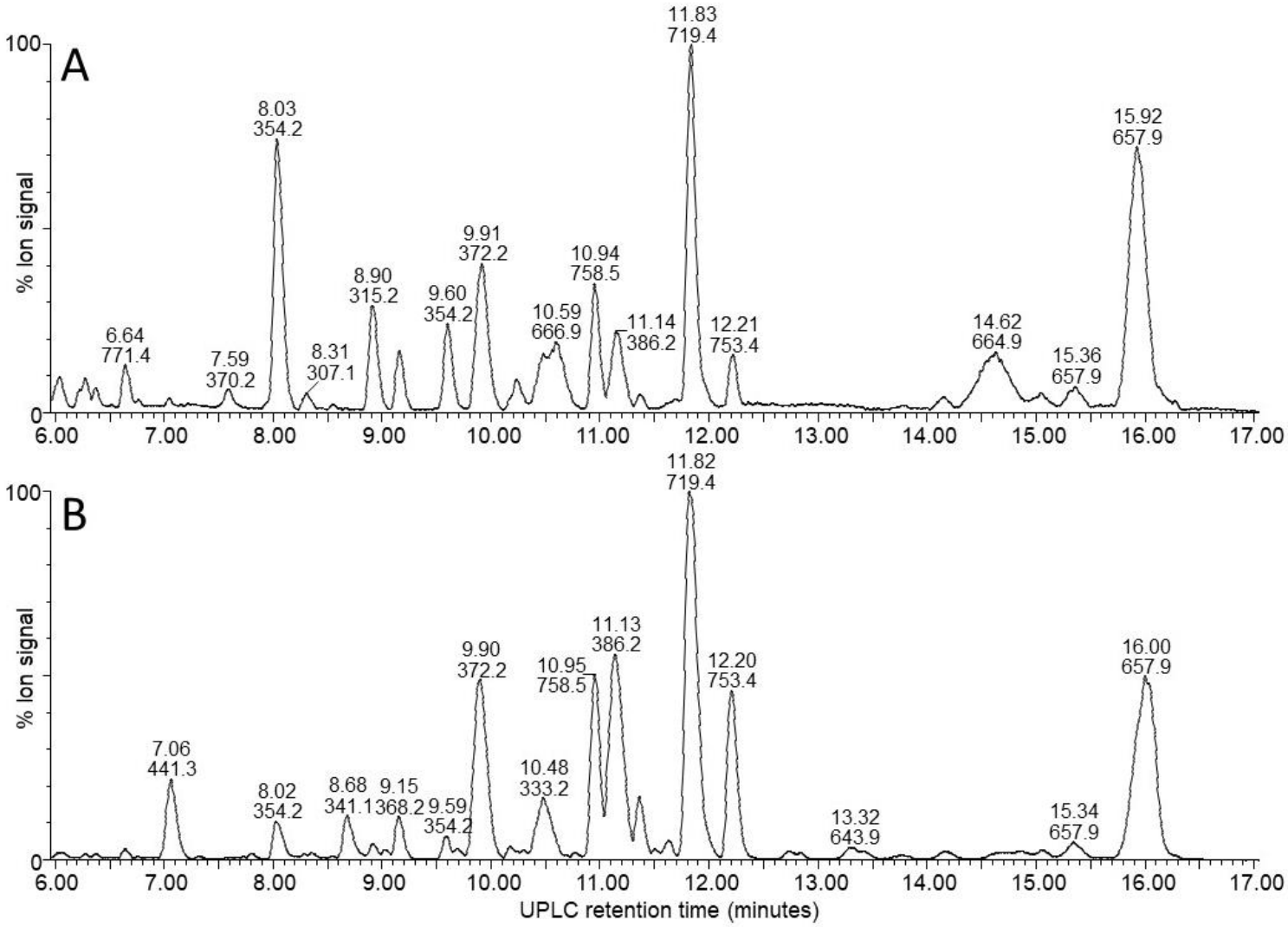

FIGURE 4. UPLC-MS of the mid-gradient eluting components (6 to 17 min) from the four *X. khoisanae* J194 extracts that showed antibacterial activity: (A) NAO fraction of nonaerated culture in broth, (B) extract from culture grown on surface of solid media. The masses in the spectra are protonated masses of the most prominent detected compounds.

Over the first 6 minutes a diverse number of compounds were identified in the UPLC analysis of which 19 were selected for fingerprinting (**Figure 3, Figure S1 and Table 2**). Similar polar compounds were found in NAO and SM extracts, while the profiles of NAA and AB correlated (**Figure 3, Figures S1 and S2**), with latter possibly due to the aqueous nature of the extract and culture media. The heatmap in table 2 indicated the differences between the extracts. Notably the compounds observed with high ion intensity, 8 (*m/z* = 427.3), 16 (*m/z* = 889.5), 17 (*m/z* = 671.4), 18 (*m/z* = 407.2) were primarily found in the NAO and SM extracts. Only compounds 15 (*m/z* = 1124.6) is observed primarily in the more aqueous extracts, AB

and NAA. We were able to purify compounds 8, 17, 15 and 18 for further study (refer to discussion below).

In the mid-gradient to late gradient (6-17 minutes) a plethora of small compounds are observed for the SM and less so for the NOA fraction (**Table 2, Figure 4, supplementary data Figures S3, S4**). None of the compounds show a particularly high intensity in comparison with those eluting from 1-6 minutes of after 13 minutes.

The hydrophobic compounds (34-44) eluting after 13 minutes were all about 1.3 kDa with 14, 16 and 22 Da differences (**Table 2**), which indicated the possibly of a related peptide complex. We identified three compounds, 39 (*m/z* = 1328.9) and 42 (*m/z* = 1314.8) with 44 (*m/z* = 1336.8) the Na-adduct of 42 for purification and further analysis. Refer to discussion below.

TABLE 2. Heatmap of UPLC-MS fingerprinting of secondary metabolite profiles in the extracts of the three different *Xenorhabdus* cultures (refer to Figs. 3 and 4). The ions were selected from the top 50 most abundant ions after confirmation in the UPLC-MS profile.

Compound Number	Rt (min)	Culture extract				Monoisotopic M_r of major cations (1+) in UPLC run
		NAA	NAO	AB	SM	
1	2.74	1	1	98	0	479.298
2	2.75	49	16	32	4	652.401
3	2.77	4	30	8	59	445.313
4	2.81	37	24	38	2	751.367
5	2.84	45	21	32	2	758.407
6	2.85	29	34	30	7	558.330
7	2.89	17	44	27	11	627.349
8	2.92	8	53	12	26	**427.302**
9	2.98	1	0	99	0	474.342
10	2.98	17	25	36	23	473.275
11	3.01	33	24	32	12	1100.576
12	3.02	30	9	59	3	530.297
13	3.02	54	27	18	1	1025.567
14	3.16	91	7	2	0	1078.806*
15	3.40	48	4	43	4	**1124.634**
16	3.50	9	29	49	13	**889.481**
17	3.59	5	60	7	28	**671.413**
18	3.75	2	68	0	29	**407.217***
19	4.42	4	39	7	50	434.265

Table 2 continued

20	7.05	3	2	10	86	881.543
21	8.02, 9.59	3	46	1	50	354.220
22	8.93	4	12	5	80	758.455
23	9.90	3	28	4	66	394.211
24	9.90	1	14	2	83	372.229
25	10.47	5	28	4	62	355.198
26	10.49	1	18	1	80	333.217
27	11.14	1	7	2	90	386.244
28	11.35	2	5	4	89	792.416
29	11.82	1	17	4	77	719.432
30	11.83	2	1	11	87	1437.882
31	11.85	5	28	12	56	741.431
32	11.90	3	13	2	83	347.235
33	12.20	2	7	2	89	753.433
34	13.33	0	7	9	84	1286.809
35	13.7, 14.2, 14.7	0	24	0	76	1322.803
36	13.8, 14.2, 14.8	0	15	1	84	1300.823
37	14.63	0	0	4	96	1330.840
38	14.74	0	78	0	22	1350.832
39	14.86	0	66	2	32	1328.853
40	14.89	0	7	1	92	1312.822
41	15.97	0	16	1	83	1331.860
42	15.97	0	17	1	82	**1314.838**
43	15.97	0	23	7	70	1352.794
44	15.99	0	32	1	67	**1336.817**

The numbers within blocks indicate the relative signal in the ESMS detection of the different compounds (total sample signal was normalised and then the relative signal for each ion was calculated). The *m/z* values in bold indicated most abundant ions, those underlined were purified further for more detailed structural analyses (refer to Figs. 5-8, supplementary data Figs. S1-4) and known compounds and detected metabolites (refer to Table 3, Fig. 5) are indicated with an * and #, respectively.

Identification of known compounds

AntiSMASH identified 17 known biosynthetic gene clusters, of which eight were native to *Xenorhabdus* spp. (**Figure 5**). This presence of the xenocoumacin, xenoamicin and PAX peptide biosynthetic gene clusters led us to search for these compounds in the extracts

Closer inspection of the compounds eluting from 1-6 minutes revealed compound 8 (*m/z* = 1078.8) as PAX 7E in the NAA extract. We also found PAX1', PAX3' and PAX5 at lower levels in this extract **(Figure 6B)**. The production of the PAX peptides in this *Xenorhabdus* strain was much lower than that found by Dreyer *et al.* (2019), and we were unable to purify any member of this family further. However, accurate mass analysis and the PAX biosynthetic gene cluster in this strain's genome supported our identification (**Table 3**).

Compound 18 (*m/z* = 407.2) that eluted early at 3.71 min was observed in the NAO and SM fractions (**Table 2**). The compound displays a distinct yellow colour and was purified and subsequently identified as xenocoumacin II (**Figure 5, Table 3, supplementary data Figure S6**).

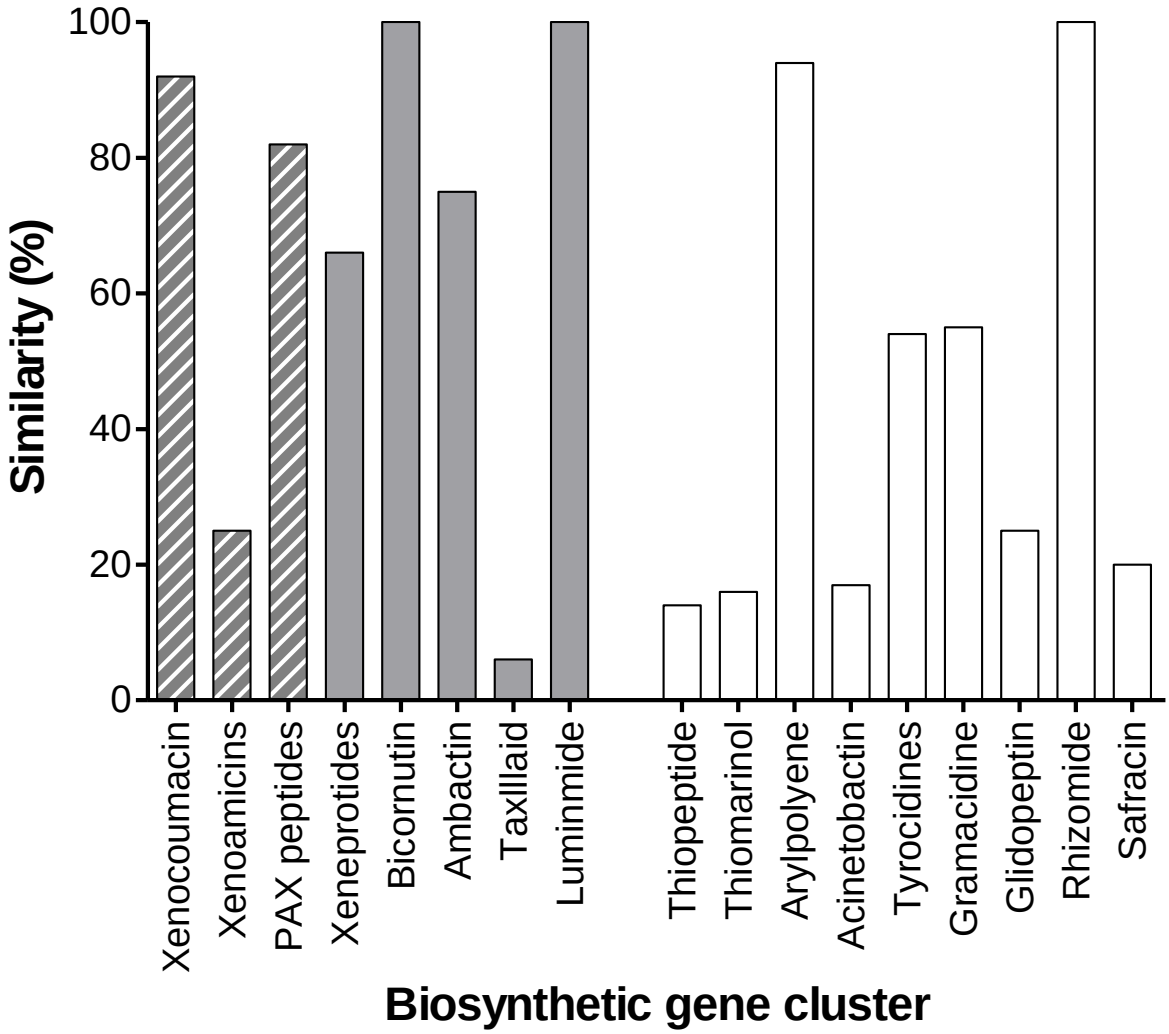

FIGURE 5. Graph depicting the various operons identified in the whole genome of *X. khoisanae* J194 by the antiSMASH algorithms. The * indicates operons native to *Xenorhabdus* bacteria. Operons for xeneprotides, bicornutin, ambactin, taxlllaid and luminmide were also detected by antiSMASH, but was not identified in the crude extracts.

TABLE 3. Summary of previously identified secondary metabolites in the extracts othe three different *Xenorhabdus* cultures using high resolution UPLC-MS and MS analysis, as well as genetic analysis to confirm group identity. Refer to Table 2, Figs. 2-4 for UPLC-MS and Figs 5, S1 and S2 (supplementary data) for high resolution MS analyses and structures.

Nr	Experimental M_r		Proposed Identity	Theoretical M_r		Mass error (ppm)	Comment/ Reference
	Protonated	Sodiated		Protonated	Sodiated		
-	1050.7719	-	PAX5	1050.7766	-	4	Low concentration (Fuchs et al. 2011)
-	1052.7937	-	PAX1'	1052.7923	-	-1	Low concentration (Fuchs et al. 2011)
-	1066.8075	-	PAX3'	1066.8079	-	0.4	Low concentration (Fuchs et al. 2011)
8	1078.8058	-	PAX7E	1078.8079	-	2	Low concentration, (Dreyer et al., 2019)
18	407.2171	-	Xenocoumacin II	407.2182	-	3	(Reimer et al., 2011) (Dreyer et al., 2019)
34	1286.8077	1308.7849	Xenoamicin D1	1286.8077	1308.7901	0, 4	Novel Xenoamicin? (Zhou et al., 2013, this study)
35, 36	1300.8235	1322.8052	Xenoamicin A1,2,3	1300.8238	1322.8058	0.2, 0.5	Novel Xenoamicins? (Zhou et al., 2013, this study)
37	1330.8326	-	Xenoamicin B2 +OH	1330.8344	-	1	Novel Xenoamicin
38, 39	1328.8552	1350.8311	Xenoamicin B1 (V→I/L)	1328.8552	1350.8371	0, 4	Novel Xenoamicin (Zhou et al., 2013, this study)
42, 44	1314.8390	1336.8177	Xenoamicin B2 (I→V, I/L→V)	1314.8395	1336.8215	0.4, 3	Novel Xenoamicin (Zhou et al., 2013, this study)

With the analysis of the late eluting compounds, we noted a compound range around 1.3 kDa that may be part of a peptide complex. As the xenoamicin biosynthetic gene cluster were found in this strain's genome (**Figure 5**) this family was considered as possible candidate compounds. These peptide complexes were primarily identified in the SM fraction, although some of the members were also observed in the NAO fraction. We were able to co-purify compound 42 (*m/z* = 1314.8) and compound 38 (*m/z* = 1328.8) (**Table 2, supplementary data Figure S7**) and confirmed that both are members of the xenoamicin family (**Table 3, Figure 6 and supplementary data Figure S7**). However, the MS-MS structural analysis of compounds 38 and 42 showed a number of different fragments to that of xenoamicin G and B/C, respectively. Compound 38 shares the b1-b5 fragments with Xenoamicin B and X (Zhou

et al., 2013) but differs by +14 dalton in the observed y fragments. This indicated either a -CH_2CH_3 group in R_4(Val→Ile) or iso/secondary butyl group in R_5 (Val→Ile/Leu) (**Figure 6, supplementary data Figure S7**). Compound 38 was labelled as xenoamicin $B2^{V→I/L}$. Compound 42 shares the b1-b4 fragments with Xenoamicin B and C (Zhou et al., 2013) but differs by -14 dalton in b5 indicating a -CH_3 group in R_3(Ile→Val). Compound 42 also differed in the y'8 fragment by +14 dalton. Similar to compound 40. This indicated either a -CH_2CH_3 group in R_4 (Val→Ile) or iso/secondary butyl group in R_5 (Val→Ile/Leu) (**Figure 6, supplementary data Figure S7**). Compound 42 was labelled as xenoamicin $B3^{I→V,\ I/L→V}$. Compound 37 (*m/z* = 1330.8), was also further characterised. This compound was labelled as a xenoamicin $B1^{+OH,\ x}$ after its fragmentation pattern was compared with that of compound 42 (**Table 3, Supplementary data, Figure S8**). The MS-MS analysis indicated that the terminal group was hydroxylated while R_3 group or residue was different from that of 42 and other reported xenoamicins. A number of other xenoamicins were also found in this peptide complex. Compound 34 with an identical Mr to xenoamicin D was denoted xenoamicin D1. Compound 35 and its sodium adduct (36) had three elution peaks (**Table 2**) indicating 3 different compounds with all three having an identical mass to xenoamicin A (Zhou et al., 2013) and was denoted xenoamicin A1,2,3 (**Table 3**). Three more compounds may be part of this complex, 40 (*m/z* = 1312.8), 41 (*m/z* = 1331.7) and 43 (*m/z* = 1352.8). This xenoamicin complex contains novel analogues that warrants future exploration.

Novel antimicrobial compounds

The observed antibacterial activity of SM, NAA and NAO could be due to the PAX peptides and/or xenocoumacin II. However, other novel compounds could also contribute to this observed antibacterial activity. Furthermore, no known compounds with antibacterial activity were identified in the AB fraction, which could indicate that this fraction contains novel antimicrobial components. Twenty-one possible NRP synthetase operons were identified after utilising the tblastn function of the NCBI website. This was further narrowed down to two putative operons by searching for the core motifs of the catalytic domains of the NRP synthetases. From this result we then predicted that at least two small non-ribosomally synthesised antimicrobial peptides or peptide analogues may be present in the extracts. Refer to the supplementary data (**Figure S9**) for the protein sequences of the two putative domains.

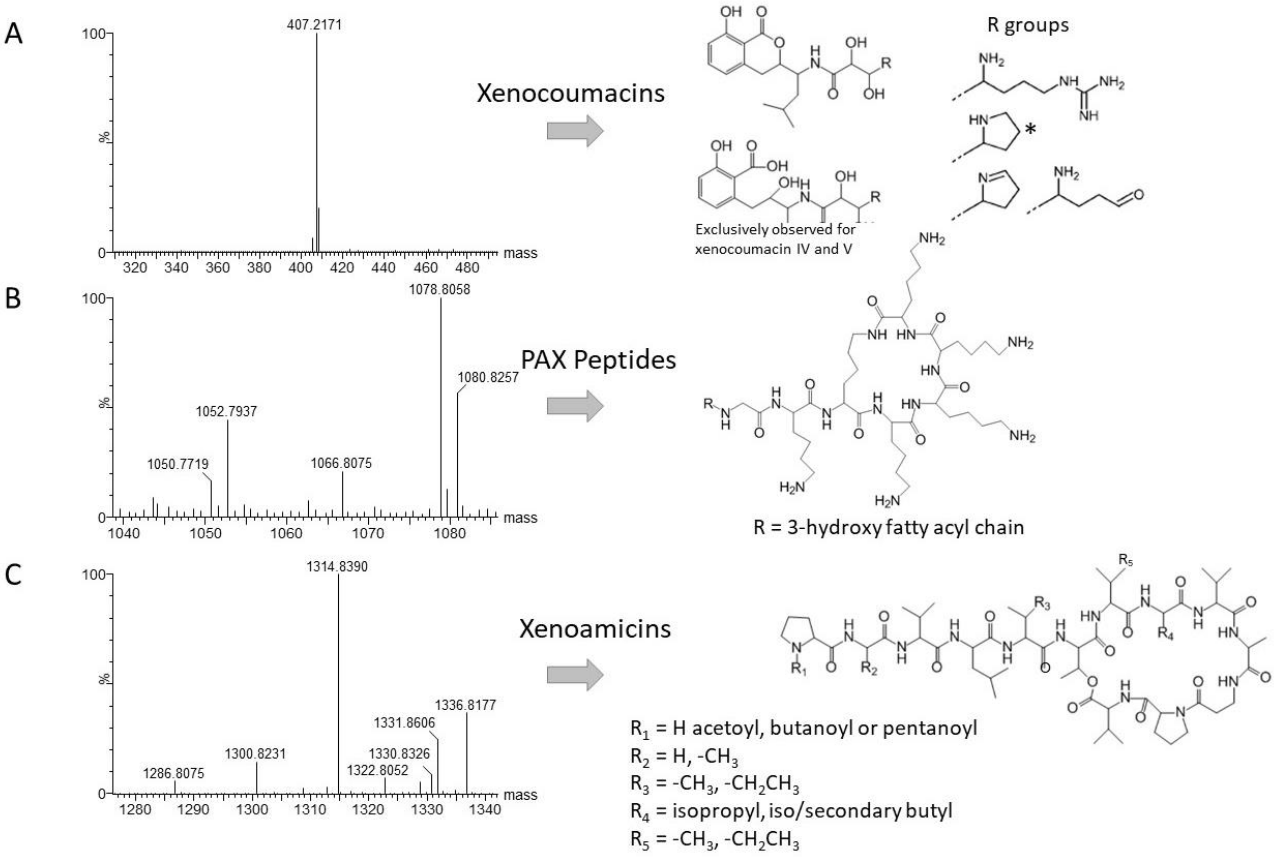

FIGURE 6. High resolution MS analysis and the structures of compounds in the three most prominent known families identified in J194 culture: (A) Xenocoumacin II, identified with a * (McInerney et al., 1991b; Reimer et al., 2009); (B) PAX peptides (Fuchs et al., 2011; Dreyer et al., 2019), and (C) xenoamicins (Zhou et al., 2013 and this study). Refer to supplementary data Figs. S6-S7 for more structure analyses details.

Three possible novel compounds and putative non-ribosomal antibacterial peptides namely compounds 8 (*m/z* = 427.3), 17 (*m/z* = 671.4) and 15 (*m/z* = 1124.6), were identified and purified from the various extracts (**Figures 7-9**). All three compounds were produced at appreciable amounts that assisted further purification to >80% purity (**Figures 7-9**). The antimicrobial activity of the three compounds were confirmed by screening the purified compounds against a library of bacterial targets (**Table 4)** Summary of previously identified secondary metabolites in the extracts of the three different *Xenorhabdus* cultures using high resolution UPLC-MS and MS analysis, as well as genetic analysis to confirm group identity. Refer to Table 2, Figs. 2-4 for UPLC-MS and Figs 5, S1 and S2 (supplementary data) for high resolution MS analyses and structures.

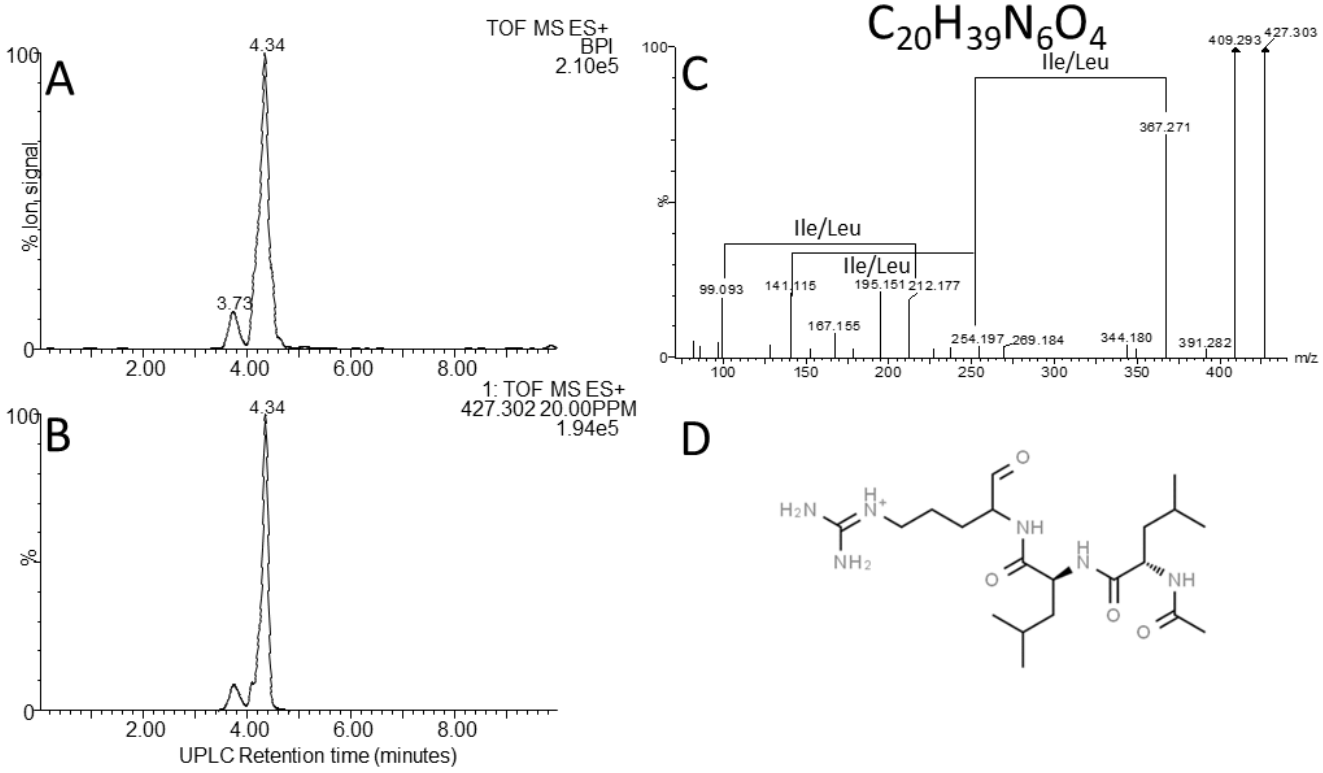

FIGURE 7. Structural analyses of compound **8** – khoicin. (A) UPLC-MS analysis of the purified compound and (B) the extracted *m/z* chromatogram of the khoicin ion with *m/z*= 427.302, (C) high resolution MS-MS spectrum of 427.302; (D) proposed working structure for khoicin.

Compound 8 – Khoicin

The first novel compound was named khoicin (8, *m/z* = 427.3) and exhibited a broad spectrum of potent Gram-positive and Gram-negative activity (**Table 4**). It is mainly produced in oxygen-limiting conditions and the highest amounts were extracted from a non-aerated broth culture (NAO) and a culture grown on solid media (SM). It was detected in the extracts in the following order: NAO>SM>AB>NAA (**Figures 3 B and D, Table 4**). We determined the accurate mass of khoicin and derived its most probable elemental composition as $C_{20}H_{39}N_6O_4$. The MS-MS structural analysis of khoicin revealed that it fragmented into two major fragments, namely a dehydration product as *m/z* = 409.3 and a fragment ion at *m/z* = 367.3 which could be the result of the loss of an acetyl (CH_2CO) group from the molecular ion (**Figure 7**). The rest of the fragment ions were at a much lower intensity. However, we could

identify, a fragment of 113.08 that indicated a Leu/Ile residue correlating with an immonium ion of Ile/Leu at *m/z* = 86.098. The fragments ions 254.197 and 227.101 could be mapped to an acetylated dipeptide containing Leu/ Ile, respectively. One of the minor fragments at *m/z* = 156.113 mapped to Arg, which could explain the early elution of this compound. These results further indicate the peptide nature of khoicin and considering the elemental composition khoicin could consist of a formylated Arg linked to an acetylated Leu/Ile dipeptide, with Mr 426.2949, correlating with the experimental Mr of 426.2956 (-2 ppm mass error) (**Figure 7**).

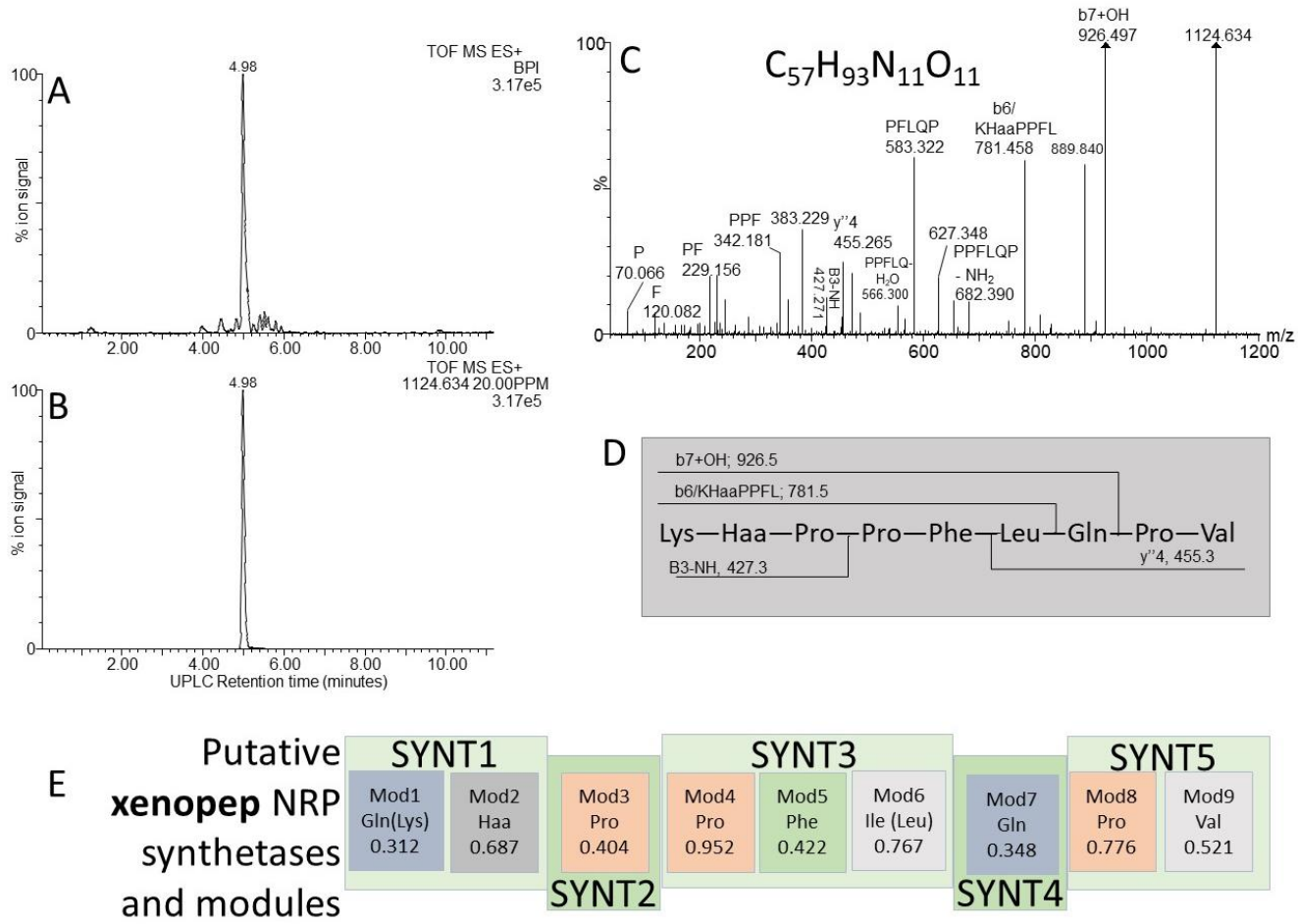

FIGURE 8. Structural analyses of compound **15** – xenopep. (A) UPLC-MS analysis of the purified compound and (B) the extracted *m/z* chromatogram of the xenopep ion with *m/z*= 1124.364; (C) high resolution MS-MS spectrum of 1124.364 annotated with putative ion identities; (D) proposed working structure for xenopep; (E) putative NRPS operon for xenopep with the predicted amino acids for each module (Mod) in the synthetase (SYNT) and probability score (the greater the number the lower the probability). The amino acids found with amino acid analysis and MS-MS are given in brackets.

Compound 15 – Xenopep

Compound 15, named, xenopep (*m/z* = 1124.6), was one of the early eluting peptide-like compounds primarily produced by aerated broth cultures (AB), suggesting that xenopep production could be oxygen dependent (**Table 2**). We were able to purify xenopep from AB cultures to >85% purity for further analysis (**Figures 8A, B**). Xenopep (16) is only active against Gram-positive bacteria (*S. aureus, S. epidermidis* and *L. monocytogenes*) and could thus be responsible for the inhibition of *S. epidermidis* and *L. monocytogenes* in AB and NAA extracts (**Table 1, 4**). The purified peptide was subjected to amino acid analysis which revealed the amino acid composition to contain Val, Leu, Lys, Glu, Phe and three Pro residues.

We considered the two NRP synthetase operons to assist with the structure determination of xenopep, the first putative operon is located within node 7 and consist out of five genes encoding for the nine amino acids, with a predicted sequence of Gln-Haa-Pro-Pro-Ile-Gln-Pro-Val (Haa = hydrophobic amino acid) (**Figure 8E**). The sequence partially correlated with the determined amino acid composition. A conservative replacement of Ile with Leu improved this correlation, but one of the Gln residues must be replaced with Lys for a better correlation. The high-resolution MS-MS sequencing did not reveal a classical b- and y''-ion pattern of a linear peptide acid but yielded a number of internal fragments (**Figure 8C**). Using the MS-MS analysis and predicted sequence from the xenopep putative operon, a working sequence was deduced as Lys-Haa-Pro-Pro-Leu-Gln-Pro-Val (**Figure 8D**), with Haa an undetermined hydrophobic residue.

Compound 17 – Rhabdin

Compound 17 (*m/z* = 671.4) was named rhabdin and its production was exclusive to the non-aerated broth (NAO) and SM (**Table 2**). This compound was purified to >80% (**Figure 9A, B**). Of the three early eluting peptide-like compounds, rhabdin is the second most active and inhibited the growth of *S. aureus, L. monocytogenes, K. pneumoniae, P. aeruginosa* and *E. coli* (**Table 4**).

Amino acid analysis conducted on rhabdin indicated the following amino acid composition: 2xPro, Val, Leu and Phe. This composition shares some similarities with xenopep. In the MS-MS structural analysis there was also significant correlation between the fragments observed for rhabdin and xenopep, with eight major fragments (*m/z* = 672.4, 383.2, 342.2, 245.1, 229.2,217.1,120.1 and 70.1) being identical (**Figures 8C, 9C)**. These fragments all map to the N-terminal part of xenopep. If the first three synthetases of the putative xenopep

operon is used for rhabdin synthesis it would suggest the sequence as Val-Haa-Pro-Pro-Leu-Phe. We confirmed the sequence with MS-MS analysis, in which the fragmentation yielded classical y''-ions suggesting a linear peptide acid (**Figures 8C and D**). Preliminary NMR and MS findings indicate that the Haa residue of both xenopep and rhabdin might be a modified aromatic residue with *M*r =99.07 (C_5H_5ON), but more in-depth NMR analysis is needed to confirm this.

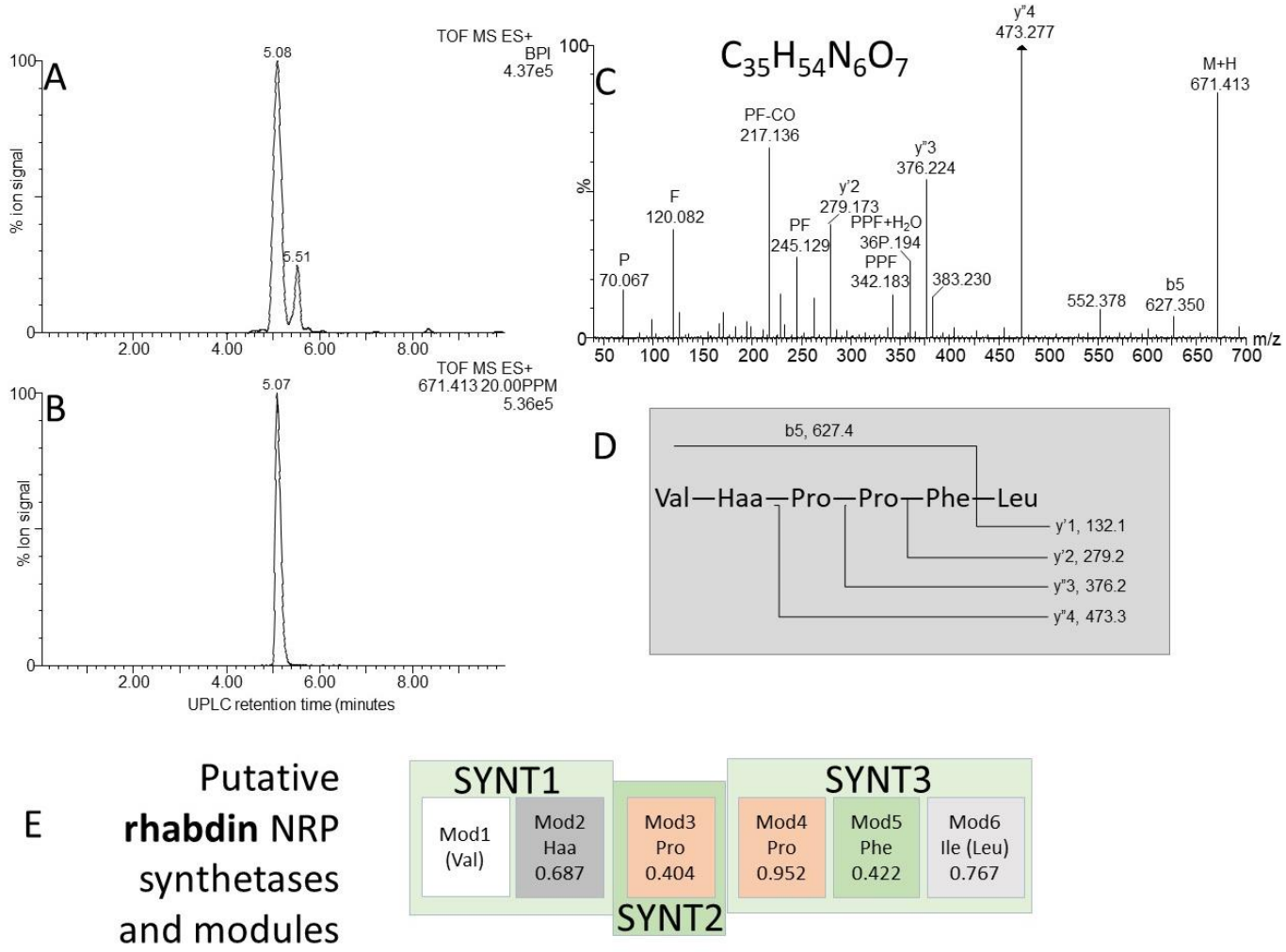

FIGURE 9. Structural analyses of compound **17** – rhabdin. (A) UPLC-MS analysis of the purified compound and (B) the extracted *m/z* chromatogram of the rhabdin ion with *m/z*= 671.413; (C) high resolution MS-MS spectrum of 671.413 annotated with putative ion identities; (D) proposed working structure for rhabdin; (E) putative NRPS operon for xenopep with the predicted amino acids for each module (Mod) in the synthetase (SYNT) and probability score (the greater the number the lower the probability). The amino acids found with amino acid analysis and MS-MS are given in brackets.

TABLE 4. Comparison of the antimicrobial activity spectrum of purified and partially purified novel compounds identified in the four *X. khoisanae* J194 extracts.

Compound number, proposed name	**Activity against Gram-positive strains***		**Activity against Gram-negative strains***	
8, Khoicin	*S. aureus* ATCC 25923 +++ *L. monocytogenes* +++ *S. epidermidis* +++ *B. subtilis* +	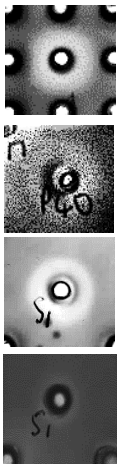	*E. coli* ++ *A. baumannii* +++ *K. pneumoniae* + *S. typhimurium* + *P. aeruginosa* ++	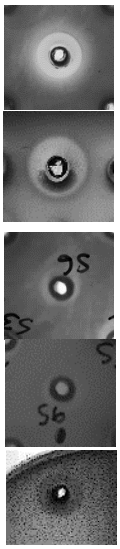
17, Rhabdin	*S. aureus* ATCC 25923 +++ *S. aureus* Xen 31 +++ *L. monocytogenes* +++	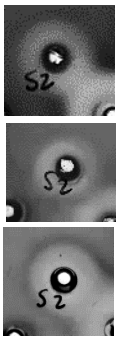	*K. pneumonia* + *P. aeruginosa* ++ *E. coli* +	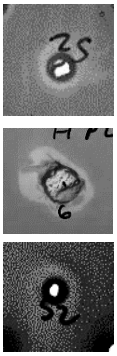
14, Xenopep	*S. aureus* ATCC 25923 + *L. monocytogenes* ++ *S. epidermidis* +++		*Inactive*	NA

*Activity +++ = very high, ++ = high, + = medium, if target cell of library tests (refer to methods) is not indicated, no activity was detected. The photos show the clear zones detected with the well diffusion assay with each of the respective target organisms.

DISCUSSION

Bacteria from the genus *Xenorhabdus* are well known for their ability to produce a wide range of antimicrobial compounds, active against Gram-positive and -negative bacteria. Here we report on the activity of *X. khoisanae* J194 extracts against *P. aeruginosa, E. coli, S. aureus, S. epidermidis* and *L. monocytogenes* under different culture conditions. A previous study on *X. khoisanae* SB10 (Dreyer et al., 2019) also reported activity against *Bacillus subtilis* subsp. *subtilis* and *Candida albicans*. This suggests that some strains of *X. khoisanae* produce a range of antimicrobial compounds active against bacteria, yeast and possible also mycelial fungi.

The *in situ* analysis of the whole genome of *X. khoisanae* J194 confirmed the identification of xenocoumacin II, PAX peptides and xenoamicins. The analysis also gave insight into the sequence of two potential novel peptides, rhabdin and xenopep, identified in this study. The whole genome analysis gave additional support to the MS analysis that xenopep and rhabdin are novel but related peptides.

PAX 1', 3', 5 and 7E and xenocoumacin II were previously identified in cell-free extracts of *X. khoisanae* SB 10 (Dreyer et al., 2019). PAX 7E and PAX1', 3' and 5 are lipopeptides known for its activity against *Bacillus subtilis* BD170 and *E. coli* Xen 14 (Gualtieri et al., 2009; Dreyer et al., 2019) and could thus be present in fractions NAA and NAO. The second known compound, xenocoumacin II, is known for its antimicrobial and anti-ulcer activity. Xenocoumacin II is active against *S. aureus* and *E. coli*, as observed in studies on *X. nematophilia* (McInerney et al., 1991b) and *X. khoisanae* SB10 (Dreyer et al., 2019). It is thus safe to assume that xenocoumacin 2, produced by *X. khoisanae* J194 and present in the NAA fraction, was below MIC levels required to kill *S. aureus* ATCC 25923. The presence of xenocoumacin II in the NAO and SM fractions could be responsible for the activity observed against *E. coli* Xen 14 and *S. aureus* ATCC 25923. The production of xenocoumacin in surface cultures and non-aerated broth indicated a role of oxygen in the control of its synthesis in this *X. khoisanae* strain and correlated with the results obtained by Dreyer *et al.* (2019). Due to its hydrophobic nature, the third family of compounds, xenoamicins, eluted much later (Zhou et al., 2013). We show that the xenoamicins in the produced complex exhibited some distinctly different fragments when compared to xenoamicin B/C and G described by Zhou et al. (2013), indicating that the xenoamicins produced by this strain might be novel. This is an important finding as xenoamicins are depsipeptides known for their anti-plasmodial activity (Zhou et al., 2013). However, they may not have contributed to the antimicrobial activity observed in NAO and SM fractions. Activity observed against *P. aeruginosa* ATCC 27853, *S. epidermidis* SE1 and *L. monocytogenes* EDGe is possibly due to novel compounds such as rhabdin and khoicin.

Khoicin and rhabdin, are small early eluting compounds and provisionally characterised as a tri- and hexapeptide respectively, that are present in NAO and SM fractions. These could be responsible for inhibiting *P. aeruginosa* ATCC 27853, *S. epidermidis* SE1 and *L. monocytogenes* EDGe (**Table 2 and 4**). The size of both khoicin and rhabdin makes them ideal candidates for future antibiotics. The lack of known compounds identified in the AB fraction also indicated that *X. khoisanae* produces a plethora of possibly novel compounds, such as xenopep. Xenopep, a larger peptide also elutes early, but is primarily produced under aerated conditions, with a putative NRPS operon in node 7. The fact that a non-classical MS/MS fragmentation with internal fragments was observed could indicate that the peptide is modified and or cyclic. The Xenopep and rhabdin, share structural moieties, such as the sequence Pro-Pro-Leu-Phe. They may share an operon with differential expression with the synthetase 4 and 5, only expressed under anaerobic conditions to yield xenopep, while synthetases 1-3 are expressed under all conditions to yield rhabdin. *Xenorhabdus* bacteria are known for their ability to produce a wide range of secondary metabolites from a single synthetase (Gualtieri et al, 2009; Kronenwerth et al, 2014; Park et al, 2009; Zhou et al, 2013). These bacteria also utilise different starting points in the assembly line to further expand their repertoire of secondary metabolites (Kegler and Bode 2020; Trietze et al, 2020). The limited amounts of pure khoicin, rhabdin and xenopep precluded further structural analyses, which will be addressed in a future study.

Apart from the known compounds and the three novel compounds in this study an additional 28 compounds were detected and high ion signals. The bioactivity of these compounds is unknown and it is possible that strain J194 probably produce compounds with a wider bioactive profile than recorded in this study.

In an era where there is a dire need for new antibiotics, this study highlights the potential of discovering novel antibiotics from the rich complex of antimicrobials produced by *X. khoisanae* J194. The use of powerful techniques such as UPLC-MS and HPLC, combined with advanced microbiological techniques, proved to be a successful strategy. Further research is required to determine the full antimicrobial potential of rhabdin and khoicin. This study also showed the immense influence aeration have on the secondary metabolism of *X. khoisanae* J194. Indicating that researchers should investigate a more diverse range of conditions when mining for novel antibiotics from microorganisms. The variation in antimicrobial compounds produced by *X. khoisanae* J194 may lead to the discovery of novel antibiotics.

MATERIALS AND METHODS

Isolation, stock and growth conditions of strains

Xenorhabdus khoisanae J194 was isolated from the nematode *Steinernema jeffreyense* J194 (Dreyer et al., 2017), collected from soil in the Eastern Cape, South Africa (Malan et al., 2016). Cells of *X. khoisanae* J194 were plated onto nutrient agar, supplemented with 0.025% (w/v) bromothymol blue and 0.04% (*w/v*) TTC (NTBA), and incubated at 30 °C for a minimum of 48 h. Blue colonies, representative of cells in phase I (Dreyer et al., 2017), were selected and cultured in Tryptone Soy Broth (TSB) at 37 °C for 24 h on an orbital shaker. Pure colonies were stored at -80 °C in the presence of 40% (*v/v*) sterile glycerol. *Staphylococcus aureus* ATCC 25923, *S. aureus* Xen 31, *S. epidermidis* SE1, *L. monocytogenes* EDGe, *E. coli* Xen 14 and *P. aeruginosa* ATCC 27853 were from the culture collection of the Department of Microbiology, Stellenbosch University, and were grown in Brain Heart Infusion (BHI). These strains were streaked to purity on BHI Agar. Colonies were resuspended into sterile phosphate buffer (PBS), transferred to 80% (*v/v*) sterile glycerol (final 40%, *v/v*) and stored at -80 °C.

Isolation of Antimicrobial Compounds

Xenorhabdus khoisanae J194 was cultured in TSB for 24 h at 30 °C and then streaked onto Tryptone Soy Agar (TSA). Colonies were suspended in 5 mL TSB and used as inoculum in each of the three following culturing methods.

In method A, 10 mL of TSB in a 100 mL Erlenmeyer flask was inoculated with 100 µL cell suspension and incubated at 26 °C for 24, 48, 72 and 96 h, respectively. At each of these time points, 1.0 mL was sampled to record the pH and optical density (OD_{595}). The pH was of each sample was adjusted to 4.0 with 10.2 N HCl and kept at 4 °C for 3 h. Cells were harvested (5000 x *g*, 20 min, 4 °C) and the cell-free supernatants (CFSs) concentrated by freeze-drying. Freeze-dried samples were re-suspended, separately, in 10 mL 75% (*v/v*) acetonitrile. The acetonitrile upper fraction and oily bottom fraction were separated by carefully removing the top layer with a pipette and freeze-dried. Harvested cells were resuspended in 10 mL 90% (*v/v*) acetonitrile to extract intracellular antimicrobial compounds, vortexed and centrifuged (5000 × *g*, for 20 min, 4 °C) to remove cell debris. Cell-free supernatants were concentrated by freeze-drying.

In method B, 250 mL TSB, in a 250 mL Erlenmeyer flask was inoculated with 2.5 mL active growing cell suspension and incubated at 26°C for 24, 48, 72 and 96 h, respectively, on an orbital shaker (220 rpm). Samples (1.0 mL) were collected after 24, 48, 72 and 96 h, and the pH and OD readings determined as described in method A. At each time point, cells were

harvested, as described above, 10g Amberlite XAD-16 resin (Sigma-Aldrich, Missouri, USA) were added to 250 mL cell-free supernatant (CFS) and left on an orbital shaker (180 rpm) at 4 °C for 3 h. The beads were removed by filtration, washed with 1 L of double distilled water and incubated with 30% (*v/v*) ethanol (25 mL/5 g) for 30 min to remove weakly bound polar compounds. After 30 min the beads were collected by filtration and ethanol was washed of with 1 L of double distilled water. The more hydrophobic and amphipathic compounds were released from the beads by incubating the beads with 80% (*v/v*) isopropanol containing 0.1% (*v/v*) TFA (Trifluoroacetic acid) (ISO-TFA; 40 mL per 5.0 g)for 1 hour. The 80% isopropanol and beads were separated by filtration and the isopropanol was removed under vacuum, using a Rotavapor R-114 (Büchi) connected to a water bath (B-480, Büchi). Further concentration was accomplished by freeze-drying.

In method C, 5.0 mL cell suspension was mixed with 5.0 g sterile Amberlite XAD-16 resin and then plated onto TSA (TSB with 2.0%, w/v, agar) in four sets of 150 mm diameter plates. TSB was pre-treated with Amberlite XAD-16 resin to remove most of the hydrophobic compounds before agar was added. Plates were incubated at 26 °C for 24, 48, 72 and 96 h, respectively. At each of these time points, the Amberlite XAD-16 resin were removed from the surface of the agar with a sterile metal scraper, added to 200 mL analytical quality water and agitated on an orbital shaker (180 rpm) at 4 °C for 1 h. The beads were then collected and incubated with 30% (*v/v*) ethanol (25 mL per 5.0 g) as described above to remove polar compounds. After 30 min the hydrophobic and amphipathic compounds were released from the Amberlite XAD-16 resin by incubating the resin in 80% (*v/v*) isopropanol, containing 0.1% (*v/v*) TFA (ISO-TFA; 40 mL per 5.0 g) for 1 h. The isopropanol and resin were separated as described above and the isopropanol was removed by evaporation and the hydrophobic and amphipathic fraction concentrated by freeze-drying, as described elsewhere.

Antimicrobial Activity Tests

Overnight-grown cultures of *S. aureus* ATCC 25923, *L. monocytogenes* EDGe, *E. coli* Xen 14 and *P. aeruginosa* ATCC 27853 were inoculated (1.0%, *v/v*) into separate volumes of sterile molten TSA (approximately 45 °C), carefully swirled, immediately transferred to wells (100 µL per well) in a 96-well microtiter plate (Greiner Bio-One, Austria) and left to solidify. Refer to Du Toit and Rautenbach (2000) for a more detailed description Freeze-dried fractions were each suspended in 50% (*v/v*) acetonitrile in water to yield a final volume of 1.0 mL. Twenty microliters of each suspension of the freeze-dried crude extracts (24 h, 48h, 72h and 96h)were added onto the surface of TSA-imbedded cells in the 96-well plate and the plate was incubated

for 24 h at 37°C.Optical density readings (595 nm) were recorded for each well before and after 24 h of incubation at 37°C, using an iMark Microplate reader (Biorad, California, USA).

Activity assays of the 96 h crude extracts were repeated to determine specific activity. Freeze-dried CFS collected from 96 h-old cultures were each re-suspended in sterile distilled water (4.0 mg/mL) and antimicrobial activity tested against *P. aeruginosa* ATCC 27853, *E. coli* Xen 14, *S. aureus* ATCC25923, *S. aureus* Xen 31, *S. epidermidis* SE1 and *L. monocytogenes* EDGe. The strains were inoculated (1.0%, *v/v*) into separate volumes of sterile molten TSA (approximately 45 °C), carefully mixed and immediately transferred to round petri dishes of 145 mm in diameter in the first step of the well diffusion agar assay. A 96-well PCR plate was sterilized under UV, placed into the inoculated molten agar and the agar was allowed to set before the PCR plate were removed. Once the agar was set, 20.0 µL crude extract was placed into each well and incubated for 24 hours at 37°C. The same method was used to determine the antimicrobial activity of the partially purified compounds, except all the fractions collected were dissolved in 100 µL of 50% acetonitrile. Specific activity was determined using the following equation:

$$\text{Specific activity} = \frac{area/mL}{4.00\ mg/mL}$$

In situ Identification of Putative Operons

The whole genome of *X. khoisanae* J194 was subjected to AntiSMASH (Antismash.secondarymetabolites.org) to identify secondary metabolites biosynthesis gene clusters (Blin et al., 2019). The whole genome was also analysed for putative operons relating to rhabdin and xenopep. Operons were identified by aligning the protein sequence of gramicidin S and tyrocidine synthetases to the whole genome sequence of *X. khoisanae* J194 using the tblastn function of the NCBI website (blast.ncbi.nlm.nih.gov/Blast.cgi). The open reading frames of the possible operons were translated to protein sequence using the CLC Main Workbench 7.6.1 software. Thereafter the various domains present in non-ribosomal peptide (NRP) synthetases (condensation, adenylation, epimerization, thiolation and thioesterase) were identified by searching for the highly conserved core motifs of the catalytic NRP domains. The synthetases identified were subjected to the LSI based A-domain function predictor (http://bioserv7.bioinfo.pbf.hr/LSOpredictor/AdomainPrediction.jsp), the NRPSsp adenylation domain predictor (http://www.nrpssp.com) and the PKS/NRPS Web Server/Predictive Blast Server (http://sourceforge.net/projects/secmetdb/. Validity of the prediction was based on the prediction score given by the software.

Partial Purification of Antimicrobial Compounds

Compounds produced by *X. khoisanae* J194 cultured on solid media were extracted and partially purified by means of high-performance liquid chromatography (HPLC; Agilent, California, USA). The freeze-dried extract was dissolved in 50% (*v/v*) acetonitrile and loaded onto a Poroshell 120 EC-C_{18} HPLC column (120 Å, 4 µm, 4.6 mm x 150 mm, Agilent) and eluted with a linear gradient created with 0.1% (*v/v*) trifluoracetic acid (TFA) in analytically pure water (eluent A) and 0.1% (*v/v*) TFA in acetonitrile (eluent B). The flow rate was set at 1.5 mL/min and the elution program utilised was as follows: 20% eluent A from 0 to 0.5 min (initial conditions), 0.5 to 12.5 min linear gradient from 20% to 90% eluent B, 12.5 to 13 min linear gradient from 90% to 100% eluent B, 13 min to 14 min at 100% eluent B, followed by column equilibration (14 to 20 min linear gradient from 100% to 20% eluent B and 20 to 25 min at initial conditions). Separation was performed on an Agilent 1260 Infinity II LC system. Data were recorded at 230 nm and 245 nm. Fractions of the peaks were collected, freeze-dried and tested for antimicrobial activity as described above.

Identification of Antimicrobial Compounds

Samples that were active against one or more of the target strains were analysed using a Waters Acquity UPLC^{TM} (ultraperformance liquid chromatography), linked to a Waters Synapt G2 quadrupole time-of-flight mass spectrometer (QTOF; Waters Corporation, Milford, USA) housed at the Central Analytical Facility at Stellenbosch University. Sample volumes of 1.0 to 5.0 µL were analysed on a HSS T3 column (1.8 µm, 2.1 mm × 100 mm) developed with an elution program created with 0.1% (*v/v*) formic acid in analytically pure water (eluent A) and 0.1% (*v/v*) formic acid in acetonitrile (eluent B). The flow rate was set at 300 µL/min and the elution program utilised was as follows: 100% eluent A from 0 to 0.5 min (initial conditions), 0.5 to 1.0 min linear gradient from 0 to 30.0% eluent B, 1.0 to 10.0 min linear gradient from 30.0 to 60.0% eluent B, 10 to 15 min linear gradient from 60.0 to 80.0% eluent B, followed by column equilibration (15.0 to 15.1 min linear gradient from 80.0 B to 100% A and 15.1 to 20.0 min at initial conditions). The rest of the instrument settings for mass spectrometric analysis were as follows: cone voltage 15 V, capillary voltage 2.5 kV, extraction cone voltage 4V, source temperature 120 ºC, desolvation gas (N_2) of 650 L/h and temperature 275 ºC. Spectral data were collected in positive mode by scanning through *m/z* = 100 to 2000 in continuum mode. Mass-spectrometry data of the detected ion peaks in chromatography of the different samples were processed with the MaxEnt 3 function of MassLynx 4.1. For comparison of

samples, signals were normalised to the highest signal over a specific elution range (0-6 min and 6-17 min).

Preliminary structure analysis was done by high resolution collision induced dissociation (CID) analyses in the MS^E mode (tandem MS or MS/MS) during UHPLC-MS and monitored on a second MS channel, as described by Dreyer et al. (2019). A collision energy gradient of 20 to 60 eV at 1 s MS/MS scan time were used for CID and data was collected in the second mass analyser (MS2) through *m/z* = 40 to 2000 in continuum mode. Reliable high-resolution MS data was ensured by calibrating the MS instruments with sodium formate. A single point lock spray (leucine encephalin, *m/z* = 556.2771) was used as a calibrant during analysis to compensate for any *m/z* drift. Elemental composition was fitted using Masslynx software and formulas were considered that has a mass accuracy of 5 ppm or better. The elution time, number of hetero atoms, isotope patterns and double bond equivalence were taken into consideration when probable formulas were selected. Candidate formulas were not selected for larger molecules, due to high number of possibilities, and therefore a high uncertainty, unless they were previously identified compounds.

DATA AVAILABILITY STATEMENT

The datasets generated for this study are available on request to the corresponding authors.

AUTHOR CONTRIBUTIONS

All authors contributed to the writing of the manuscript. Experimental work was done by E Booysen. Analysis and experimental setup of UPLC-MS was done by MA Stander and M Rautenbach. All authors have given approval to the final version of the manuscript.

REFERENCES

Arbeit, R., Maki, D., Tally, F. O., Campanaro, E., and Eisenstein, B. I. (2004). The safety and efficacy of daptomycin for the treatment of complicated skin and skin-structure infections. *Clin. Infect. Dis. an Off. Publ. Infect. Dis. Soc. Am*. 38, 1673–1681. doi:10.1097/01.idc.0000144912.27311.19.

Blin, K., Shaw, S., Steinke, K., Villebro, R., Ziemert, N., Lee, S. Y., et al. (2019). antiSMASH 5.0: updates to the secondary metabolite genome mining pipeline. *Nucleic Acids Res*. 47, W81–W87. doi:10.1093/nar/gkz310.

Booysen, E., and Dicks, L. M. T. (2020). Does the future of antibiotics lie in secondary metabolites produced by *Xenorhabdus* spp.? *A Review. Probiotics Antimicrob. Proteins* 12, 1310–1320. doi:10.1007/s12602-020-09688-x.

Böszörményi, E., Érsek, T., Fodor, A. M., Fodor, A. M., Földes, L. S., Hevesi, M., et al. (2009). Isolation and activity of *Xenorhabdus* antimicrobial compounds against the plant pathogens *Erwinia amylovora* and *Phytophthora nicotianae*. *J. Appl. Microbiol*. 107, 746–759. doi:10.1111/j.1365-2672.2009.04249.x.

Cai, X., Challinor, V. L., Zhao, L., Reimer, D., Adihou, H., Grün, P., et al. (2017). Biosynthesis of the antibiotic nematophin and its elongated derivatives in entomopathogenic bacteria. *Org. Lett*. 19, 806–809. doi:10.1021/acs.orglett.6b03796.

Chen, G., Maxwell, P., Dunphy, G. B., and Webster, J. M. (1996). Culture conditions for *Xenorhabdus* and *Photorhabdus* symbionts of entomopathogenic nematodes. *Nematologica* 42, 127–130.

Crawford, J. M., Kontnik, R., and Clardy, J. (2010). Regulating alternative lifestyles in entomopathogenic bacteria. *Curr. Biol.* 20, 69–74. doi:10.1016/j.cub.2009.10.059.

Crawford, J. M., Portmann, C., Kontnik, R., Walsh, C. T., and Clardy, J. (2011). NRPS substrate promiscuity diversifies the xenematides. *Org. Lett. 13*, 5144–5147. doi:10.1021/ol2020237.

Crawford, J. M., Portmann, C., Zhang, X., Roeffaers, M. B. J., and Clardy, J. (2012). Small molecule perimeter defense in entomopathogenic bacteria. *Proc. Natl. Acad. Sci. U. S. A.* 109, 10821–10826. doi:10.1073/pnas.1201160109.

D'Costa, V. M., King, C. E., Kalan, L., Morar, M., Sung, W. W. L., Schwarz, C., et al. (2011). Antibiotic resistance is ancient. *Nature* 477, 457–461. doi:10.1038/nature10388.

Dreyer, J., Malan, A. P., and Dicks, L. M. T. (2017). Three novel *Xenorhabdus – Steinernema* associations and evidence of strains of *X. khoisanae* switching between different clades. *Curr. Microbiol*. 74, 938–942. doi:10.1007/s00284-017-1266-2.

Dreyer, J., Malan, A. P., and Dicks, L. M. T. (2018). Bacteria of the genus X*enorhabdus*, a novel source of bioactive compounds. *Front. Microbiol*. 9, 1–14. doi:10.3389/fmicb.2018.03177.

Dreyer, J., Rautenbach, M., Booysen, E., Van Staden, A. D., Deane, S. M., and Dicks, L. M. T. (2019*). Xenorhabdus khoisanae* SB10 produces Lys-rich PAX lipopeptides and a Xenocoumacin in its antimicrobial complex. *BMC Microbiol*. 19, 1–11. doi:10.1186/s12866-019-1503-x.

Du Toit, E. A., and Rautenbach, M. (2000). A sensitive standardised micro-gel well diffusion assay for the determination of antimicrobial activity. *J. Microbiol. Methods* 42, 159–165. doi:10.1016/S0167-7012(00)00184-6.

Dunphy, G. B., and Webster, J. M. (1991). Antihemocytic surface components of *Xenorhabdus nematophilus* var. *dutki* and their modification by serum nonimmune larvae of *Galleria mellonella. J. Invertebr. Pathol*. 58, 40–51.

Fair, R. J., and Tor, Y. (2014). Antibiotics and bacterial resistance in the 21st century. *Perspect. Medicin. Chem*. 6, 25–64. doi:10.4137/PMC.S14459.

Ferreira, T., van Reenen, C. A., Endo, A., Spröer, C., Malan, A. P., and Dicks, L. M. T. (2013). Description of *Xenorhabdus khoisanae* sp. nov., the symbiont of the entomopathogenic nematode *Steinernema khoisanae*. *Int. J. Syst. Evol. Microbiol*. 63, 3220–3224. doi:10.1099/ijs.0.049049-0.

Fuchs, S. W., Grundmann, F., Kurz, M., Kaiser, M., and Bode, H. B. (2014). Fabclavines: Bioactive peptide – polyketide-polyamino hybrids from *Xenorhabdus*. *Chembiochem* 15, 512–516. doi:10.1002/cbic.201300802.

Fuchs, S. W., Proschak, A., Jaskolla, T. W., Karas, M., and Bode, H. B. (2011). Structure elucidation and biosynthesis of lysine-rich cyclic peptides *in Xenorhabdus namtophila*. *Org. Biomol. Chem*. 9, 3130–3132. doi:10.1039/c1ob05097d.

Grundmann, F., Kaiser, M., Kurz, M., Schiell, M., Batzer, A., and Bode, H. B. (2013). Structure determination of the bioactive depsipeptide xenobactin from *Xenorhabdus* sp. PB30.3. *RSC Adv*. 3, 22072–22077. doi:10.1039/c3ra44721a.

Gualtieri, M., Aumelas, A., and Thaler, J.-O. (2009). Identification of a new antimicrobial lysine-rich cyclolipopeptide family from *Xenorhabdus nematophila*. *J. Antibiot*. (Tokyo). 62, 295–302. doi:10.1038/ja.2009.31.

Guo, S., Zhang, S., Fang, X., Liu, Q., Gao, J., Bilal, M., et al. (2017). Regulation of antimicrobial activity and xenocoumacins biosynthesis by pH in *Xenorhabdus nematophila*. *Microb. Cell Fact*. 16, 1–14. doi:10.1186/s12934-017-0813-7.

Hacker, C., Cai, X., Kegler, C., Zhao, L., Weickhmann, A. K., Wurm, J. P., et al. (2018). Structure-based redesign of docking domain interactions modulates the product spectrum of a rhabdopeptide-synthesizing NRPS. *Nat. Commun*. 9. doi:10.1038/s41467-018-06712-1.

Ji, D., Yi, Y., Kang, G. H., Choi, Y. H., Kim, P., Baek, N. I., et al. (2004). Identification of an antibacterial compound, benzylideneacetone, from *Xenorhabdus nematophila* against major plant-pathogenic bacteria. *FEMS Microbiol. Lett*. 239, 241–248. doi:10.1016/j.femsle.2004.08.041.

Kaufman, G. (2011). Antibiotics: mode of action and mechanisms of resistance. *Nurs. Stand.* 24, 49–55.

Kegler, C., Bode, H. B. (2020). Artificial splitting of a non-ribosomal peptide synthetase by inserting natural docking domians. *Angew. Chem.* 132, 13565-13569

Kronenwerth, M., Bozhüyük, K. A. J., Kahnt, A. S., Steinhilber, D., Gaudriault, S., Kaiser, M., et al. (2014). Characterisation of taxlllaids A-G; natural products *from Xenorhabdus indica. Chem. - A Eur. J*. 20, 17478–17487. doi:10.1002/chem.201403979.

Lee Ventola, C. (2015). The antibiotic resistance crisis: part 2: management strategies and new agents. *Pharm. Ther*. 40, 344–352.

Li, B., Wever, W. J., Walsh, C. T., and Bowers, A. A. (2014). Dithiolopyrrolones: Biosynthesis, synthesis and activity of a unique class of disulfide containing antibiotics. *Nat. Prod. Rep*. 31, 905–923. doi:10.1039/b000000x.

Malan, A. P., Knoetze, R., and Tiedt, L. R. (2016). *Steinernema jeffreyense* n. Sp. (Rhabditida: Steinernematidae), a new entomopathogenic nematode from South Africa. *J. Helminthol.* 90, 262–278. doi:10.1017/S0022149X15000097.

McInerney, B. V, Gregson, R. P., Lacey, M. J., Akhurst, R. J., Lyons, G. R., Rhodes, S. H., et al. (1991a). Biologically active metabolites from *Xenorhabdus* spp., Part 1. Dithiolopyrrolone derivatives with antibiotic activity. *J. Nat. Prod*. 54, 774–784.

McInerney, B. V, Taylor, W. C., Lacey, M. J., Akhurst, R. J., and Gregson, R. P. (1991b). Biologically active metabolites from *Xenorhabdus* spp., Part 2. Benzopyran-1-one Derivatives with Gastroprotective activity. *J. Nat. Prod.* 54, 785–795.

Park, D., Ciezki, K., van der Hoeven, R., Singh, S., Reimer, D., Bode, H. B., et al. (2009). Genetic analysis of xenocoumacin antibiotic production in the mutualistic bacterium *Xenorhabdus nematophila. Mol. Microbiol*. 73, 938–949. doi:10.1111/j.1365-2958.2009.06817.x.

Proschak, A., Zhou, Q., Schöner, T., Thanwisai, A., Kresovic, D., Dowling, A., et al. (2014). Biosynthesis of the insecticidal xenocyloins in *Xenorhabdus bovienii. Chembiochem* 15, 369–372. doi:10.1002/cbic.201300694.

Qin, Z., Huang, S., Yu, Y., and Deng, H. (2013). Dithiolopyrrolone natural products: Isolation, synthesis and biosynthesis. *Mar. Drugs* 11, 3970–3997. doi:10.3390/md11103970.

Reimer, D., Luxenberger, E., Brachmann, A. O., and Bode, H. B. (2009). A new type of pyrrolidine biosynthesis is involved in the late steps of xenocoumacin production in *Xenorhabdus nematophila. Chembiochem* 10, 1997–2001. doi:10.1002/cbic.200900187.

Reimer, D., Nollmann, F. I., Schultz, K., Kaiser, M., and Bode, H. B. (2014). Xenortide biosynthesis by entomopathogenic *Xenorhabdus nematophila. J. Nat. Prod*. 77, 1976–1980. doi:10.1021/np500390b.

Reimer, D., Pos, K. M., Thines, M., Grün, P., and Bode, H. B. (2011). A natural prodrug activation mechanism in nonribosomal peptide synthesis. *Nat. Chem. Biol*. 7, 888–890. doi:10.1038/nchembio.688.

Singh, J., and Banerjee, N. (2008). Transcriptional analysis and functional characterization of a gene pair encoding iron-regulated xenocin and immunity proteins of *Xenorhabdus nematophila*. *J. Bacteriol*. 190, 3877–3885. doi:10.1128/JB.00209-08.

Spellberg, B., Guidos, R., Gilbert, D., Bradley, J., Boucher, H. W., Scheld, M. W., et al. (2008). The epidemic of antibiotic-resistant infections: a call to action for the medical community from the infectious diseases society of America. *Clin. Infect. Dis*. 46, 155–164. doi:10.1086/524891.

Thaler, J. O., Baghdiguian, S., and Boemare, N. (1995). Purification and characterization of xenorhabdicin, a phage tail-like bacteriocin, from the lysogenic strain F1 of *Xenorhabdus nematophilus*. *Appl. Environ. Microbiol*. 61, 2049–2052.

Tietze, A., Shi, Y., Kronenwerth, M., Bode, H. B. (2020). Nonribosomal peptides produced by minimal and engineered synthetases with terminal reductase domains. ChemBioChem. 21. 2750-2754

Ventola, C. L. (2015). Antibiotic Resistance Crisis: part 1: causes and threats. *Pharm. Ther*. 40, 277–283. doi:10.24911/ijmdc.51-1549060699.

Wang, Y., Fang, X., An, F., Wang, G., and Zhang, X. (2011a). Improvement of antibiotic activity of *Xenorhabdus bovienii* by medium optimization using response surface methodology. *Microb. Cell Fact*. 10, 98. doi:10.1186/1475-2859-10-98.

Wang, Y., Fang, X., Cheng, Y., and Zhang, X. (2011b). Manipulation of pH shift to enhance the growth and antibiotic activity of *Xenorhabdus nematophila*. *Journalof Biomed. Biotechnol.* 2011, 1–9. doi:10.1155/2011/672369.

Wang, Y. H., Feng, J. T., Zhang, Q., and Zhang, X. (2008a). Optimization of fermentation condition for antibiotic production by *Xenorhabdus nematophila* with response surface methodology. *J. Appl. Microbiol*. 104, 735–744. doi:10.1111/j.1365-2672.2007.03599.x.

Wang, Y. H., Li, Y. P., Zhang, Q., and Zhang, X. (2008b). Enhanced antibiotic activity of *Xenorhabdus nematophila* by medium optimization. *Bioresour. Technol*. 99, 1708–1715. doi:10.1016/j.biortech.2007.03.053.

Webster, J. M., Li, J., and Chen, G. (1996). Xenorxides with antibacterial and antimycotic properties. 1–12.

Yang, J., Zeng, H.-M., Lin, H.-F., Yang, X.-F., Liu, Z., Guo, L.-H., et al. (2012). An insecticidal protein from *Xenorhabdus budapestensis* that results in prophenoloxidase activation in the wax moth, *Galleria mellonella*. *J. Invertebr. Pathol*. 110, 60–67. doi:10.1016/j.jip.2012.02.006.

Zavascki, A. P., Goldani, L. Z., Li, J., and Nation, R. L. (2007). Polymyxin B for the treatment of multidrug-resistant pathogens: A critical review. *J. Antimicrob. Chemother*. 60, 1206–1215. doi:10.1093/jac/dkm357.

Zhou, Q., Grundmann, F., Kaiser, M., Schiell, M., Gaudriault, S., Batzer, A., et al. (2013). Structure and biosynthesis of xenoamicins from entomopathogenic *Xenorhabdus*. *Chem. Eur. J.* 19, 16772–16779. doi:10.1002/chem.201302481.

SUPPLEMENTARY MATERIAL

UPLC-MS/UV fingerprinting of *Xenorhabdus khoisanae* J194 culture extracts

Figs. S1 and S2 depict the UPLC profiles of four culture extracts of aqueous fraction of non-aerated broth culture (NAA), fraction of non-aerated broth culture, (NAO), extract from aerated broth culture and (AB) and extract from culture grown on surface of solid medium(SM). over the first 6 minute. of chromatography. The linked mass spectra and UV spectra of the selected UPLC peaks is also supplied. The ions detected first 6 minutes represent the most polar and overt amphipathic compounds in the extract.

Figs. S3 and S4 depict the UPLC profiles of four culture extracts of NAO and SM over the mid gradient of 6-13 minutes of chromatography. The linked mass spectra and UV spectra of the selected UPLC peaks is also supplied. The ions detected from 6-13 minutes represent the amphipathic compounds in the extract.

Figs. S5 depicts the UPLC profiles of four culture extracts NAA, NAO, AB and SM over the late gradient of 13-17 minutes of chromatography. The linked mass spectra of the selected UPLC peaks are also supplied. These compounds did not show any appreciable UV spectrum apart from absorption above 240 nm (results not shown). The ions detected from 13-17 minutes represent the more hydrophobic compounds in the extract.

Compounds ion that was selected are indicated in bold, while those indicated with * represent non-covalent dimers of the main ion (+1) that were detected.

Figs. S6 depicts the structural analyses of compound **18** – xenocoumacin II. UPLC-MS analysis of the purified compound and the extracted *m/z* chromatogram of the xenocoumacin II ion with *m/z*= 407.210 and the high-resolution MS-MS spectrum of 407.210 can be seen in this figure, as well as the Uv spectrum of the xenocoumacin II.

Figs. S7 depicts the structural analyses of compounds **38** and **42** – xenoamicins. UPLC-MS-MS analysis showing the m/z extracted chromatogram of ion at *m/z* 1314.841 and ion at 1328.856 can be seen in this figure as well as the high-resolution MS-MS spectra of *m/z* 1314.841 and *m/z* 1328.856.

Figs. S8 is a comparison of the high-resolution MS-MS of compounds **37 (***m/z* 1314.841) and **42** (*m/z* 1330.856).

Figs. S9 depicts the conserved core motif sequences of the condensation, adenylation and thiolation domains. Conserved sequences are highlighted.

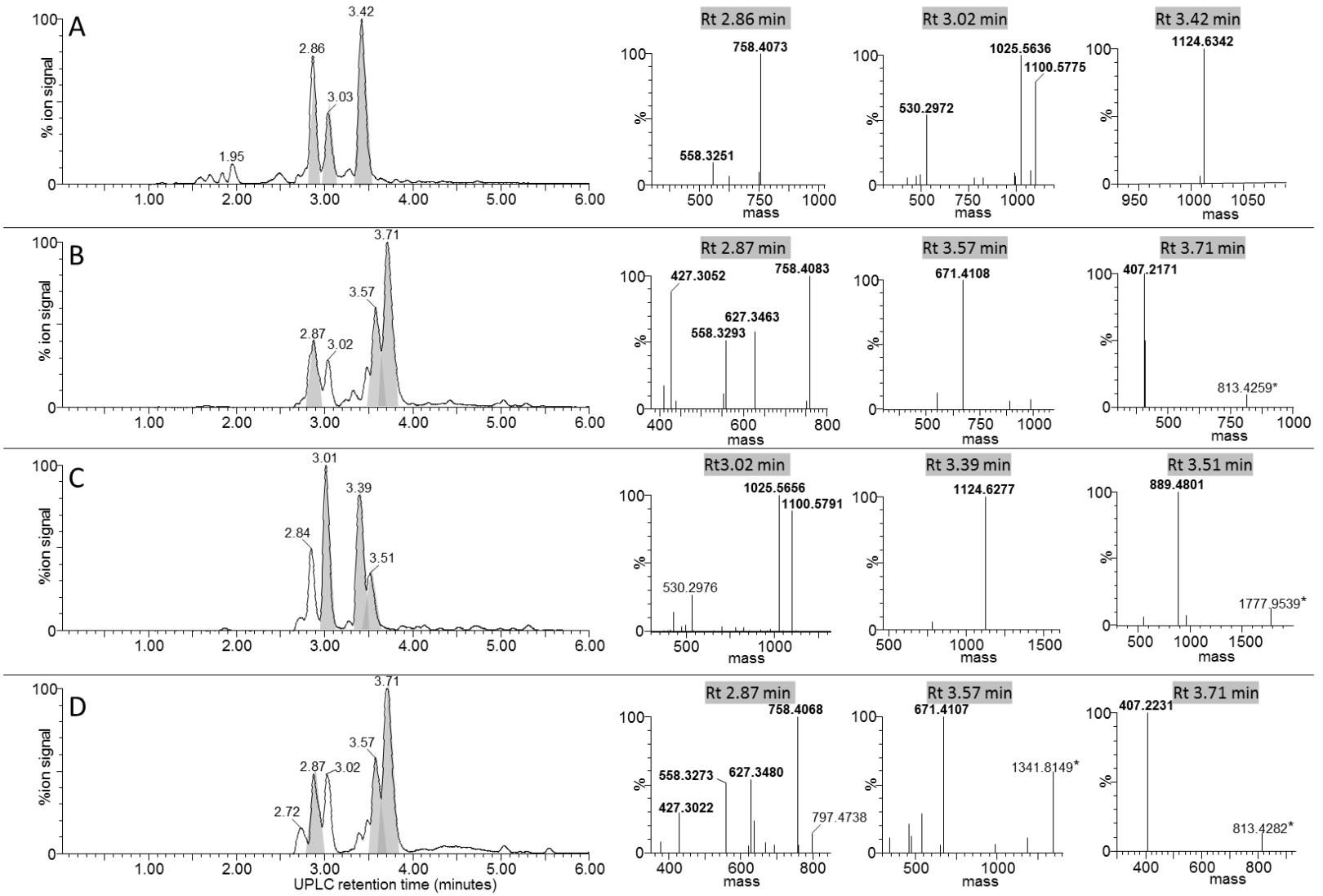

FIGURE S1. UPLC-MS of the early eluting components (0 to 6 min) from the four *X. khoisanae* J194 extracts that showed antibacterial activity: (A) NAA, (B) NAO, (C) AB (D) SM. The UPLC profiles are shown on left and the mass spectra from multi-protonated isotopic resolved spectra (deconvoluted with MassLynx 4.01 MaxEnt 3 algorithm) of the selected peaks shaded in grey are shown on right. The masses in the spectra are protonated masses of the most prominent detected compounds.

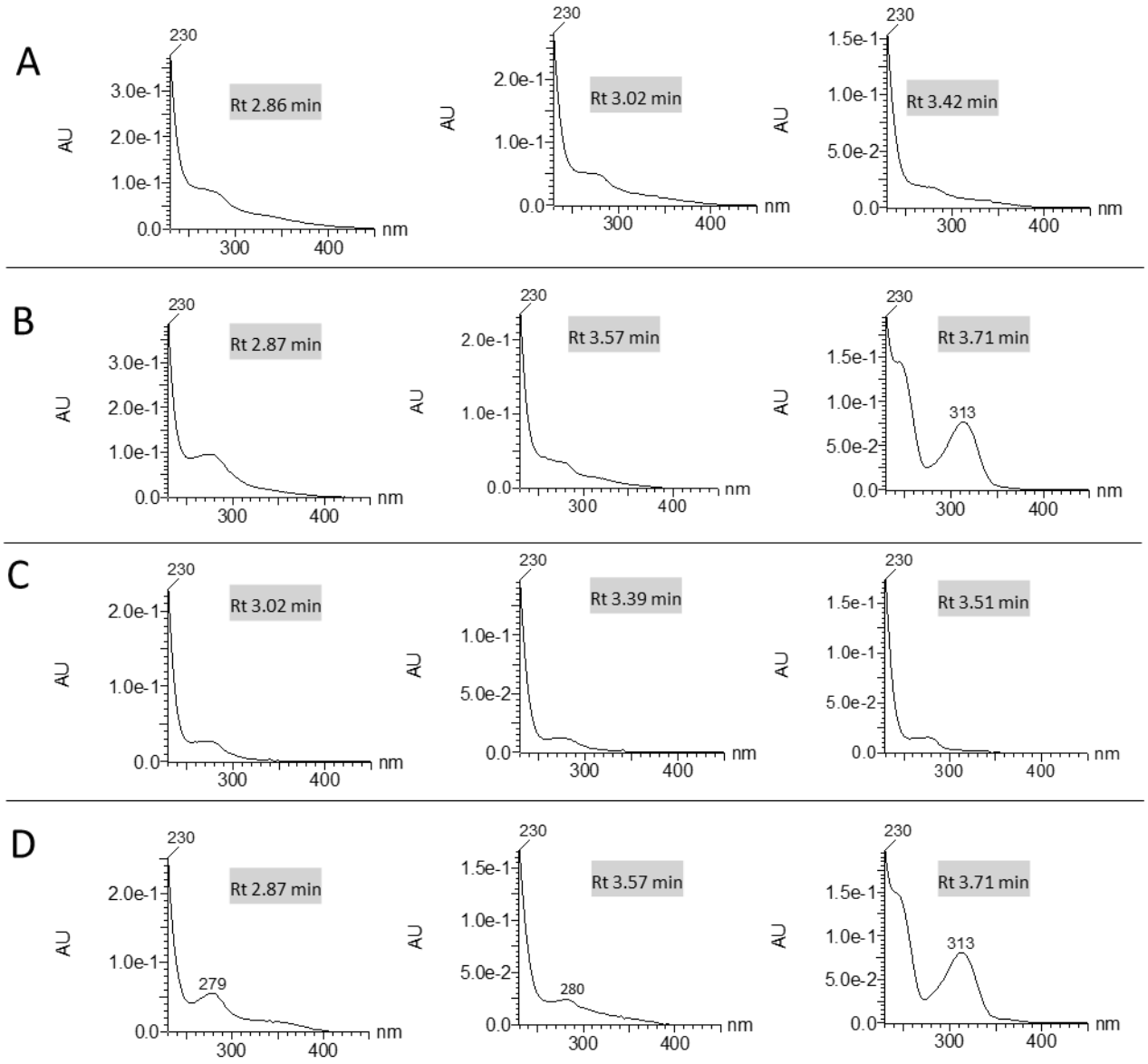

FIGURE S2. UV spectra of the early eluting components (0 to 6 min) from the four *X. khoisanae* J194 extracts that showed antibacterial activity: (A) NAA, (B) NAO, (C) AB (D) SM. The retention time correlate with the selected peaks selected in grey in Fig. S1.

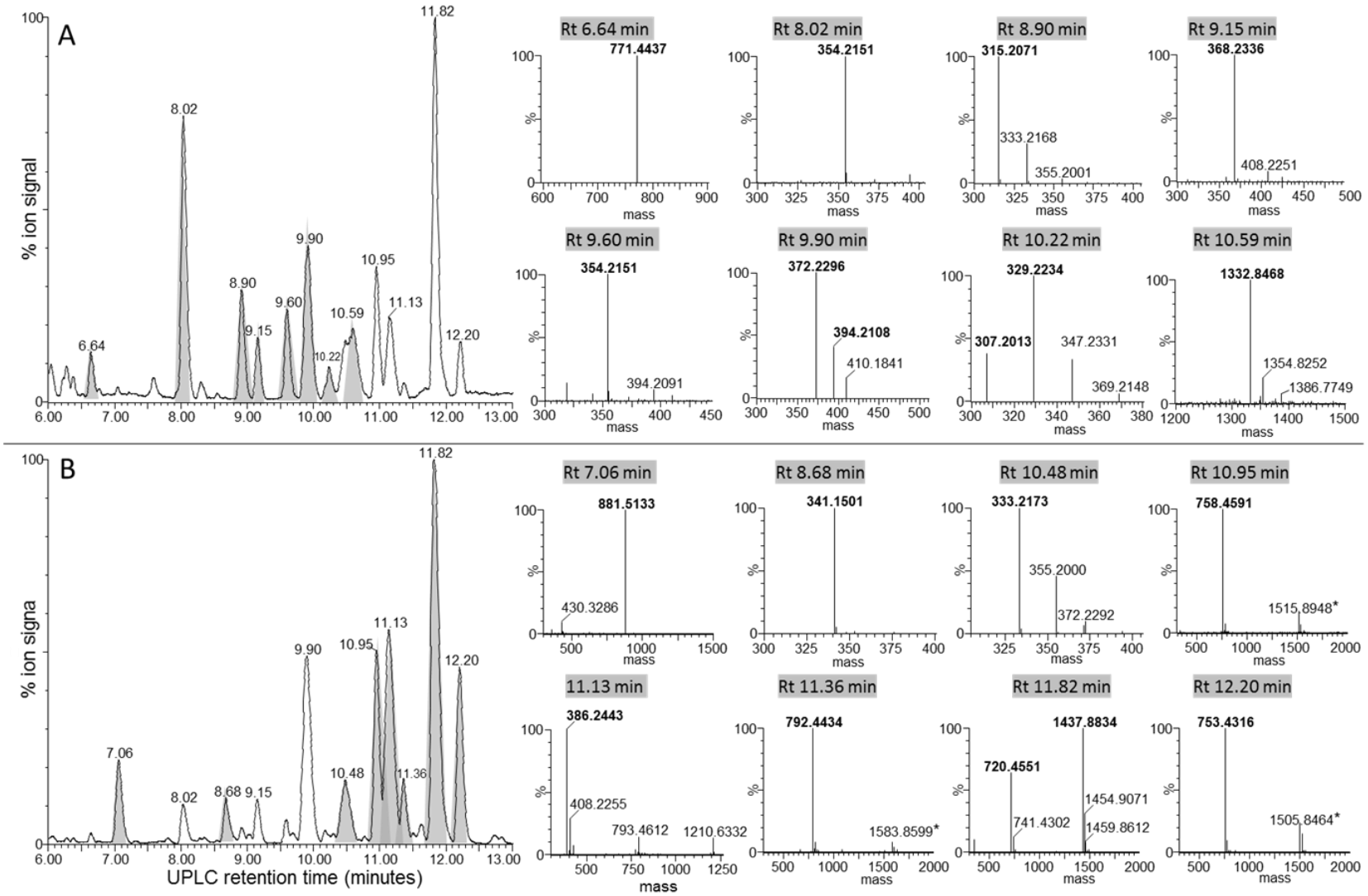

FIGURE S3. UPLC-MS of the mid-gradient eluting components (6 to 13 min) from the two *X. khoisanae* J194 extracts that showed antibacterial activity: (A) NAO and (B) SM. The UPLC profiles are shown on left and the extracted mass spectra from multi-protonated isotopic resolved spectra (deconvoluted with MassLynx 4.01 MaxEnt 3 algorithm) of the selected peaks shaded in grey are shown on the right. The masses in the spectra are protonated masses of the most prominent detected compounds.

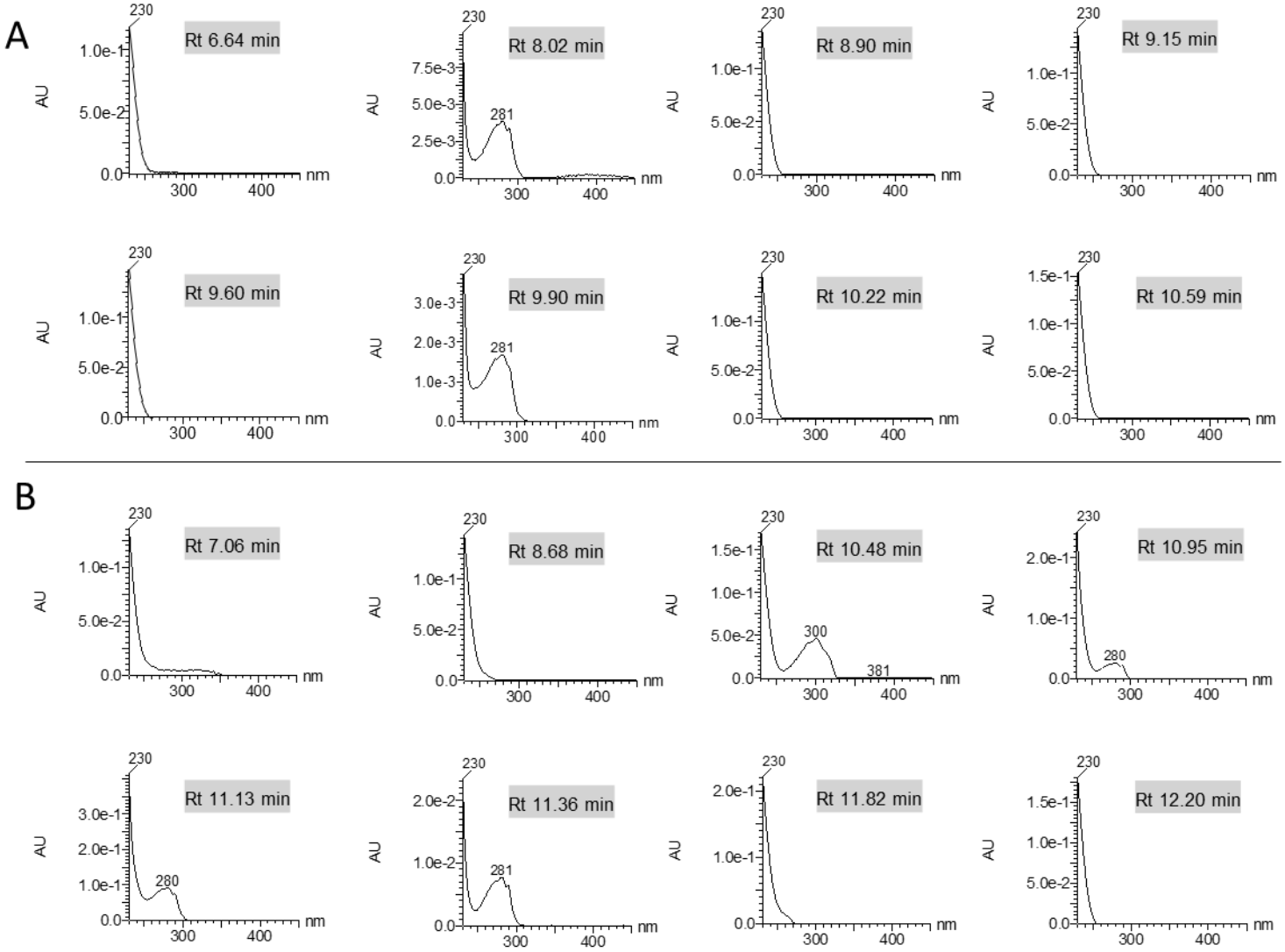

FIGURE S4. UV spectra of the early eluting components (6 to 13 min) from the two *X. khoisanae* J194 extracts that showed antibacterial activity: (A) NAO and (B) SM. The retention time correlate with the selected peaks selected in grey in Fig. S3.

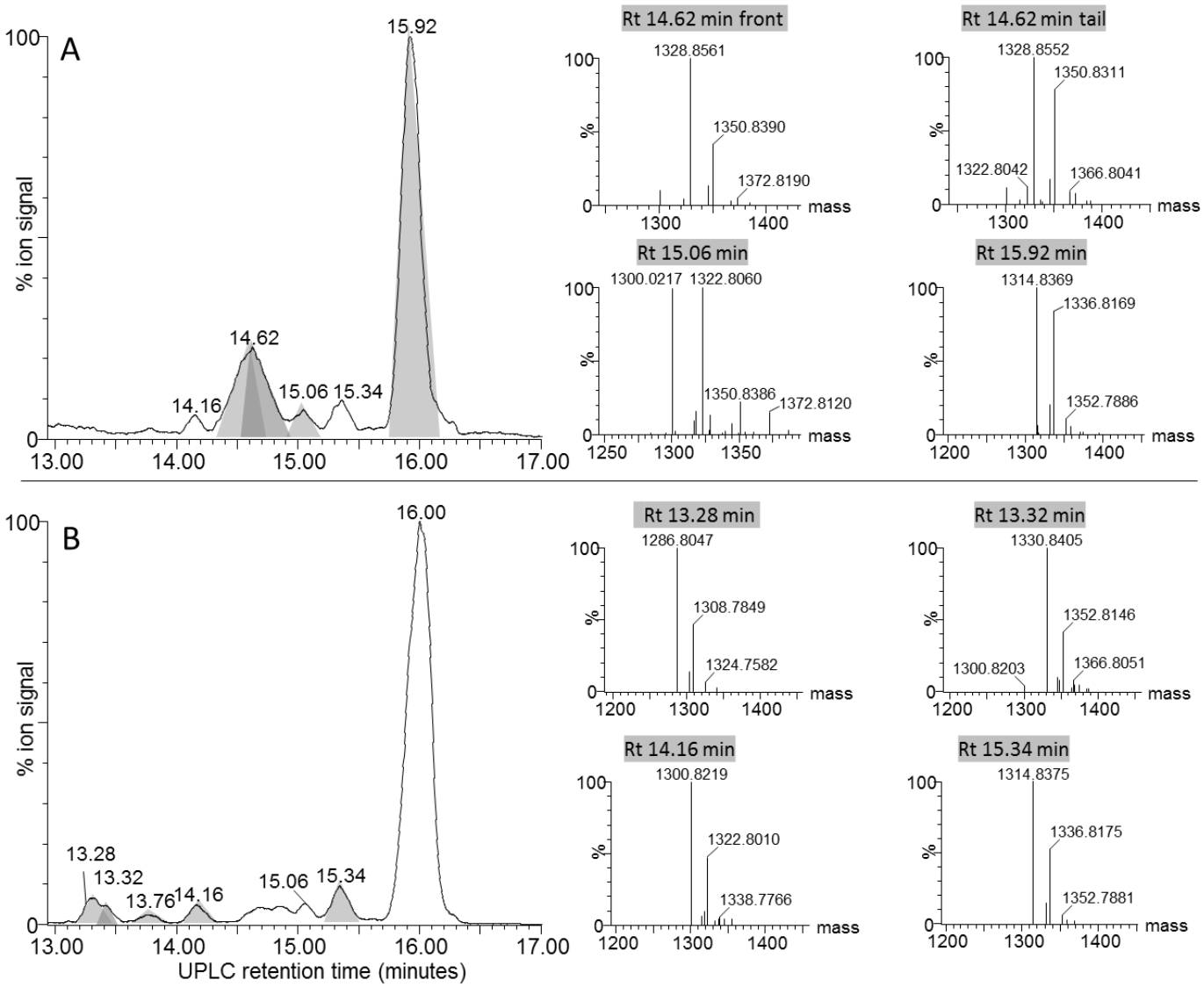

FIGURE S5. UPLC-MS of the late eluting components (13 to 17 min) from the *X. khoisanae* J194 extracts that showed antibacterial activity: (A) NAO (B) SM. The UPLC profiles are shown on the left and the extracted mass spectra from multi-protonated isotopic resolved spectra (deconvoluted with MassLynx 4.01 MaxEnt 3 algorithm) of the selected peaks are shaded in grey are shown on right. The masses in the spectra are protonated masses of the most prominent detected compounds.

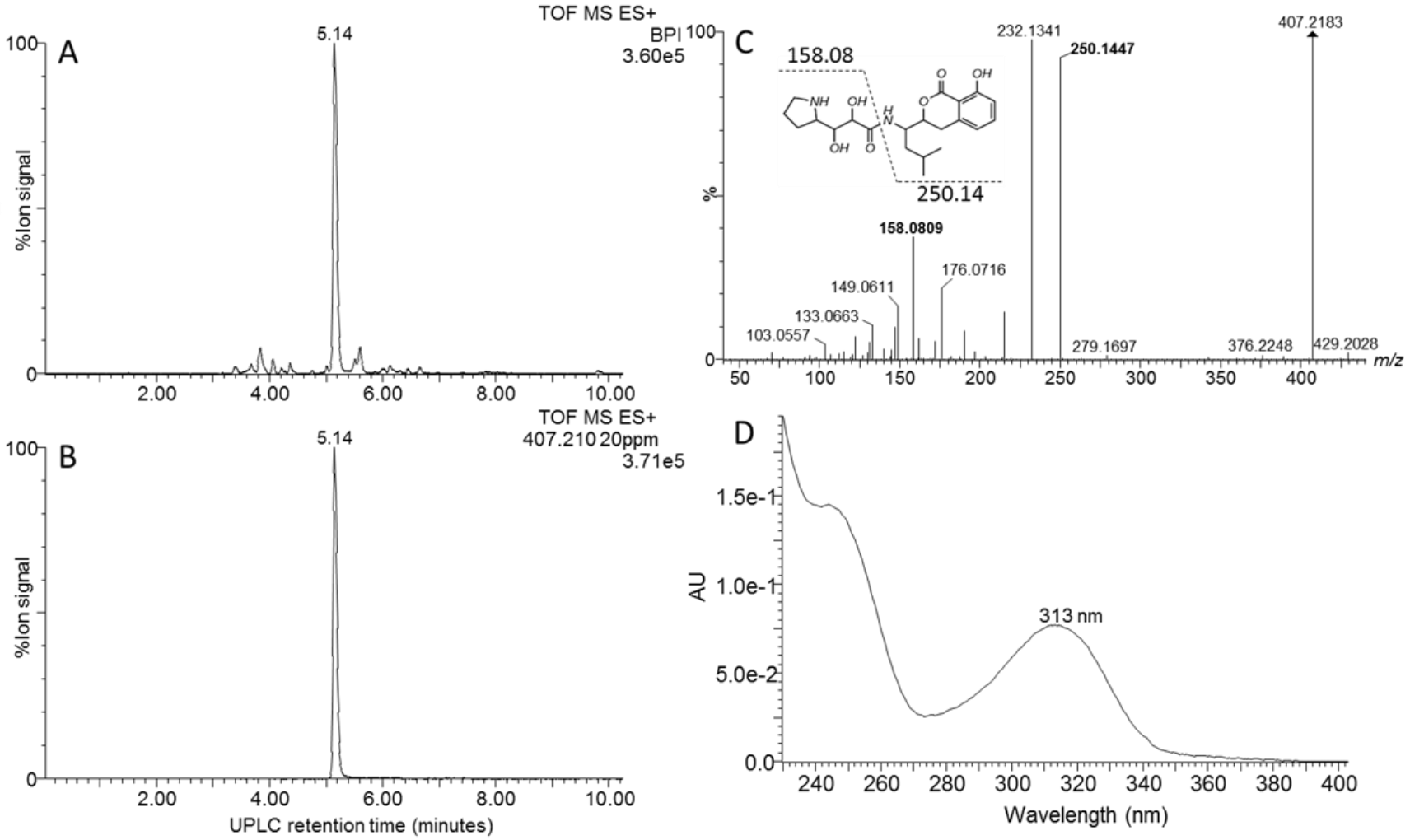

FIGURE S6. Structural analyses of compound **18** – xenocoumacin II. (A) UPLC-MS analysis of the purified compound, (B) the extracted *m/z* chromatogram of the xenocoumacin II ion with *m/z*= 407.210, (C) high resolution MS-MS spectrum of 407.210; (D) Uv spectrum of the xenocoumacin II.

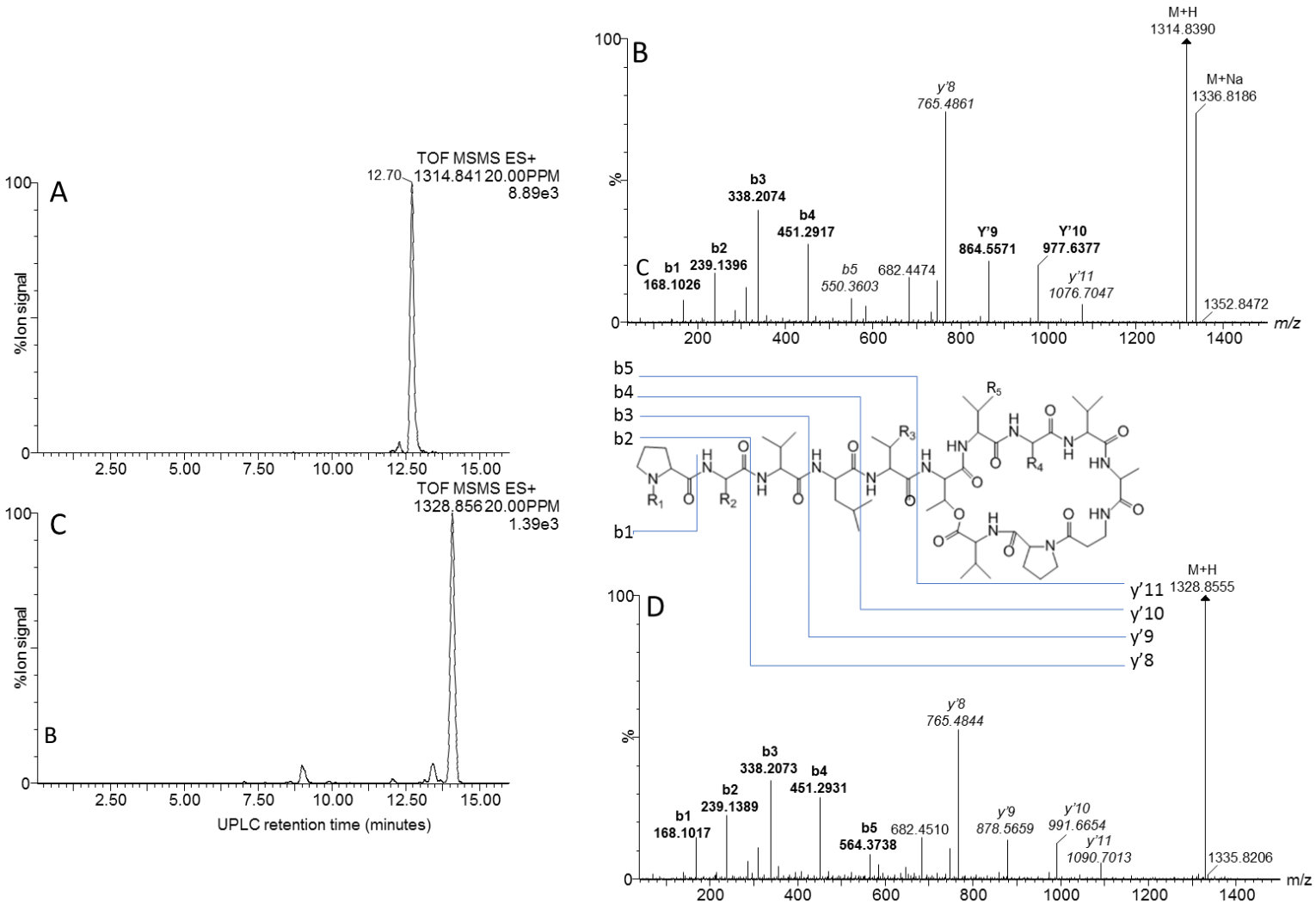

FIGURE S7. Structural analyses of compounds **38** and **42** – xenoamicins. UPLC-MS-MS analysis showing the m/z extracted chromatogram of ion at *m/z* 1314.841 (A) and ion at 1328.856 (B). High resolution MS-MS spectra of *m/z* 1314.841 (C) and *m/z* 1328.856 (D).

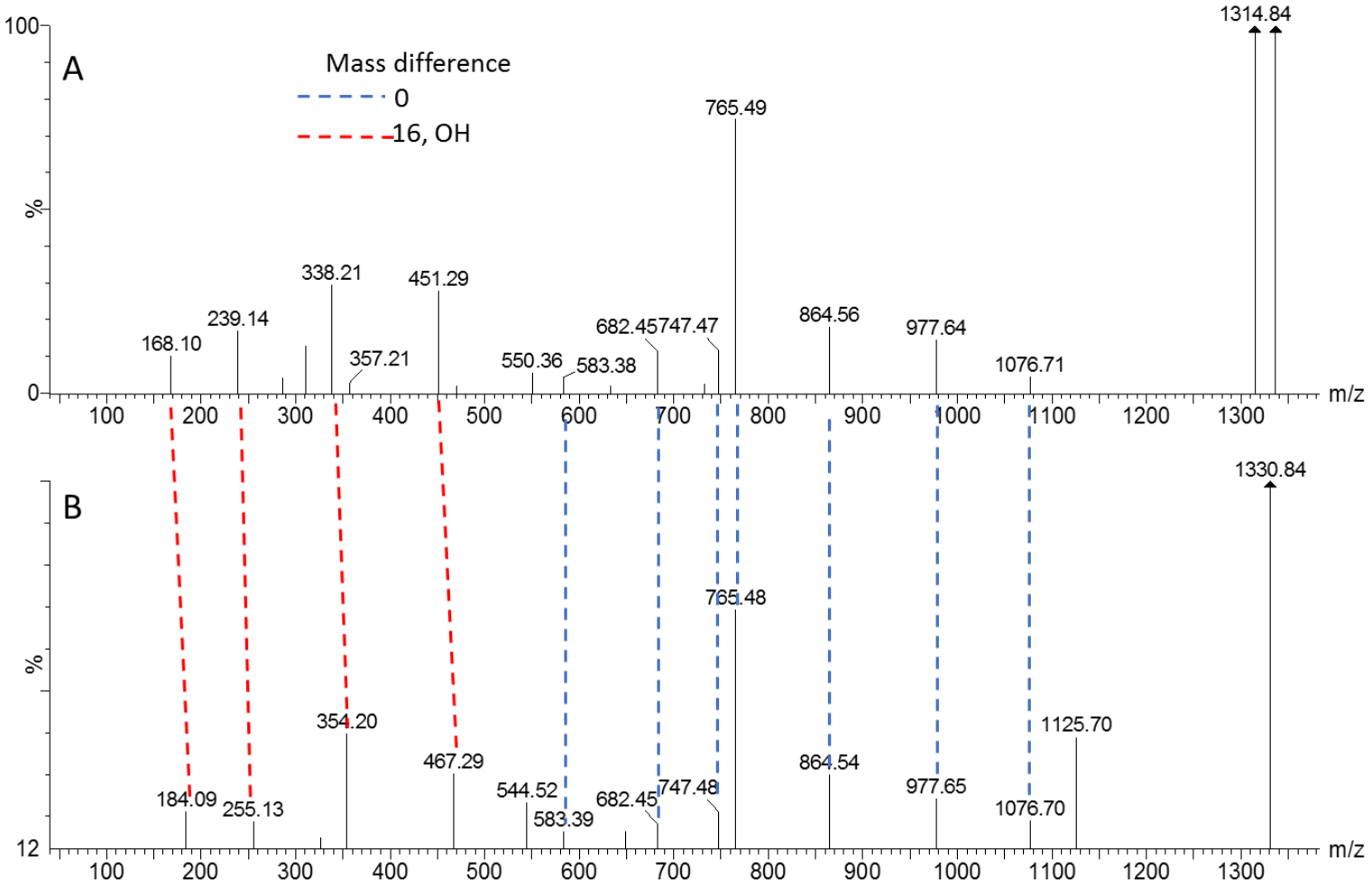

FIGURE S8. Comparison of the MS-MS of **37** and **42** – xenoamicins. High resolution MS-MS spectra of *m/z* 1314.841 (A) and *m/z* 1330.856 (B).

C Domains

	Core/Motif 1 SxAQxRxxxL	Core/Motif 2 RHExLRTxF	Core/Motif 3 MHHxISDGxS
SYNT 1 – MOD 1	----------	----------	----------
SYNT 1 – MOD 2	HLAQPRDDAY	RFPILRTAF	QHHSIIDGWS
SYNT 2 – MOD 3	----------	----------	----------
SYNT 3 – MOD 4	----------	----------	----------
SYNT 3 – MOD 5	SFAQQRLWFL	RQEILHTRF	HHHIISDGWS
SYNT 3 – MOD 6	SFAQQRLWFL	RQEILRTRF	QHHIISDGWS
SYNT 4 – MOD 7	----------	----------	----------
SYNT 5 – MOD 8	----------	----------	----------
SYNT 5 – MOD 9	SFAQQSLWFL	RHESLRTRF	LHHIITDGWS

	Core/Motif 4 YxDxAVW	Core/Motif 5 XGxFVNTxxxR	Core/Motif 6 xQDxPFE
SYNT 1 – MOD 1	----------	----------	----------
SYNT 1 – MOD 2	AESEAYW	VGLYINTLPLM	HSLFVFE
SYNT 2 – MOD 3	----------	----------	----------
SYNT 3 – MOD 4	----------	----------	----------
SYNT 3 – MOD 5	YADYAVW	MGFFVNTLALR	HQDLPFE
SYNT 3 – MOD 6	YADYAVW	IGFFVNTLALR	HQDLPFE
SYNT 4 – MOD 7	----------	----------	----------
SYNT 5 – MOD 8	----------	----------	----------
SYNT 5 – MOD 9	YADYAVW	MGFFVNTLALR	HQDLPFE

A Domains

	Core/Motif 1 LxYxEL	Core/Motif 2 LKAGxAYLxPxD	Core/Motif 3 LAYxxYTSGxTGxPKG	Core/Motif 4 FDxS	Core/Motif 5 NxYGPTE
SYNT 1 – MOD 1	LTYRQL	LKAGGAYVPIS	LAYIIYTSGTTGQPKG	FDAS	NLYGPTE
SYNT 1 – MOD 2	LTYRQL	LKAGGAYVPIS	LAYIIYTSGTTGQPKG	FDGS	NAYGPTE
SYNT 2 – MOD 3	LTYRQL	LKAGGAYVPIS	LAYIIYTSGTTGQPKG	FDAS	NQYGPTE
SYNT 3 – MOD 4	LSYGEL	LKAGGAYVPLD	VAYVIYTSGSTGLPKG	FDVA	NHYGPTE
SYNT 3 – MOD 5	LSYEEL	LKAGGAYVPLD	LAYVIYTSGSTGLPKG	FDAS	NAYGPTE
SYNT 3 – MOD 6	LSYGEL	LKTGGAYVPLD	LAYVIYTSGSTGKPKG	FDFS	NMYGITE
SYNT 4 – MOD 7	LSYDEL	LKAGGAYVPLD	RAYIIYTSGSTGLSKG	FDAA	HMYGPTE
SYNT 5 – MOD 8	MSYGEL	LKAGGAYVPLD	LAYVIYTSGSTGLPKG	FDVA	NHYGPTE
SYNT 5 – MOD 9	ISYGEL	LKAGGAYVPLD	LAYVIYTSGSTGQPKG	FDAS	NGYGPTE

	Core/Motif 6 GELxIxGxGxARGYL	Core/Motif 7 YxTGDL	Core/Motif 8 GRxDxQVKIRGxRIELGEIE	Core/Motif 9 LPxYMxP	Core/Motif 10 NGKxDR
SYNT 1 – MOD 1	GELYIGGAGLARGYR	YKTGDL	GRNDFQVKIRGYRIELGEIE	LPEYMIP	NGKLDR
SYNT 1 – MOD 2	GELYIGGAGLARGYL	YKTGDL	GRNDFQVKIRGYRIELGEIE	LPEYMLP	NGKLDR
SYNT 2 – MOD 3	GELYIGGAGLARGYW	YKTGDR	GRNDFQVKIRGYRIELGEIE	LPEYMLP	NGKLNR
SYNT 3 – MOD 4	GEIHIAGAGVARGYL	YKTGDL	GRNDFQVKLRGFRIELGEIE	LAEYMLP	NGKLDR
SYNT 3 – MOD 5	GEIYIAGAGVARGYL	YRTGDL	GRNDFQVKLRGFRIELGEIE	LAEYMLP	NGKLDR
SYNT 3 – MOD 6	GEIYIVGAGVTRGYL	YKTGDL	GRNDFQVKIRGFRIELGEIE	LAEYMLP	NGKLDR
SYNT 4 – MOD 7	GEIYVAGAGVARGYL	YKTGDL	GRNDFQIKLRGFRIELGEIE	LAEYMLP	NGKTDR
SYNT 5 – MOD 8	GEIHIAGAGVARGYL	YKTGDL	GRNDFQIKIRGFRIELGEIE	LAEYMLP	NGKLDR
SYNT 5 – MOD 9	GEIHIAGAGVARGYL	YKTGDL	GRNDFQVKLRGFRIELGEIE	LAEYMIP	NGKLDR

Thiolation domain

	Core/Motif T DxFFxLGGxSx
SYNT 1 – MOD 1	DNFFRIGGDSI
SYNT 1 – MOD 2	DNFFRIGGNSL
SYNT 2 – MOD 3	DNFFRLGGNSL
SYNT 3 – MOD 4	DHFFELGGHSL
SYNT 3 – MOD 5	DHFFELGGHSL
SYNT 3 – MOD 6	DHFFELGGHSL
SYNT 4 – MOD 7	DHFFELGGHSL
SYNT 5 – MOD 8	DHFFELGGHSL
SYNT 5 – MOD 9	DHFFELGGHSL

FIGURE S9. Alignment of conserved sequences of the (A) condensation domain, (B) adenylation domain and (C) thiolation domain (Marahiel et al., 1997).

REFERENCE

Marahiel, M. A., Stachelhaus, T., and Mootz, H. D. (1997). Modular peptide synthetases involved in nonribosomal peptide synthesis. *Chem. Rev*. 97, 2651–2674. doi:10.1021/cr960029e.

STELLENBOSCH UNIVERSITY

Chapter 4

Characterisation of Xenopep and Rhabdin, novel antilisterial peptides produces by *Xenorhabdus khoisanae*

This paper has been prepared for publication in Journal of Antimicrobial Chemotherapy

Characterisation of Xenopep and Rhabdin, novel antilisterial peptides produced by *Xenorhabdus khoisanae*

E. Booysen[1], M. Rautenbach[2] and LMT Dicks[1]

[1]Department of Microbiology, [2]Biopep peptide group, Department of Biochemistry, Stellenbosch University, Stellenbosch, South Africa

Abstract

Objectives: To characterise two antilisterial peptides, xenopep and rhabdin, isolated from *Xenorhabdus khoisanae* J194, based on structure, stability, activity spectrum and mode of action

Methods: The structure of xenopep and rhabdin was investigated with ultraperformance liquid chromatography linked to mass spectrometry and nuclear magnetic resonance (NMR). The stability of xenopep and rhabdin was performed by exposing the peptides to various proteases, pH values, long-term storage conditions and heat treatment. Mode of action was determined by studying the effect xenopep has on the cell membrane of *Listeria monocytogenes.*

Results: Xenopep and rhabdin share a tetra-peptide sequence but differ in antimicrobial activity. Xenopep is active against *L. monocytogenes* and *Staphylococcus epidermidis*, whilst rhabdin is active against *L. monocytogenes, S. epidermidis, Staphylococcus aureus* and *Escherichia coli.* The antimicrobial activity of xenopep and rhabdin increased after heat treatment, but storing xenopep in suspension caused a loss in activity. After exposing *L. monocytogenes* to xenopep, the cell membrane was depolarised, propidium iodide uptake increased and ATP leakage was observed. Higher concentrations of xenopep resulted in the formation of elongated cells.

Conclusion: Xenopep is a narrow spectrum antilisterial peptide prone to aggregation and forms pores or lesions in the cell membrane of *L. monocytogenes.*

Introduction

Species from the genus *Xenorhabdus* are endosymbionts of *Steinernema* nematodes and produce several antibacterial and antifungal compounds, some of which are anti-parasitic[1]. The ability of these bacteria to produce more than 23 different classes of antimicrobial compounds makes them an attractive source for discovery of novel antibiotics[2,3] and insecticides[1]. The discovery and registration of novel antimicrobial compounds is crucial, especially with the

increase in antibiotic resistance amongst strains of *Enterococcus faecium*, *Staphylococcus aureus*, *Klebsiella pneumoniae*, *Actinobacter baumannii*, *Pseudomonas aeruginosa* and *Enterobacter* spp[4]. Control of *L. monocytogenes* infections is equally important, as the species is often associated with the contamination of ready-to-eat food[5] and systemic infections of immunocompromised individuals, newborns, pregnant woman and the elderly[6]. Infection may also lead to miscarriages, spontaneous abortion and premature birth[7–9]. In severe cases infection may cause rhombencephalitis, encephalitis and meningitis[10].

Listeria infections are generally treated with tetracycline, ampicillin, gentamycin and erythromycin[11] but with a long history of infections, it is no surprise that strains of *L. monocytogenes* have developed resistance to many of the commonly used antibiotics[12]. The first antibiotic-resistant strains of *L. monocytogenes* were isolated in 1988[13]. Since then, numerous strains of antibiotic resistant *L. monocytogenes* have been isolated. Prazak *et al.*[14] reported that 95% of environmental strains (20 out of 21) isolated in Texas, USA, were resistant to two or more commonly used antibiotics. In 2005 a research group in Turkey reported that 66% of isolates from raw or cooked meat were resistant to ampicillin, sulfamethoxale and trimethoprim[15]. In another study, 60% of *L. monocytogenes* strains isolated from dairy products in Iran were resistant to ampicillin[16]. From the above and numerous other studies documented by Olaimat *et al.*[17] it is clear that the prevalence of antibiotic-resistant *L. monocytogenes* isolates have increased significantly over the last two decades.

The 1998 outbreak of listeriosis in the USA, caused by a single strain of *L. monocytogenes* in contaminated deli meats and hot dogs, spread over 10 states. Forty cases of infection were reported, resulting in 14 deaths and four miscarriages. Two years later a further 29 cases of *L. monocytogenes* infections were reported. This outbreak resulted in three miscarriages and four deaths. The source of the contamination was traced to turkey meat[18].Reported cases of listeriosis in the European Union (EU) increased from 667 in 1999 to 1583 in 2006. A multi-country outbreak was reported in 2018 by the EU with, 32 reported cases and six deaths. For further information on listeria infections in the EU the reader is referred to Tchatchouang *et al*[18]. In 2003 Australia experienced one of the worst listeriosis outbreaks to date, with a mortality rate of 30%. In 2009 an outbreak was reported, linked to contaminated chicken wraps sold on domestic flights, followed by another outbreak in 2010, caused by contaminated melons[18]. Several listeriosis outbreaks have also been reported in Asia, with the majority of the cases registered in Bangkok[19], Taiwan[20] and Japan[6]. In Africa listeriosis outbreaks have been reported in Nigeria and South Africa. In 2017 a severe listeriosis

outbreak occurred in South Africa, with 1060 cases and 216 deaths reported. The majority of these cases were reported in newborns[18]. All of the cases in South Africa were linked to contaminated processed meat[21]. The outbreak in SA led to an estimated cost of US $380 million[18]. It is clear from the statistics on *L. monocytogenes* outbreaks and the increased resistance to antibiotics that novel antimicrobial compounds need to be developed to control infections. This requires more research on, and an in-depth understanding of, antimicrobial compounds produced by bacteria from novel niches.

Not much is known about the mode of action of antimicrobial peptides produced by *Xenorhabdus* ssp., except for PAX peptides[22] and nematophin[23]. PAX peptides interact with the cell membrane of *E. coli*[22]. In contrast to other cationic antimicrobial peptides (AMP), PAX peptides did not interact with chromosomal DNA[24]. In 2019 Zhang *et al.* reported that *Rhizoctonia solani* exposed to nematophin had shrivelled growing points as well as deformed mitochondrial structures, indicating that nematophin interacted with the cell wall and internal membrane structures[23]. Similar to PAX peptides, xenopep also interact with the cell membrane, although further research is needed to determine if xenopep flood the cytosol. Here we reported on the effect of xenopep on the cell membrane of *L. monocytogenes* ATCC 7644.

Materials and methods

Growth conditions of strains

L. monocytogenes ATCC 7644, EDGe and RTE9 were cultured in Listeria Enrichment Broth (LEB), *S. epidermidis SE1* and *S. aureus* ATCC 25923 was cultured in Brain Heart Infusion (BHI) and *E. coli* xen 14 was cultured in Luria Broth (LB). All cultures were incubated at 37°C for 24 h on a rotating test tube wheel. *Xenorhabdus khoisanae* J194 was cultured on nutrient agar, supplemented with 0.025% (*w/v*) bromothymol blue and 0.04% (*w/v*) triphenyl tetrazolium chloride (NBTA), and incubated at 30°C for a minimum of 48 h. Blue colonies, representative of cells in phase I[25], were selected and cultured in Tryptone Soy broth (TSB) at 30°C for 24 h on an orbital shaker.

Isolation of xenopep and rhabdin

Method A:

Ten millilitres of TSB were inoculated with a blue, phase I, *X. khoisanae* J194 colony and incubated at 30°C on a rotating wheel for 18 hours. Five millilitres of a 18 h-old culture of *X.*

khoisanae J194 (OD = 1.00) was mixed with 5.0 g sterile Amberlite XAD-16 and plated onto TSA (TSB with 2.0%, *w/v*, agar). Plates were incubated at 26°C for 96 h. After incubation the resin was washed with 30 % (*v/v*) ethanol to remove non-specific binding. Xenopep and rhabdin were eluted from the beads using 80% (*v/v*) isopropanol, containing 0.1 % (*v/v*) Trifluoroacetic acid (TFA). Isopropanol was removed by rotary evaporation and the crude extract concentrated by freeze-drying.

Method B:

Clarified TSB was prepared by adding 20 g XAD-16 resin to 800 mL TSB and left at 4°C for 1 h. The resin was removed by filtration and the clarified TSB (filtrate) autoclaved and the entire volume inoculated with 10 mL of an actively growing *X. khoisanae* J194 culture. After 96 h of incubation at 26°C, the culture was centrifuged (4700 *x* g, 10 min), 20 g of XAD-16 resin added to the cell-free supernatant and left at 4°C for 3 h. The resin was collected as described elsewhere and washed with 30% (*v/v*) ethanol to remove non-specific binding. Xenopep was eluted from the resin with 80% (*v/v*) isopropanol containing 0.1% (*v/v*) TFA. The latter was removed by rotary evaporation. The xenopep crude extract was freeze-dried. A detailed description of the methods used can be found in the supplementary document.

Purification of xenopep and rhabdin

Freeze-dried crude extracts of xenopep and rhabdin were suspended in 50 % (*v/v*) acetonitrile and loaded onto a Poroshell 120 EC-C_{18} column (120 Å, 4 µm, 4.6 mm x 150 mm, Agilent, California, USA). Separation was by high-performance liquid chromatography (HPLC), using the Agilent 1260 Infinity II LC system. Compounds were eluted using a linear gradient of 0.1 % (*v/v*) TFA in analytically pure water (eluent A) and 0.1 % (*v/v*) TFA in acetonitrile (eluent B). The flow rate was set at 1.5 mL/min and the elution program used was as follows: 20% eluent A from 0.0 to 0.5 min (initial conditions), 0.5 to 12.5 min linear gradient from 20% to 90% eluent B, 12.5 to 13.0 min linear gradient from 90% to 100% eluent B, 13.0 min to 14.0 min at 100% eluent B, followed by column equilibration (14.0 to 20.0 min linear gradient from 100% to 20% eluent B and 20.0 to 25.0 min at initial conditions). Data was recorded at 245 nm and 314 nm, respectively. Fractions were collected, freeze-dried and, tested for antimicrobial activity using an agar well diffusion assay as described elsewhere[26].

Active fractions containing xenopep and rhabdin, corresponding to those reported by Booysen *et al.*[26], were identified with ultraperformance liquid chromatography (Waters Acquity UPLC™), linked to mass spectrometry (UPLC-MS). The system was coupled to a

Waters Synapt G2 quadrupole time-of-flight mass spectrometer (QTOF; Waters, Milford, USA). Fractions containing both rhabdin and xenopep were loaded onto the Poroshell 120 EC-C18 column for a second time and eluted using a linear gradient. The flow rate was set at 1.5 mL/min and the elution program was as follows: 20% eluent A from 0 to 0.5 min (initial conditions), 0.5 to 12.5 min linear gradient from 20% to 60% eluent B, 12.5 to 14.0 min linear gradient from 60% to 100% eluent B, 14.0 min to 15.0 min at 100% eluent B, followed by column equilibration (15.0 to 20.0 min linear gradient from 100% to 20% eluent B and 20.0 to 25.0 min at initial conditions). Data was recorded at 245 nm and 314 nm and fractions were collected with the Agilent 1260 Infinity II LC system fraction collector. Fractions were freeze-dried and tested for antimicrobial activity as described elsewhere. Active fractions were further analysed using UPLC-MS/MS^{E}, to confirm the presence of xenopep and rhabdin was identified with this technique. Samples were injected onto a HSS T3 column (1.8 µm, 2.1 mm x 100mm) a linear gradient was created with 0.1% (*v/v*) formic acid in analytical pure water (eluant A) and 0.1% (*v/v*) formic acid in acetonitrile (eluant B). The following elution program was used: 20% eluent B from 0.0 to 0.5 min (initial conditions), 0.5 – 12.5 min linear gradient from 20 to 90% eluent B, 12.5 – 13.0 min linear gradient from 90% to 100% eluent B, 100% eluent B from 13.0 – 14.0 min, 14.0 – 14.1 min linear gradient from 100% to 20% eluent B, followed by column equilibration (20% eluent B from 14.1 – 16.0 min). Settings for mass spectrometric detection were as follows: cone voltage 15 V, capillary voltage 2.5 kV, extraction cone voltage 4 V, source temperature 120°C, desolvation gas (N_2) at 650 L/h and temperature 275°C. Spectral data were collected in positive mode by scanning through *m/z* = 100 to 2000 in continuum mode[26].

NMR analysis of xenopep and rhabdin

The fraction containing Xenopep was dissolved in DMSO-d_6 (1.5 mM) and acetonitrile-d_3 (1.5 mM). Rhabdin, previously purified[27], was dissolved in DMSO-d_6 (1.5 mM,). Chemical shifts are expressed with respect to the DMSO-d_6 residual signal at 2.5 and the acetonitrile-d_3 residual signal at 1.9. All NMR experiments were conducted on a Varian ^{unity}*Inova* 600 Liquid State NMR spectrometer (Varian, California, USA) equipped with a 5 mm ^{1}H indirect detection PFG Probe. All data were processed with MestReNova software (version 11.0.2-18153).

Antimicrobial activity

Antimicrobial activity of xenopep and rhabdin was determined using the agar well diffusion assays were performed as follows: Target strains were cultured as described elsewhere in

respective growth media. These cultures were used to inoculate (1%, *v/v*) sterile molten BHI and LEA (approximately 45°C). The tubes were carefully swirled and the cell suspension of each immediately transferred to a petri dish (90 mm diameter). A sterilised 96-well PCR plate was inserted into the molten agar to create wells. Once the agar was set a defined concentration of peptide was carefully pipetted into each well. Erythromycin (13 µM) was used as positive control and 10 mM Tris-HCl as negative control. Plates were incubated at 37°C for 18 h and zones were measured the next day. Digital photos were taken of inhibition zones, adjusted for contrast, enlarged (from 90 to a digital 360 mm) and the zones measured using the Microsoft Powerpoint size tool for objects. The average of the vertical and horizontal diameter of a zone was taken as the inhibition size

A modified version of the Clinical Laboratory and Standard Institute (CLSI) broth microdilution method[28] was used to determine the minimum inhibitory concentration (MIC) and minimum bactericidal concentration (MBC) of xenopep and rhabdin. Cell suspensions of *S. aureus* ATCC 25923, *S. epidermidis* SE1, *E. coli* Xen 14, and *L. monocytogenes* ATCC 7644, EDGe and RTE9 (5×10^6 CFU/mL) were prepared and pipetted into the wells of a sterile 96-well microtiter plate. *S. aureus* ATCC 25923 and *S. epidermidis* SE1 was prepared in BHI, *E. coli* Xen 14 was prepared in LB and *L. monocytogenes* ATCC 7644, EDGe and RTE9 was prepared in LEB. A 2-fold concentration range of each peptide was pipetted into the wells. Plates were incubated at 37°C for 24 h, 20 µL 0.1 mg/mL resazurin added (final concentration: 10 µg/mL) and incubated for a further 2 h as described by Foerster *et al.*[29] and Elshikh *et al*[30]. The MIC and MBC of peptides were calculated according to CLSI guidelines. A change in colour was used to determine the MIC. Before adding resazurin, 20 µL from each well was serially diluted and plated onto Listeria Enrichment Agar (LEA) to determine the MBC. Plates were incubated at 37°C for 24 h. The MIC value was defined as the lowest concentration of peptide that did not cause a colour change from blue to pink/red. The MBC value was calculated from the lowest concentration of xenopep or rhabdin that inhibited cell growth or caused a log-3 reduction in cell numbers (correlating to at least 99% inhibition). Activity was considered bactericidal if the MBC/MIC ratio was ≤ 4[31,32].

Stability of xenopep and rhabdin

The effect of proteolytic enzymes changes in pH and temperature, and storage conditions on the activity of xenopep and rhabdin were determined as follows:

Pepsin (10 mg/mL) was suspended in analytically pure water containing 0.1% TFA (*v/v*), and proteinase K and trypsin (10 mg/mL each) in 10 mM Tris-HCl (pH 8.0). The proteases were added to xenopep (20 µM and 15 µM) and rhabdin (12 µM) at a final concentration of 1 mg/mL and incubated for 2 h at 37°C. Nisin (10 µM) treated the same was used as positive control. In two separate experiments, the pH of xenopep (150 µL; 30 µM) was lowered to 2.0 by adding 1.0 µL 5M HCl and increased to 12.0 by adding 1.0 µL 5M NaOH. Xenopep, suspended in 10 mM Tris-HCl (pH 7.4) to a final concentration of 20 µM, 18 µM and 15 µM were stored at -20°C and 22°C, respectively. After 60 days, activity was tested using the agar-well diffusion assay as described elsewhere. Xenopep suspensions of 20 µM, 18 µM and 15 µM, and rhabdin suspensions of 20 µM, 15 µM and 12 µM were prepared in 10 mM HCl-Tris (pH 7.4) and incubated at 100°C for 10 minutes.

In all stability test antimicrobial activity was determined using the agar-well diffusion assay as described elsewhere, with *L. monocytogenes* ATCC 7644 as target. Inhibition zone size were calculated from digital images as described elsewhere.

Mode of action

Interaction between xenopep and rhabdin

Soft BHI agar (1%, *v/v*) was inoculated with 1% (*v/v*) of an 18-h old culture of *L. monocytogenes* ATCC 7644 and *S. epidermidis* SE1 respectively. A sterile 96-well PCR plate was placed into the molten agar. Once the agar was set the PCR plate was removed and 15 µL xenopep (15 µM) and 15 µL rhabdin (12 µM) pipetted into wells in proximity. The plates were incubated at 37°C for 18 h, digital images of inhibition zones recorded, and activity determined as described elsewhere.

Time-kill kinetics assay

The bactericidal activity of xenopep was determined by measuring the reduction in viable *L. monocytogenes* ATCC 7644 cells over 6 h as described by Yasir *et al*[34]. *L. monocytogenes* ATCC 7644 was cultured in LEB (1 x 10^7 cfu/mL) and xenopep added to yield final concentrations of 15 µM and 30 µM, respectively. Aliquots were immediately sampled, and after 30, 60, 90, 120, 180, 240 and 360 min, serially diluted in LEB and plated onto LEA. Plates were incubated at 37°C for 24 h and colonies counted.

Membrane depolarisation

Depolarisation of the cytoplasmic membrane of *L. monocytogenes* ATCC 7644 was studied as follows: Cells were grown to mid-logarithmic phase in LEB (OD_{600nm} = 0.5), harvested (5000 x g, 10 min), washed and resuspended in 5 mM HEPES containing 20 mM glucose (pH 7.2) to an OD_{600} of 0.05. To each cell suspension $DiSC_{3-5}$ was added to a final concentration of 4 µM and incubated in the dark for 60 min at 22°C. After incubation, KCl (100 mM) was added to cell suspensions to equilibrate the cytoplasmic membranes and 90 µL pipetted into wells of a black 96-well microtiter plate. Xenopep was added to the cell suspensions to a final concentration of 30 µM and 15 µM, respectively. Triton X-100 (1%, v/v) was used as positive control and 10 mM Tris-HCl as negative control. Fluorescence was measured using a Tecan Spark multi-reader (Tecan, Männedorf, Switzerland), set at excitation and emission wavelengths of 622 nm and 670 nm, respectively. Fluorescence intensity was measured every 30 seconds for 6 min.

Cell leakage assay

The effect of xenopep on the integrity of the cytoplasmic membrane of *L. monocytogenes* ATCC 7644 was determined using the Syto9/propidium iodide stain (BacLight, Thermofisher, Massachusetts, USA)

Penetration of Syto9/propidium iodide was measured using flow cytometry, according to the method of Yasir *et al* [33,35]. *L. monocytogenes* ATCC 7644 was cultured to mid logarithmic phase (OD_{600} = 0.5) in LEB, washed and resuspended in 20mM phosphate buffer (PB, pH 7.4) to a final cell number of 1 x 10^6 CFU/mL (OD_{600nm} = 0.1). Syto9 (7.5 µM) and propidium iodide (PI, 30 µM) were added to the bacterial suspension and incubated for 15 min in the dark. After incubation, 15 µM and 30 µM xenopep was added, respectively, to each cell suspension. Changes in fluorescence was recorded immediately, and again after 15, 60 and 120 min. Readings were taken with the BD FACS Melody (BD Biosciences, New Jersey, USA). The excitation and emission wavelength of Syto9 was set at 525 nm and 550 nm respectively. The excitation and emission wavelength of PI was set at 610 and 620 nm, respectively. A minimum of 20000 events were recorded for each sample. Statistical analyses were performed with graph pad prism software (version 5.01) and data were expressed as standard mean and error (SEM). One-way ANOVA and Dunnett's *post hoc* test or two-way ANOVA with Bonferroni's *post hoc* test, were used to analyse applicable data sets. Values of $P < 0.05$ were regarded statistically significant. All assays were performed in triplicate.

Release of cellular components

Leakage of ATP from damaged cells of *L. monocytogenes* ATCC 7644 was recorded using the ATP bioluminescence kit (Invitrogen, Massachusetts, USA). Cells were cultured to mid-logarithmic phase (OD_{600nm} = 0.5) and xenopep added to final concentrations of 15 µM and 30 µM, respectively. Incubation was for 10 min at 37°C. Samples were withdrawn every 2 minutes and centrifuged at 5000 x g for 10 min. Cell-free supernatants were removed and kept on ice. Total ATP was determined by resuspending the bacterial pellets in boiling 100 mM Tris and, 4mM EDTA (pH 7.4), followed by boiling for an additional 2 minutes. ATP concentrations were determined according to the protocol supplied with the ATP determination kit (Invitrogen, Massachusetts, USA). In short, 90 µL of a standard reaction solution and 10 µL of sample was deposited into wells of a black 96-well microtiter plate. Luminescence was measured using a Tecan Spark multi-reader. Statistical analyses were performed as described elsewhere. The % change was calculated in terms of the control (10 mM Tris) using the following equation:

$$\% \text{ Change in ATP} = 100\ x\ (\frac{(Treatment - Tris)}{Tris})$$

Scanning electron microscopy

The method from Babii *et al.*[36] was adapted to visualise cell membrane integrity of *L. monocytogenes* ATCC 7644 exposed to xenopep. Cells were cultured to mid logarithmic phase (OD_{600} = 0.5) and xenopep added to final concentrations of 15 µM and 30 µM, respectively. After 4 h of incubation at 37°C the cells were deposited onto a 0.2 µm Isopore polycarbonate filter (Merck Milipore, Massachusetts, USA) and fixed with 2.5% (*v*/v) glutaraldehyde in phosphate buffer saline (PBS) for 2 h. After fixation, filters were washed twice with PBS and dehydrated for 15 min in a stepwise gradient of ethanol (30%, 50%, 70%, 80% and 100%). Samples were dried using hexamethyldisilazane (HMDS) as a drying liquid, sputter-coated with a 10 nm layer of gold and examined using a scanning electron microscope (Zeiss MERLIN SEM, Germany) set at an acceleration voltage of 5 kV. Tris-HCl (10 mM) was used as negative control.

Results and discussion

Production and purification of xenopep and rhabdin

Rhabdin and xenopep were produced using isolation method A in which production was on TSB (Figure S1). Separation of xenopep and rhabdin was difficult using HPLC and rhabdin

could only be isolated to approximately 75% purity. Method B yielded only xenopep (Figure S2), which was isolated to 95% purity after sequential HPLC steps (Figure S3). Molecular mass and amino acid sequences were confirmed with UPLC-MS/MS^{E} and correlated with previous findings[26]. Several other research groups have also reported on the influence of temperature, initial pH and aeration on the production of antimicrobial compounds. Examples are *Serratia* spp.[37], *Streptomyces* spp.[38,39], *Xenorhabdus khoisanae*[26] and *Lactobacillus* spp.[40].

Structure characteristics of xenopep and rhabdin

Xenopep and rhabdin are similar in structure and share the same sequence of hydrophobic amino acids (Pro-Pro-Phe-Leu), and possibly an unknown hydrophobic amino acid (Haa) in the N-terminus[26]. These findings were supported with NMR spectra of alpha and aliphatic proton regions (Figure S4 b and c), and the amide proton region (Figure S5). Two aromatic amino acid signals were putatively identified in the amide proton spectrum, namely phenylalanine and a unknown aromatic compound that may represent the Haa amino acid (Figure S5, green circles). Alpha protons for these two aromatic residues were also visible in the alpha proton region of the spectrum (Figure S4, green circles). The identity and structure of Haa with putative M_r as 99.07 (correlates to C_5H_9NO). remains unknown, as identification was complicated by peak broadening and spectral overlaps in both 1D and advanced 2D NMR analysis. Further research is required to unravel the complete amino acid sequence of xenopep and rhabdin. Although further research is necessary to confirm this hypothesis, rhabdin might be a processed form of xenopep. Many micro-organisms excrete pre-peptides with activity levels significantly lower than the processed peptide to protect themselves from the peptide's antimicrobial activity. The same might be possible for xenopep and rhabdin.

Peak broadening in ^{1}H-NMR spectra suggest that xenopep aggregates in the presence of DMSO-d_6. However, peak broadening was not observed when xenopep was resuspended in 80% (*v/v*) acetonitrile prepared with deuterated water (Figure S4 a and b; S5 a and b). Amide peak broadening observed with NMR spectra suggests that different xenopep conformations formed, similar to those found in unordered aggregates certain oligomers. Residue 3 to 6 in xenopep and rhabdin had similar chemical shifts, indicating that these two peptides share a tetra-peptide sequence.

Results obtained with UPLC-MS indicated that xenopep and rhabdin form oligomers that survives the mass spectrometric process, as had been recorded for oligomers with strong electrostatic polar interactions such as salt bridges and hydrogen bonds[42]. However,

aggregation of xenopep and rhabdin in solution could be due to both hydrophobic- and electrostatic polar interactions. Xenopep is more prone to aggregation, as observed with the formation of oligomers up to heptamers (Figure 1a). Rhabdin, on the other hand, did not form stable larger oligomers as low signals were observed for oligomers up to hexamers (Figure 1b).

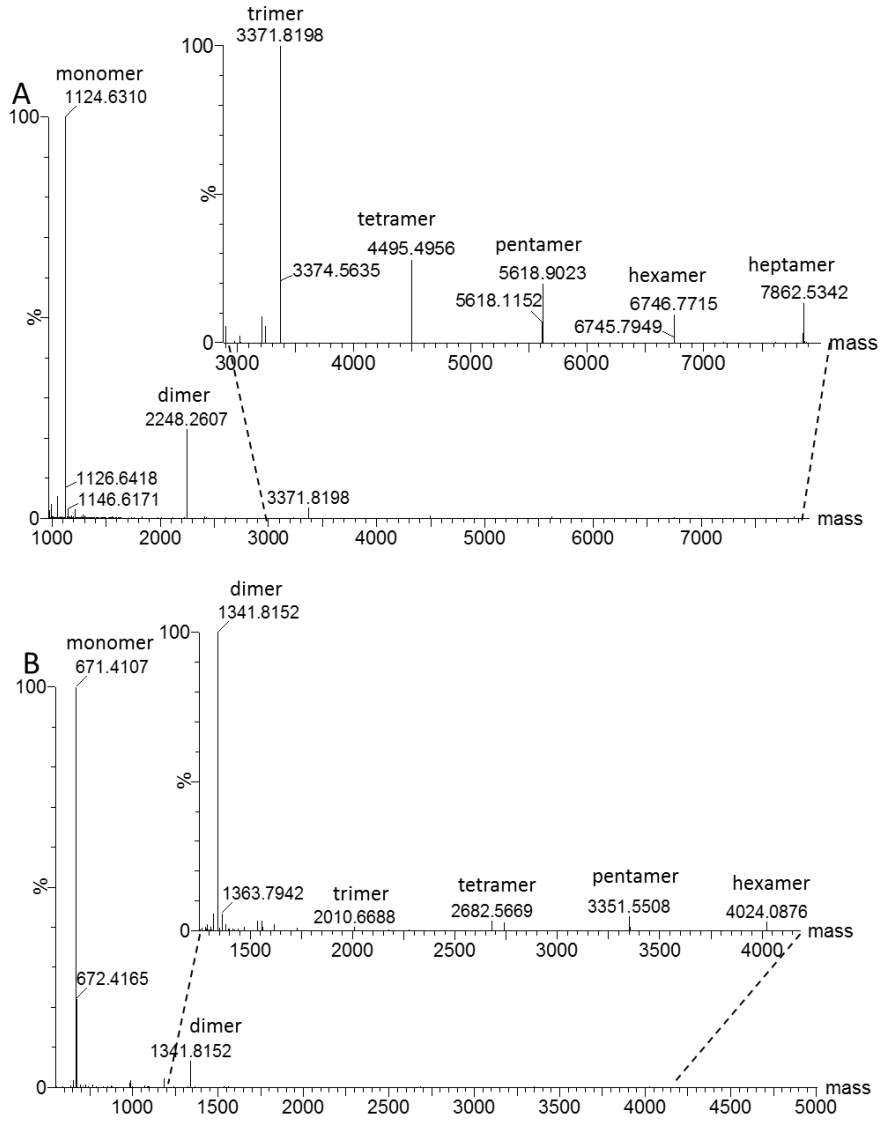

Figure 1: High resolution MS analysis of the Oligomers formed by (a) xenopep and (b) rhabdin. Xenopep forms strong stable oligomers from dimers up to heptamers. While rhabdin is less prone to form oligomers, although low signals for dimers up to hexamers were observed.

Antibacterial activity of xenopep and rhabdin

An interesting difference in activity was observed between the two peptides, although previous studies and our NMR analyses indicated that the two peptides share similar amino acid sequences. The MIC and MBC values for rhabdin is listed in Table 1.

MIC values recorded for xenopep against *L. monocytogenes* ATCC 7644, *L. monocytogenes* EDGe and *L. monocytogenes* RTE9, were 15 µM, 20 µM and 20 µM. For all three strains of *L. monocytogenes* MBC/MIC ratios were < 4 (MBC/MIC = 2), suggesting that xenopep is bactericidal. Xenopep MIC values of 11 µM were recorded against *S. epidermidis* SE1. *Lactiplantibacillus plantarum* 423 and *Lacticaseibacillus rhamnosus* R11 were sensitive to 15 µM xenopep. A much higher concentration of xenopep (45 µM) were required to kill *Lacticaseibacillus casei* 106. Xenopep had no effect on *Limosilactobacillus reuteri* DSM 17938 and *Enterococcus mundtii* ST4SA (Table 2 and S2). This is noteworthy, as lactic acid bacteria form the major group of Firmicutes in the human GIT[43].

Rhabdin was active against all three *L. monocytogenes* strains, *S. aureus* ATCC 7644 and *E. coli* xen 14 (Table 1). The MIC of rhabdin required to kill *L. monocytogenes* ATCC 7644, *L. monocytogenes* EDGe and *L. monocytogenes* RTE9 was 12 µM. The MBC/MIC ratio for all three *L. monocytogenes* strains were < 4 (MBC/MIC = 2) suggesting that rhabdin has a bactericidal mode of action. Activity against *S. aureus* ATCC 25923 and *E. coli* Xen 14 was also observed, with MIC values of 5 µM and 30 µM, respectively.

Nisin, a well-known and commercially utilised lantibiotic, has MIC values ranging between 3.75 and 8 µM towards *L. monocytogenes* EDGe[44,45]. The MIC of nisin required to kill *L. monocytogenes* ATCC 7644 was 3 µM (Table 1). The MIC values for xenopep and rhabdin against *L. monocytogenes* is in each case higher than those reported for nisin, suggesting that they are less effective compared to nisin. MIC value reported for nisin and rhabdin against *S. aureus* ATCC 25923 was similar (5 µM and 6 µM, respectively, Table 1), indicating that nisin and rhabdin is equally effective against *S. aureus* ATCC 25923.

Stability of xenopep and rhabdin

Xenopep and rhabdin were not degraded by pepsin, proteinase K and trypsin (Table 3 and S3). The activity of nisin decreased significantly after treatment with pepsin, proteinase K and trypsin. The activity of xenopep treated with 5M HCl decreased significantly in comparison to the control (pH 7, Table 3 and S3). This indicates that xenopep may have acid-labile bonds. A small zone of inhibition was observed for Tris at pH 2 (Table S3), this was expected as *L. monocytogenes* ATCC 7644 is sensitive to a below 2.5[46].

The activity of xenopep decreased significantly over 60 days, with the activity completely disappearing at 15 µM (Table 3 and S3). The activity of xenopep at 20 µM increased significantly after treatment at 100°C for 10 min (Table 3 and S3). Concluded from these

findings, xenopep forms aggregates/oligomers when in suspension and stored at room temperature (22°C). This confirmed results obtained with NMR and UPLC-MS/MS^{E} analyses.

Table 1 Summary of the antibacterial activity data for xenopep and rhabdin with CLSI Broth Assay with resazurin indicator

Target cell	**Strain**	**Peptide/antibiotic**	**MIC (µM)**	**MBC (µM)**	**MIC/MBC**
L. monocytogenes	ATCC 7644	Xenopep	15	30	2
	EDGe		20	40	2
	RTE9		20	40	2
	ATCC 7644	Rhabdin	12	30	2.5
	EDGe		12	30	2.5
	RTE9		12	30	2.5
	ATCC 7644	Nisin	3	10	3.3
	EDGe		8	16	2
	RTE9		8	16	2
S. aureus	ATCC 25923	Xenopep	N/A*	N/A	N/A
		Rhabdin	6	12	2
		Nisin	5	10	2
S. epidermidis	SE1	Xenopep	11	22	2
		Rhabdin	5	10	2
		Nisin	5	10	2
E. coli	Xen 14	Xenopep	N/A	N/A	N/A
		Rhabdin	7	21	3
		Erythromycin	20	40	2

N/A* No activity recorded

Table 2 Summary of the antibacterial activity data for xenopep with agar diffusion assay against five beneficial gut commensal bacteria. The inhibition zones are given in mm

Commensal species and strains	Erythromycin	Xenopep		
	Antibiotic/peptide challenge concentration			
	13 µM	15 µM	30 µM	45 µM
L. plantarum 423	78.1 ± 2.6	41.5 ± 2.1	43.6 ± 0.8	44.9 ± 1.1
L. rhamnosus R11	95.4 ± 0	43.6 ± 0.8	44.9 ± 1.1	47.4 ± 0.1
L. reuteri DSM 17938	60 ± 1.9	0.0 ± 0.0	0.0 ± 0.0	0.0 ± 0.0
L. casei 106	85.9 ± 3.7	0.0 ± 0.0	0.0 ± 0.0	40.9 ± 0.3
E. mundtii ST4SA	58.3 ± 0.5	0.0 ± 0.0	0.0 ± 0.0	0.0 ± 0.0

Table 3 Summary of the antibacterial activity data against *L. monocytogenes* ATCC 7644 for xenopep and rhabdin with agar diffusion assay after different treatments. The inhibition zones are given in mm. Values in bold indicate significant difference

Treatment	**Nisin**	**Xenopep**			**Rhabdin**		
Protease stability							
Concentration (µM)	10	20		15	12		
Untreated	24.2 ± 0.2	21.0 ± 0.7		18.4 ± 0.4	42.1 ± 1.3		
Proteinase K	0.0 ± 0.0	19.5 ± 0.4		17.7 ± 1.1	42.1 ± 1.3		
Pepsin	0.0 ± 0.0	20.4 ± 0.4		18.3 ± 0.4	44.5 ± 1.7		
Trypsin	0.0 ± 0.0	20.4 ± 0.4		17.8 ± 0.6	45.7 ± 0.1		
pH stability							
Concentration (µM)	N/A			30	N/A		
pH 2				**51.8 ± 2.0**			
pH 7	-			65.9 ± 1.6	-		
pH 12				64.5 ± 0.4			
Temperature stability							
Concentration (µM)	N/A	20	18	15	20	18	15
Untreated	-	31.5 ± 0.8	29.6 ± 0.6	27.7 ± 0	68.2 ± 0.7	48.7 ± 1.7	41.3 ± 1.8
Boiling for 10 min @ 100°C		**36.5 ± 2.2**	32.5 ± 0.5	29.8 ± 0.8	71.2 ± 2.3	63.2 ± 2.6	45.9 ± 0.2
Long term stability in solution stability							
Concentration (µM)	N/A	20	18	15	N/A		
Untreated		35.9 ± 0.1	33.2 ± 0.2	27.3 ± 0.4			
Storage for 6 weeks	-	**27.3 ± 0.4**	**26.5 ± 0.8**	**0.0 ± 0.0**	-		

"-"no data available
"N/A" Not applicable

Xenopep mode of action

A previous study has shown that rhabdin is highly toxic to mammalian cells[27]. Due to this and the difficulties encountered in purifying rhabdin only xenopep was further included in mode of action studies. The ability of xenopep and rhabdin to interact was tested in a competitive agar diffusion assay against *L. monocytogenes* and *S. epidermidis.* In this assay synergistic interactions would lead to an elliptical inhibition zone encompassing the two individual inhibition zones when the peptides are placed in proximity. If antagonistic the inhibition will be lost between the two peptides. As can be seen in Fig. 2 these two peptides did not influence each other's activity. This result could indicate that they do not compete for a similar target. Rhabdin is significantly smaller compared to xenopep and might have an intracellular target. Although additional research is needed to confirm this hypothesis.

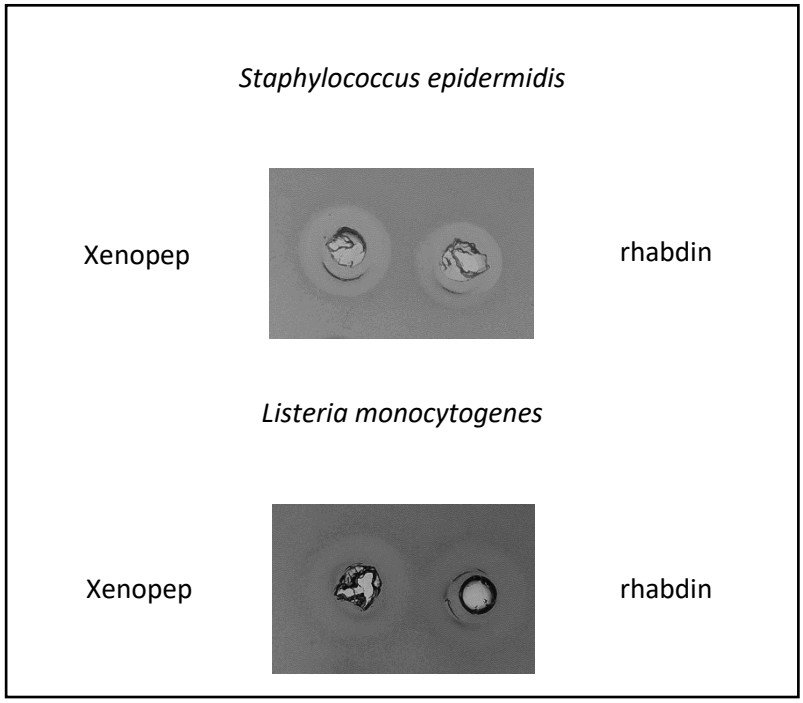

Figure 2: Interaction of between xenopep and rhabdin in a competitive agar diffusion assay against *Staphylococcus epidermidis* SE1 and *Listeria monocytogenes* ATCC 7644. If xenopep and rhabdin were synergistic an elliptical inhibition zone encompassing both individual zones would have been observed. In contrast if xenopep and rhabdin were antagonistic a loss of activity would have been visible between the two zones. Xenopep and rhabdin did not have a synergistic nor an antagonistic effect on each other.

The bactericidal activity of xenopep was studied over 6 hours. Cell numbers of *L. monocytogenes* started to decline after 180 min and led to a more than log-3 reduction after 6 h (Figure 3). A killing rate of 6 x 10^6 CFU/hour was recorded after 3h, whilst the generation time decreased to 1.5 h. This indicated that xenopep killed *L. monocytogenes* ATCC 7644 quicker than the cells could replicate. To further understand the killing kinetics of xenopep we studied it's effect on the membrane of *L. monocytogenes* ATCC 7644.

$DiSC_3(5)$ is a cationic dye that accumulates and aggregates within the bacterial cell membrane causing self-quenching. As the cell membrane is damaged the dye is released and recorded as an increase in fluorescence[47,48]. Xenopep at 15 µM and 30 µM decreased the membrane potential of *L. monocytogenes* as indicated by the increase of absorbance observed for the first 3 minutes (Figure 4), followed by a plateau. No significant difference was observed for the DMSO, 15 µM and 30 µM xenopep treated *L. monocytogenes* ATCC 7466 cells (Figure

4), although a higher signal was observed for xenopep-treated cells compared to DMSO-treated cells. The increase in fluorescence observed in Fig. 4 indicates that xenopep caused a disturbance in the cell membrane potential. A similar increase was also observed in other membrane acting antimicrobial peptides, such as melamine[33], brilacidin[49] and gramicidin S[48,50]. The membrane potential is closely linked to the ability of bacteria to replicate, which is in turn reliant on ATP production[51]. A loss in membrane potential can also lead to enhanced permeability resulting in the loss of ATP, as seen in this study when approximately 50% ATP was detected extracellularly after treating *L. monocytogenes* ATCC 7644 with xenopep.

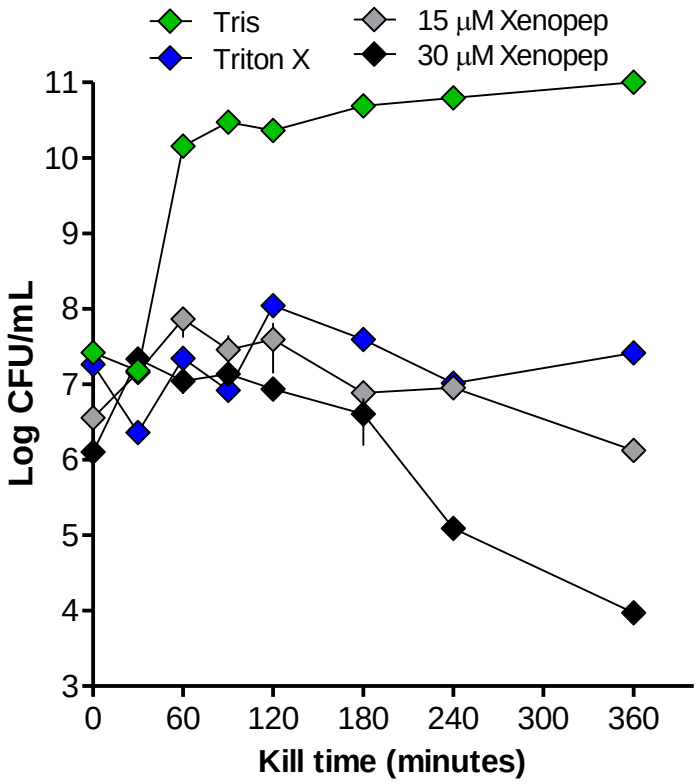

Figure 3: Time kill kinetics of xenopep. *L. monocytogenes* were cultured in LEB. Xenopep was added to *L. monocytogenes* at MIC (15 µM) and MBC (30 µM) concentrations. Triton X-100 was used as a cytotoxicity positive control and 10 mM Tris-HCl was used as a cytotoxicity negative control. Error bars represent the standard error of the mean of three independent experiments performed in triplicate.

Loss in membrane potential could be the result of membrane lesions or membrane pore formation. To assess the formation of pores/lesions the uptake of a small nucleic interacting dye, propidium iodine was tracked after *L. monocytogenes* ATCC 7644 was challenged with xenopep. The number of PI-stained cells increased drastically within the first 15 minutes, from

approximately 2% to approximately 70% and 85% for the 15 µM and 30 µM challenged cells, respectively (Figure 5a). A maximum of 95% of the cells treated with 30 µM xenopep and a maximum of 90% of the cells treated with 15 µM were stained by PI after 2 hours. The number of PI-stained cells treated with Triton-X (1%) increased with 20%, from 40% to 60%, within the first 2 h. Also confirming that membrane depolarisation is due to pore/lesion formation, rather than xenopep acting as a protonophore. Similar results were observed for nisin Z treated *L. monocytogenes* Scott A[52]. An increase in cell debris was also observed for both xenopep and Triton-X 100 treated cells (Figure 5b). The increase in cell debris for *L. monocytogenes* treated with Triton-X 100 was expected as Triton-X100 causes cell lysis[53,54]. The increase in cell debris observed for xenopep could also be due to cell lysis caused by xenopep.

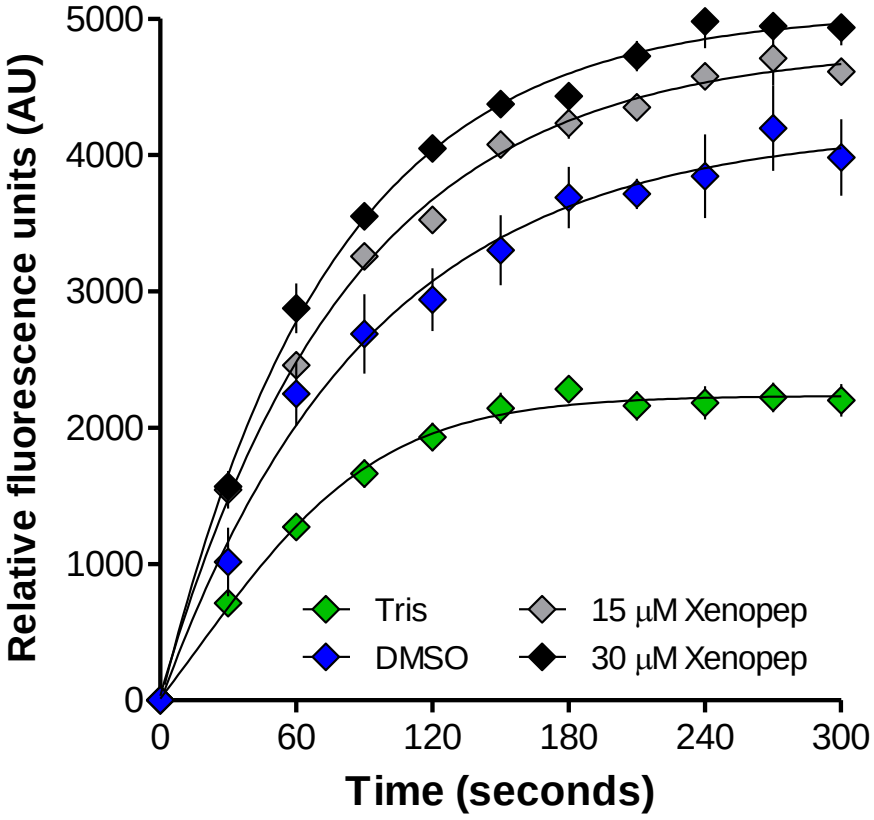

Figure 4: Cytoplasmic membrane depolarisation of *L. monocytogenes* ATCC 7644 after exposure to xenopep at MIC and MBC levels. Depolarisation was assessed spectroscopically with the potentiometric probe, $DisC_3(5)$. 20% DMSO was used as a control for depolarisation and 10 mM Tris-HCl was used as a negative control. Error bars represent the standard error of the mean of three independent experiments performed in triplicate.

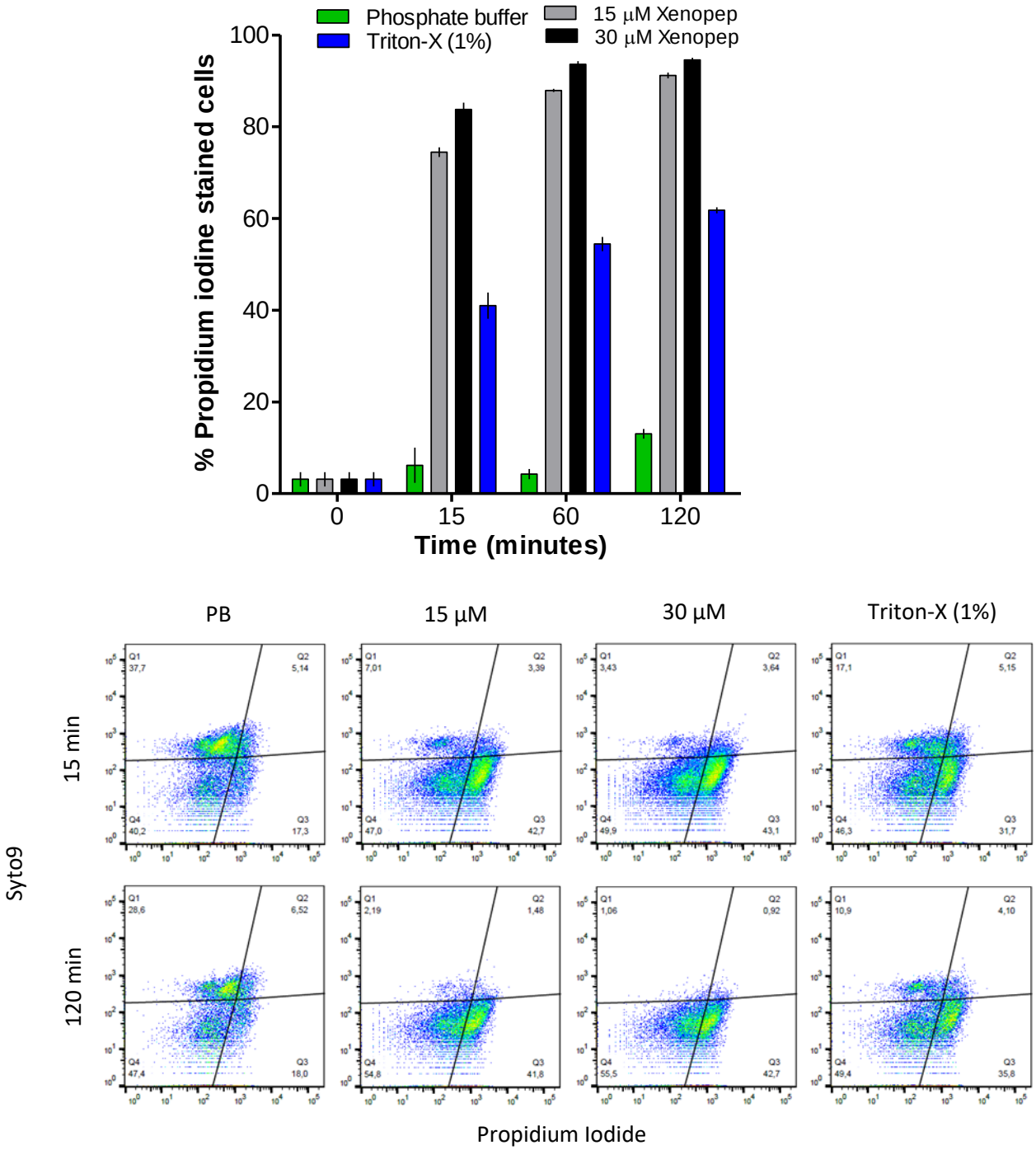

Figure 5: Membrane permeabilization of *L. monocytogenes* ATCC 7644 after exposure to xenopep determined by staining cells with Syto9 (membrane permeable) and propidium iodine (membrane impermeable) and analysing cells with flow cytometry. (a) Percentage of *L. monocytogenes* ATCC 7644 stained with propidium iodine after exposure to 15 µM and 30 µM xenopep, respectively. Error bars represent the standard error of the mean of three independent experiments performed in triplicate. (b) Flow cytometry generate images of *L. monocytogenes* ATCC 7644 after exposure to 15 µM and 30 µM of xenopep, respectively, after15 and 120 min, respectively. Triton-X (1%) was used as a positive control and 20 mM phosphate buffer (PB) was used as a negative control.

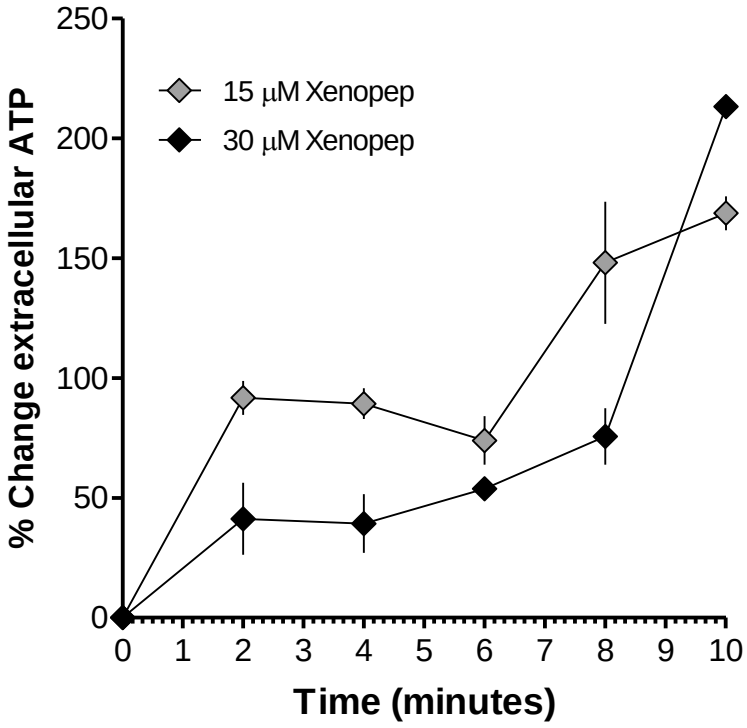

Figure 6: Leakage of ATP from the cell after treatment with xenopep. *Listeria monocytogenes* were treated with xenopep at MIC levels (15 µM) and MBC levels (30 µM). Error bars represent the standard error of the mean of three independent experiments performed in triplicate. The % change was calculated in terms of the control (10 mM Tris).

The loss of membrane functionality and increased permeability was confirmed when a release of ATP from the challenged cells were observed (Figure 6). Approximately 30% ATP was released within the first two minutes, with 92% increase for 15 µM. Whilst a 41% increase was observed for 30 µM xenopep. This was followed by a period of no release for 4 minutes, which indicated that the cells could be responding to the membrane damage or that some membrane processes were taking place limiting the leakage. This plateau was observed both for 15 and 30 µM xenopep. The lower observed extracellular ATP for the 30 µM xenopep can be due to dead cells that could not respond, whereas more cells in the 15 µM treatment could respond to osmotic stress by upregulating ATP[55]. However, a surge in extracellular ATP was observed after 8 minutes, with a maximum of 55% ATP detected after 10 minutes. This surge led to 169% and 213% increase in extracellular ATP for the 15 and 30 µM treatments, respectively. This could indicate either a time-dependent increase in membrane permeability or a surge in catabolism due to osmotic stress leading to increased ATP production to compensate for the osmotic stress and ATP loss[56].

Cell leakage and damage was further analysed by visualizing cells with SEM. Significant damage to the cells were observed when comparing *L. monocytogenes* exposed to 10 mM Tris-HCl (Figure 7a) to cells exposed to xenopep at 15 µM and 30 µM, respectively (Figure 7b and c). Small cell protrusions (indicated with blue arrows) formed on the surface of the *L. monocytogenes* ATCC 7644 cells that were treated with 15 µM of xenopep, which resembled the inner membrane protruding through the cell wall.

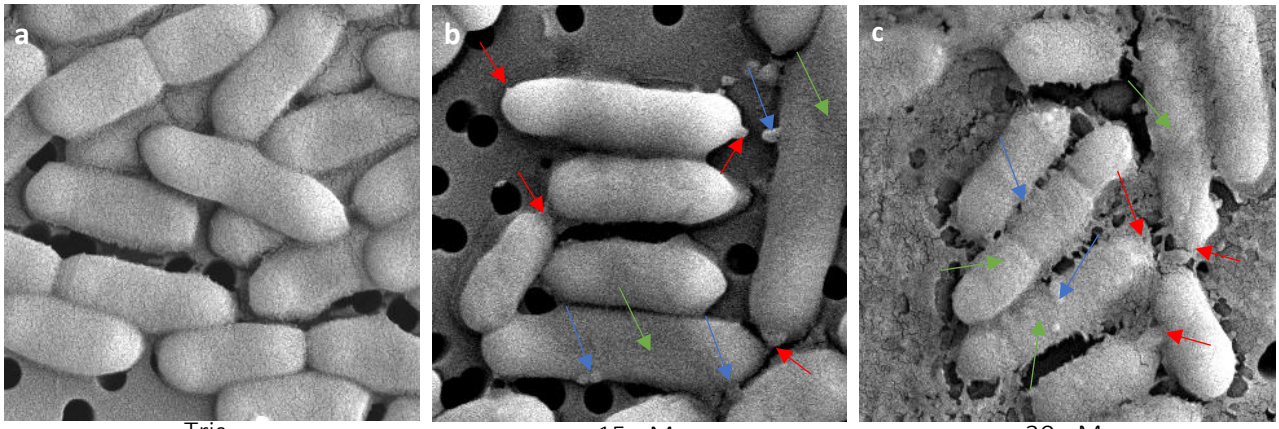

Figure 7: Scanning electron microscopy (SEM) images of *L. monocytogenes* ATCC 7644 after treatment with 10 mM Tris-HCl and xenopep. (a) *L. monocytogenes* ATCC 7644 treated with 10 mM Tris-HCl, (b) *L. monocytogenes* ATCC 7644 treated with 15 µM xenopep and (c) *L. monocytogenes* ATCC 7644 treated with 30 µM xenopep. Cells were fixed onto a Isopore membrane with 2.5% glutaraldehyde and dehydrates with ethanol using an increasing stepwise gradient. All cells are shown at 10K x magnification. Red arrows point to damage on apical end, blue arrows damage at the middle of the cell and green arrows indicate elongated cells that failed to divide/cell filamentation.

The formation of lesions, with the cell membrane protruding at the apical ends, could clearly be seen in *L. monocytogenes* ATCC 7644 treated with 15 and 30 µM xenopep (Figure 7 b and c, red arrows). These protrusions are similar in appearance as those formed by the synthetic flavonoid ClCl-flav[36] and the plant peptide NCR247[51]. Although the presence of collapsed cells was expected due to pore/lesion formation, none was observed. This could be due to the cell wall present in gram positive bacteria that will maintain cell architecture. The same was reported by Babii *et al*.[36], as they observed collapsed gram negative cells (*E. coli* and *K. pneumoniae*), but the cell architecture of gram positive cells (*S. aureus* and *Bacillus subtilis*) remained intact. This could indicate that xenopep targets the cell membrane as it appears as if

the cell wall remained intact. The blue arrows show protrusion in the middle of the cells, possibly where cell division takes place. It could also clearly be seen, specifically in the 30 µM xenopep treatment, that the cells leaked intracellular components. The leaked components formed a carpet/net covering the cells completely. A similar carpet was observed when *P. aureuginosa* ATCC 27853 was treated with *Macropis fulvipes* venom[57] and *Streptococcus pneumoniae* was treated with indolicid and ranalexin hybrid peptides[58]. String like appendages can also be observed, which could be DNA-protein networks. Some cells also appeared to be smaller in size, which might be linked to the reduction in cellular growth seen in the time kill assay. However, a number of cells, indicated with green arrows in figure 7c, were elongated indicating a failure of the daughter cells separating. Cell elongation and filamentation, as seen in a number of the *L. monocytogenes* cells treated with 30 µM xenopep (Figure 7c, green arrows), is generally associated with penicillin binding protein (PBP) 3 inhibitors[59,60]. This indicate that in addition to forming pores/lesions xenopep could also inhibit PBP3 acting in a similar way as aztreonam, piperacillin, cefureoxime, cefotaxime and ceftriaxone[61]. Although additional studies are needed to determine the extent of xenopep's affinity for PBP3.

Conclusions

In summary *X. khoisanae* J194 produces a multitude of antimicrobial compounds of which two, xenopep and rhabdin, show potent antilisterial activity. NMR proton spectrum analysis indicated that the two peptides share some sequence similarity, and two aromatic amino acid signals were identified. Although the two peptides share various characteristics differences were observed in their activity. A broader spectrum of activity was recorded for rhabdin when compared to that of xenopep. The formation of broad peaks, increase in activity after heat treatment and decrease in activity for xenopep stored in solution confirm the formation of aggregates/oligomers observed in the UPLC-MS/MS^{E} spectrums. Upon analysis of the effect of xenopep on the membrane of *L. monocytogenes* ATCC 7644 it was demonstrated that xenopep causes the formation of pores/lesions in the cell membrane. The formation of elongated cells and filamentation observed in cells treated with xenopep also led to the hypothesis that xenopep could have an affinity for PBP3.

From this study it is clear that *Xenorhabdus* spp. are an unexploited niche for novel antibiotics. Although additional studies are needed to fully characterise xenopep and rhabdin, these two peptides show great potential as novel antilisterial drugs that could either be used for the

treatment of listeriosis or as an additive to prevent the growth of *L. monocytogenes* in ready to eat foods.

References:

1. Booysen E, Dicks LMT. Does the future of antibiotics lie in secondary metabolites produced by *Xenorhabdus* spp.? A Review. Probiotics Antimicrob Proteins 2020; 12: 1310–20.

2. Reimer D, Nollmann FI, Schultz K *et al*. Xenortide biosynthesis by entomopathogenic *Xenorhabdus nematophila*. J Nat Prof 2014; 77: 1976-80.

3. Dreyer J, Malan AP, Dicks LMT. Bacteria of the genus *Xenorhabdus*, a novel source of bioactive compounds. Front Microbiol 2018; 9: 1–14.

4. Shlaes DM. *Antibiotics: the perfect storm*. 1st ed. The Neverlands: Springer, 2010.

5. Thakur M, Asrani RK, Patial V. Foodborne diseases. In: Holban AM, Grumezescu AM, eds. *Handbook of food bioengineering*. London: Academic Press, 2018; 157–92.

6. Okutani A, Okada Y, Yamamoto S, *et al*. Overview of *Listeria monocytogenes* contamination in Japan. Int J Food Microbiol 2004; 93: 131–40.

7. Goulet V, King LA, Vaillant V *et al*. What is the incubation period for listeriosis? BMC Infect Dis 2013; 13.

8. Craig S, Permezel M, Doyle L *et al*. Perinatal infection with *Listeria monocytogenes*. Aust New Zeal J Obstet Gynaecol 1996; 36: 286–90.

9. Vázquez-Boland JA, Krypotou E, Scortti M. *Listeria* placental infection. MBio 2017; 8: 1–6.

10. Vázquez-Boland JA, Kuhn M, Berche P *et al*. *Listeria* pathogenesis and molecular virulence determinants. Clin Microbiol Rev 2001; 14: 584–640.

11. Teuber M. Spread of antibiotic resistance with food-borne pathogens. Cell Mol Life Sci 1999; 56: 755–63.

12. Lungu B, O'Bryan CA, Muthaiyan A, *et al. Listeria monocytogenes*: Antibiotic resistance in food production. Foodborne Pathog Dis 2011; 8: 569–78.

13. Poyart-Salmeron C, Carlier C, Trieu-Cuot P *et al*. Transferable plasmid-mediated antibiotic resistance in *Listeria monocytogenes*. Lancet 1990; 335: 1422–6.

14. Prazak AM, Murano EA, Mercado I *et al*. Antimicrobial resistance of *Listeria monocytogenes* isolated from various cabbage farms and packaging sheds in Texas. J Food Prot 2002; 65: 1796–9.

15. Yücel N, Çitak S, Önder M. Prevalence and antibiotic resistance of *Listeria* species in meat products in Ankara, Turkey. Food Microbiol 2005; 22: 241–5.

16. Harakeh S, Saleh I, Zouhairi O *et al*. Antimicrobial resistance of *Listeria monocytogenes* isolated from dairy-based food products. Sci Total Environ 2009; 407: 4022–7.

17. Olaimat AN, Al-Holy MA, Shahbaz HM, *et al.* Emergence of antibiotic resistance in *Listeria monocytogenes* isolated from food products: A Comprehensive Review. Compr Rev Food Sci Food Saf 2018; 17: 1277–92.

18. Tchatchouang C-DK, Fri J, De Santi M, *et al*. Listeriosis outbreak in south africa: A comparative analysis with previously reported cases worldwide. Microorganisms 2020; 8: 1–18.

19. Indrawattana N, Nibaddhasobon T, Sookrung N, *et al*. Prevalence of L*isteria monocytogenes* in raw meats marketed in Bangkok and characterization of the isolates by phenotypic and molecular methods. J Heal Popul Nutr 2011; 29: 26–38.

20. Hsieh WS, Tsai LY, Jeng SF, et al. Neonatal listeriosis in Taiwan, 1990-2007. Int J Infect Dis 2009; 13: 193–5.

21. Thomas J, Govender N, McCarthy KM, et al. Outbreak of listeriosis in South Africa associated with processed meat. N Engl J Med 2020; 382: 632–43.

22. Duy Vo T. Target identification of peptides from *Xenorhabdus* and *Photorhabdus*. 2020.

23. Zhang S, Liu Q, Han Y, *et al*. Nematophin, an antimicrobial dipeptide compound from *Xenorhabdus nematophila* YL001 as a potent biopesticide for *Rhizoctonia solani* control. Front Microbiol 2019; 10: 1–15.

24. Zhu Y, Mohapatra S, Weisshaar JC. Rigidification of the *Escherichia coli* cytoplasm by the human antimicrobial peptide LL-37 revealed by super resolution fluorescence microscopy. Proc Natl Acad Sci 2019; 116: 1017–26.

25. Dreyer J, Malan AP, Dicks LMT. Three Novel *Xenorhabdus – Steinernema* associations and evidence of strains of *X. khoisanae* switching between different clades. Curr Microbiol 2017; 74: 938–42.

26. Booysen E, Rautenbach M, Stander MA, Dicks LMT. Profiling the production of antimicrobial secondary metabolites by *Xenorhabdus khoisanae* J194 under different culturing conditions. Front Chem 2021; 9: 1–15.

27. Booysen E, Dicks LM, Sadie-Van Gijsen H. Characterization of a novel antibiotic isolated from *Xenorhabdus khoisanae* and encapsulation of vancomycin in nanoparticles. 2018.

28. Methods for Dilution Antimicrobial Susceptibility Tests for Bacteria That Grow Aerobically; Approved Standard — Ninth Edition. CLSI document M07-A9. *Clin Lab Standars Inst* 2018; **32**: 18.

29. Foerster S, Desilvestro V, Hathaway LJ *et al*. A new rapid resazurin-based microdilution assay for antimicrobial susceptibility testing of *Neisseria gonorrhoeae*. J Antimicrob Chemother 2017; 72: 1961–8.

30. Elshikh M, Ahmed S, Funston S, *et al.* Resazurin-based 96-well plate microdilution method for the determination of minimum inhibitory concentration of biosurfactants. Biotechnol Lett 2016; 38: 1015–9.

31. Keepers TR, Gomez M, Celeri C *et al*. Bactericidal activity, absence of serum effect, and time-kill kinetics of ceftazidime-avibactam against β-lactamase-producing Enterobacteriaceae and *Pseudomonas aeruginosa*. Antimicrob Agents Chemother 2014; 58: 5297–305.

32. Godballe T, Mojsoska B, Nielsen HM *et al*. Antimicrobial activity of GN peptides and their mode of action. Biopolymers 2016; 106: 172–83.

33. Carson CF, Mee BJ, Riley T V. Mechanism of action of *Melaleuca alternifolia* (tea tree) oil on *Staphylococcus aureus* determined by time-kill, lysis, leakage, and salt tolerance assays and electron microscopy. Antimicrob Agents Chemother 2002; 46: 1914–20.

34. Yasir M, Dutta D, Willcox MDP. Comparative mode of action of antimicrobial peptide melimine and its derivative Mel4 against *Pseudomonas aeruginosa*. Sci Rep 2019; 9: 1–12.

35. Yasir M, Dutta D, Willcox MDP. Mode of action of the antimicrobial peptide Mel4 is independent of *Staphylococcus aureus* cell membrane permeability. PLoS One 2019; 14: 1–22.

36. Babii C, Mihalache G, Bahrin LG, *et al.* A novel synthetic flavonoid with potent antibacterial properties: *In vitro* activity and proposed mode of action. PLoS One 2018; 13: 1–15.

37. Jafarzade M, Yahya NA, Shayesteh F *et al.* Influence of culture conditions and medium composition on the production of antibacterial compounds by marine *Serratia* spp. WPRA3. J Microbiol 2013; 51: 373–9.

38. Hassan MN, El-Naggar MY, Said WY. Physiological factors affecting the production of an antimicrobial substance by *Streptomyces violatus* in batch cultures. Egypt J Biol 2001; 3: 1–10.

39. da Silva IR. The effect of varying culture conditions on the production of antibiotics by *Streptomyces* spp., isolated from the Amazonian soil. Ferment Technol 2012; 1: 1–5.

40. Omain TJ and van der Donk WA. Follow the leader: The use of leader peptides to guide natural product biosynthesis. Nat Chem Biol 2010; 6: 9-18

41. Talluri VP. Optimization of cultural parameters for the production of antimicrobial compound from *Lactobacillus fermentum* (MTCC No. 1745). J Bacteriol Mycol Open Access 2017; 4: 154–7.

42. Rautenbach M, Vlok NM, Eyéghé-Bickong HA *et al*. An electrospray ionization mass spectrometry study on the “In Vacuo” hetero-oligomers formed by the antimicrobial peptides, surfactin and gramicidin S. J Am Soc Mass Spectrom 2017; 28: 1623–37.

43. Pessione E. Lactic acid bacteria contribution to gut microbiota complexity: lights and shadows. *Front Cell Infect Microbiol* 2012; 2: 86.

44. Dreyer L, Smith C, Deane SM *et al*. Migration of bacteriocins across gastrointestinal epithelial and vascular endothelial cells, as determined using *in vitro* simulations. Sci Rep 2019; 9: 1–11.

45. Campion A, Casey PG, Field D *et al*. *In vivo* activity of nisin A and nisin V against *Listeria monocytogenes* in mice. BMC Microbiol 2013; 13.

46. Cheng C, Yang Y, Dong Z, *et al*. *Listeria monocytogenes* varies among strains to maintain intracellular pH homeostasis under stresses by different acids as analyzed by a high-throughput microplate-based fluorometer. Front Microbiol 2015; 6: 1–10.

47. Sims PJ, Waggoner AS, Wang CH *et al*. Mechanism by which cyanine dyes measure membrane potential in red blood cells and phosphatidylcholine vesicles. Biochemistry 1974; 13: 3315–30.

48. Wu M, Maier E, Benz R *et al*. Mechanism of interaction of different classes of cationic antimicrobial peptides with planar bilayers and with the cytoplasmic membrane of *Escherichia coli*. Biochemistry 1999; 38: 7235–42.

49. Mensa B, Howell GL, Scott R *et al*. Comparative mechanistic studies of brilacidin, daptomycin, and the antimicrobial peptide LL16. Antimicrob Agents Chemother 2014; 58: 5136–45.

50. Zhang L, Dhillon P, Yan H *et al*. Interactions of bacterial cationic peptide antibiotics with outer and cytoplasmic membranes of *Pseudomonas aeruginosa*. Antimicrob Agents Chemother 2000; 44: 3317–21.

51. Suh SJ, Shuman J, Carroll LP *et al*. BEEP: An assay to detect bio-energetic and envelope permeability alterations in *Pseudomonas aeruginosa*. J Microbiol Methods 2016; 125: 81–6.

52. Abee T, Rombouts FM, Hugenholtz J, *et al.* Mode of action of nisin Z against *Listeria monocytogenes* Scott A grown at high and low temperatures. 1994; 60: 1962–8.

53. Pizzirusso A, De Nicola A, Sevink GJA, *et al*. Biomembrane solubilization mechanism by Triton X-100: A computational study of the three stage model. Phys Chem Chem Phys 2017; 19: 29780–94.

54. Koley D, Bard AJ. Triton X-100 concentration effects on membrane permeability of a single HeLa cell by scanning electrochemical microscopy (SECM). Proc Natl Acad Sci U S A 2010; 107: 16783–7.

55. Csonka LN. Physiological and genetic responses of bacteria to osmotic stress. Microbiol Rev 1989; 53: 121–47.

56. Bremer E, Krämer R. Responses of microorganisms to osmotic stress. Annu Rev Microbiol 2019; 73: 313–34.

57. Ko SJ, Kim MK, Bang JK *et al*. *Macropis fulvipes* venom component macropin exerts its antibacterial and anti-biofilm properties by damaging the plasma membranes of drug resistant bacteria. Sci Rep 2017; 7: 1–15.

58. Jindal HM, Zandi K, Ong KC *et al*. Mechanisms of action and *in vivo* antibacterial efficacy assessment of five novel hybrid peptides derived from indolicidin and ranalexin against *Streptococcus pneumoniae*. PeerJ 2017; 2017:5e3887.

59. Spratt BG. Distinct penicillin binding proteins involved in the division, elongation and shape of *Escherichia coli* K12. Proc Natl Acad Sci 1975; 72: 2999–3003.

60. Kohanski MA, Dwyer DJ, Collins JJ. How antibiotics kill bacteria: from targets to networks. Nat Rev Microbiol 2010; 8: 423–35.

61. Kocaoglu O, Tsui HCT, Winkler ME *et al*. Profiling of β-Lactam selectivity for penicillin-binding proteins in *Streptococcus pneumoniae* D39. Antimicrob agents 2015; 59: 3548–55.

Supplementary material:

Production of xenopep and rhabdin

Method A

A 5 mL test tube of tryptic soy broth (TSB) was inoculated with a single phase I colony of *Xenorhabdus khoisanae* J194 from a fresh NBTA (nutrient agar supplemented with 0.025% (*w/v*) bromothymol blue and 0.04 % (*w/v*) 2,3,5-triphenyltetrazolium) plate and incubated on a rotating test tube wheel at 26°C for 18 hours. XAD-16 resin was activated by incubating the resin with 80% (*v/v*) isopropanol (40 g resin in 250 ml 80% isopropanol) for 1 hour at 4°C on an orbital shaker at 80 rpm. After activation, vacuum filtration apparatus was used to separate the beads from the 80% isopropanol. The beads were washed with 500 ml of double distilled water. This was repeated three times to ensure all the isopropanol was washed away. The beads were resuspended in 100 mL of double distilled water and pipetted into eight Macartney bottles (10 mL resin at 50% in each bottle). The resin was sterilised by autoclaving for 20 min. Eight petri dishes (145 X 20MM) of tryptic soy broth with 2% (*w/v*) agar was poured and dried in a biosafety cabinet for 15 min.

The double distilled water was removed aseptically with a pipette and the resin were mixed with the 5 ml culture of *X. khoisanae* J194. The resin was spread over the plates by swirling (1 Macartney bottle per plate) and the excess liquid was removed aseptically with a pipette. The plates were left to dry in the biosafety for 15 min and incubated at 26°C for 96 hours. After incubation the resin was removed from the plates by pouring 10 mL double distilled water onto the plate and scraping the resin with a metal scraper. The resin was collected in a glass beaker and incubated at 4°C for 3 hours. After incubation the resin was separated from the double distilled water with vacuum filtration apparatus and rinsed with 500 mL of double distilled water. See elution of compounds from resin for further details

Method B

A 10 mL test tube of TSB was inoculated with a single phase I colony of *X. khoisanae* J194 from a fresh NBTA plate and incubated on a rotating test tube wheel at 26°C for 18 hours. Tryptic soy broth (800 mL) was prepared and clarified with activated XAD-16 resin. The XAD-16 resin was activated by incubating the resin with 80% (*v/v*) isopropanol (20 g resin in 250 mL 80% isopropanol) for 1 hour at 4°C on an orbital shaker at 80 rpm. After activation, vacuum filtration apparatus was used to separate the beads from the 80% isopropanol and the resin was

washed with 500 mL double distilled water three times. The resin was resuspended in the TSB and incubated at 4°C for 1 hour. After incubation the resin was separated from the media with vacuum filtration apparatus, the media was collected and autoclaved. The autoclaved media was inoculated with the *X. khoisanae* J194 culture (1%, *v/v*) and incubated for 96 hours at 26°C on an orbital shaker at 180 rpm.

After 96 hours the culture was spun down at 4700 x g for 10 min and the supernatant was collected. Twenty grams of the activated XAD-16 resin was resuspended in the supernatant and incubated on an orbital shaker (80 rpm) for 3 hours at 4°C. After incubation the resin was collected via vacuum filtration apparatus and rinsed with 500 mL double distilled water. See elution of compounds from resin for further details

Elution of compounds from resin

The hydrophilic compounds were eluted from the resin by resuspending the resin in 150mL of 30% (*v/v*) ethanol and incubating the resin at 4°C for 1 hour in a glass beaker. After 1 hour the 30% ethanol and resin was separated with the vacuum filtration apparatus. The remaining ethanol was removed by washing the resin three times with 500 mL double distilled water. The amphiphilic and hydrophobic compounds were eluted from the resin by resuspending the resin in 100 mL 80% (*v/v*) isopropanol and incubating the resin in a glass beaker at 4°C for 1 hour. After incubation the resin and isopropanol were separated with vacuum filtration apparatus and the isopropanol was collected. The isopropanol was removed under vacuum, using a Rotavapor R-114 (Büchi, Flawil, Switzerland) connected to a water bath (B-480, Büchi). The crude extract was frozen at -80°C for a minimum of 2 hours and freeze dried.

Purification of compounds with High-performance liquid chromatography (HPLC)

The freeze-dried extract from both methods were dissolved in 50% (*v/v*) acetonitrile and loaded onto a Poroshell 120 EC-C_{18} HPLC column (120 Å, 4 µm, 4.6 mm × 150 mm, Agilent) and eluted with a linear gradient created with 0.1% (*v/v*) trifluoracetic acid (TFA) in analytically pure water (eluent A) and 0.1% (*v/v*) TFA in acetonitrile (eluent B). The flow rate was set at 1.5 mL/min and the elution program utilized was as follows: 20% eluent A from 0 to 0.5 min (initial conditions), 0.5–12.5 min linear gradient from 20 to 90% eluent B, 12.5–13.0 min linear gradient from 90 to 100% eluent B, 13.0–14.0 min at 100% eluent B, followed by column equilibration (14.0–20.0 min linear gradient from 100 to 20% eluent B and 20.0–25.0 min at initial conditions). The fractions were collected with an Agilent 1260 Infinity II LC system fraction collector set to collect a fraction every 30 seconds. The fractions were subjected to

ultraperformance liquid chromatography, linked to a Waters Synapt G2 quadrupole time-of-flight mass spectrometer (QTOF; Waters Corporation, Milford, United States) and fractions containing xenopep and rhabdin was identified and freeze-dried.

The freeze-dried fractions were dissolved in 50% (*v/v*) acetonitrile and loaded onto a 120 EC-C18 HPLC column (120 Å, 4 µm, 4.6 mm × 150 mm, Agilent) for a sequential HPLC step. Xenopep and rhabdin was eluted with a linear gradient created with 0.1% (*v/v*) trifluoracetic acid (TFA) in analytically pure water (eluent A) and 0.1% (*v/v*) TFA in acetonitrile (eluent B). The flow rate was set at 1.5 mL/min and the elution program utilized was as follows: 20% eluent A from 0 to 0.5 min (initial conditions), 0.5–12.5 min linear gradient from 20 to 60% eluent B, 12.5–14.0 min linear gradient from 60 to 100% eluent B, 14.0–15.0 min at 100% eluent B, followed by column equilibration (15.0–20.0 min linear gradient from 100 to 20% eluent B and 20.0–25.0 min at initial conditions). The fractions were collected with an Agilent 1260 Infinity II LC system. Data was recorded at 245 nm and 314 nm and the fractions were collected manually every 10 seconds. The fractions were subjected to ultraperformance liquid chromatography, linked to a QTOF mass spectrometer and fractions containing xenopep and rhabdin was identified and freeze-dried. Both xenopep and rhabdin was produced in method A, while only xenopep was produced in method B.

Figures:

Figure S1 and S2 depicts the HPLC profiles of crude extract obtained either by culturing *X. khoisanae* J194 on solid media (Figure S1) or in aerated broth (Figure S2). Figure S3 is the HPLC profile of the sequential HPLC step to purify xenopep.

Figure S4 depicts the proton NMR spectra of xenopep and rhabdin in the alpha proton and aliphatic proton regions. Figure S5 depicts the proton NMR spectra of xenopep and rhabdin in the amide proton region.

Tables:

Table S1 depicts the putative allocation of ^{1}H chemical shifts (ppm) of xenopep and rhabdin dissolved in DMSO (1:1, *v/v*) at 298K.

Table S2 depicts the antimicrobial activity of xenopep against beneficial gut bacteria.

Table S3 depicts the stability of the antimicrobial activity of xenopep and rhabdin after exposing the peptides to various environmental factors.

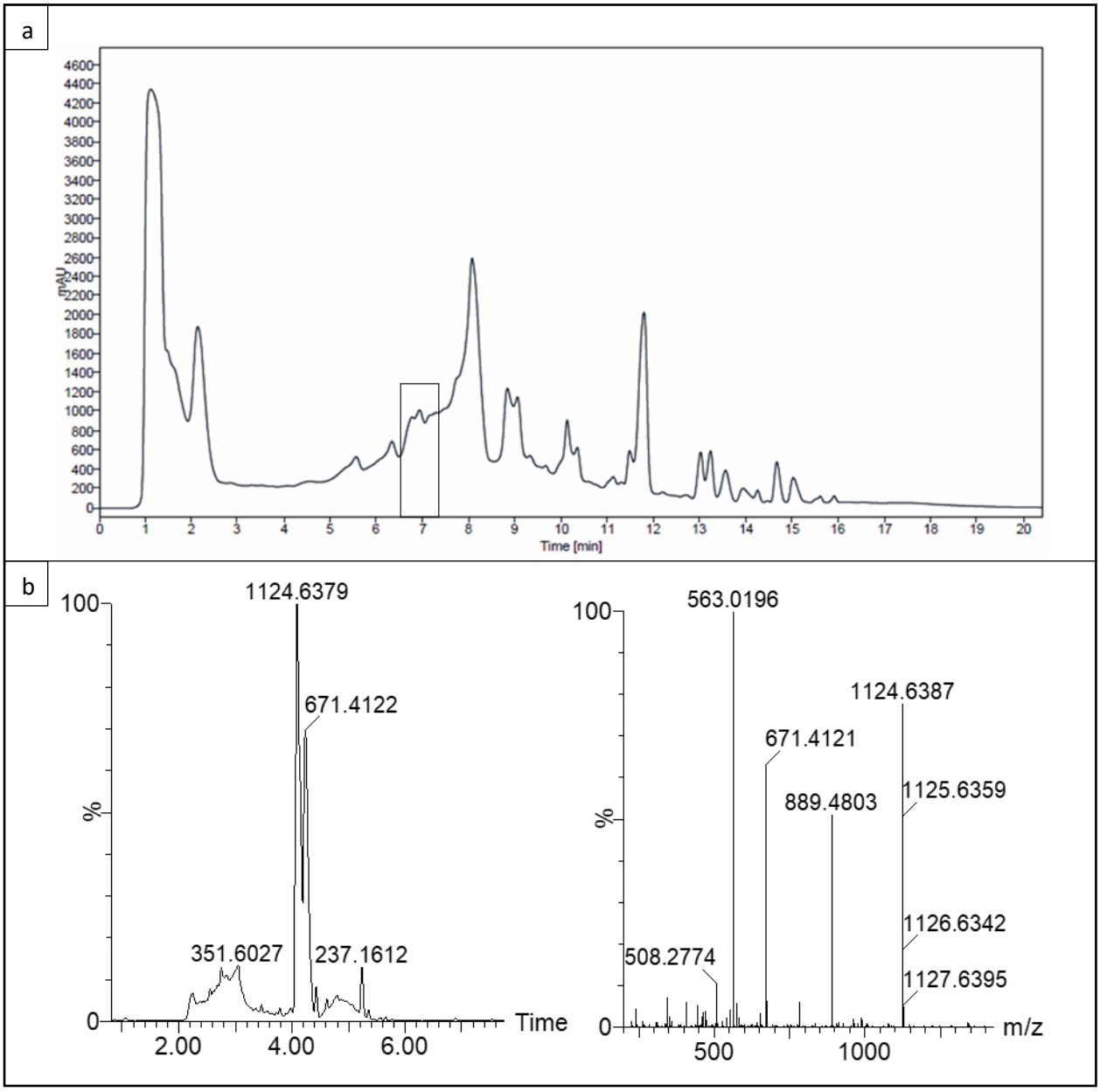

Figure S1: Purification of xenopep and rhabdin from method a crude extract. (a) HPLC chromatogram of purified xenopep and rhabdin. The peak containing xenopep and rhabdin (indicated with square) had a retention time of 7 minutes. (b) The UPLC-MS chromatograms of the peak containing xenopep and rhabdin. (c) High resolution MS analysis of the peak containing xenopep and rhabdin

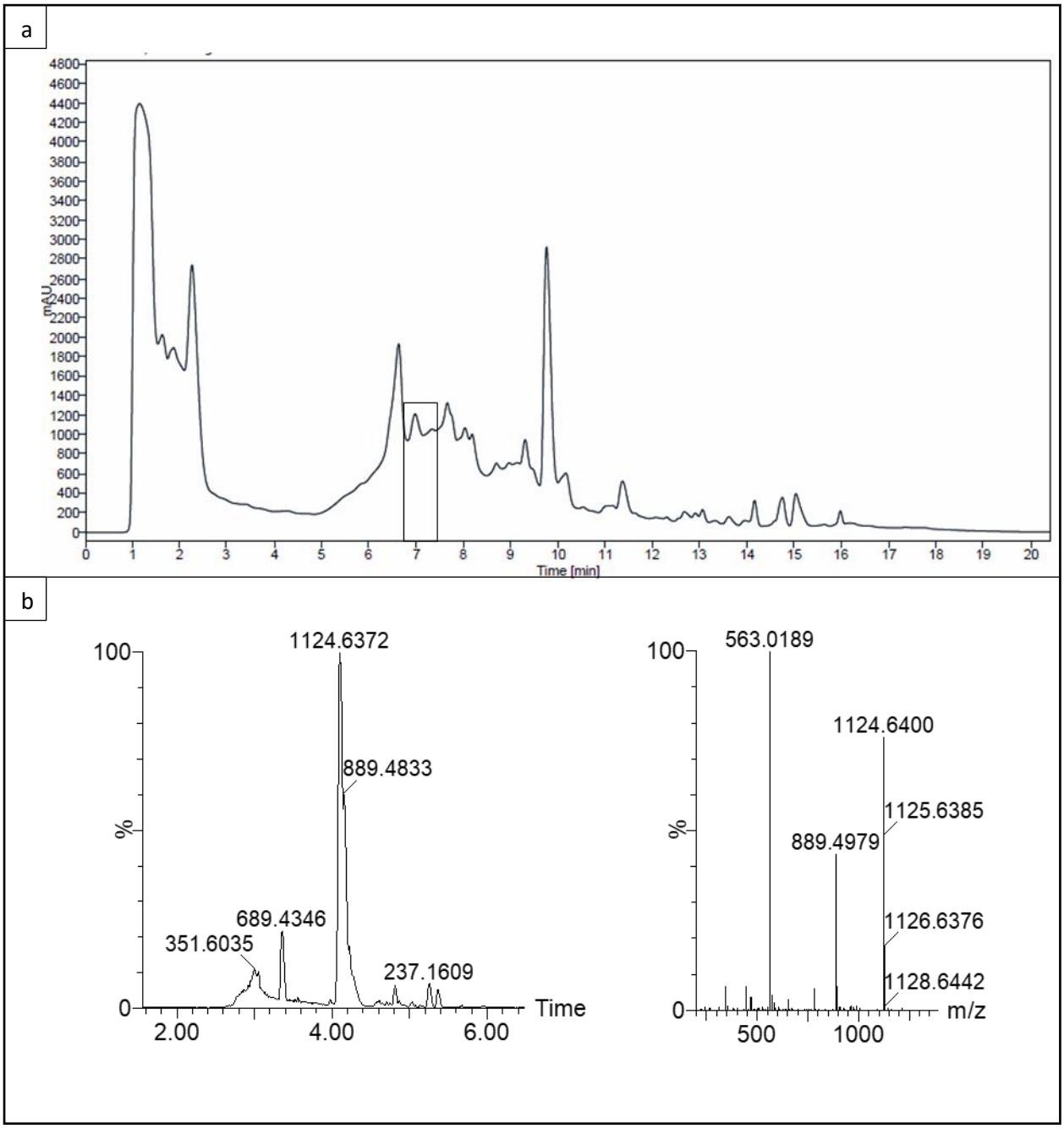

Figure S2: Purification of xenopep from method b crude extract. (a) HPLC chromatogram of purified xenopep. The peak containing xenopep (indicated with square) had a retention time of 7 minutes. (b) The UPLC-MS chromatograms of the peak containing xenopep. (c) High resolution MS analysis of the peak containing xenopep.

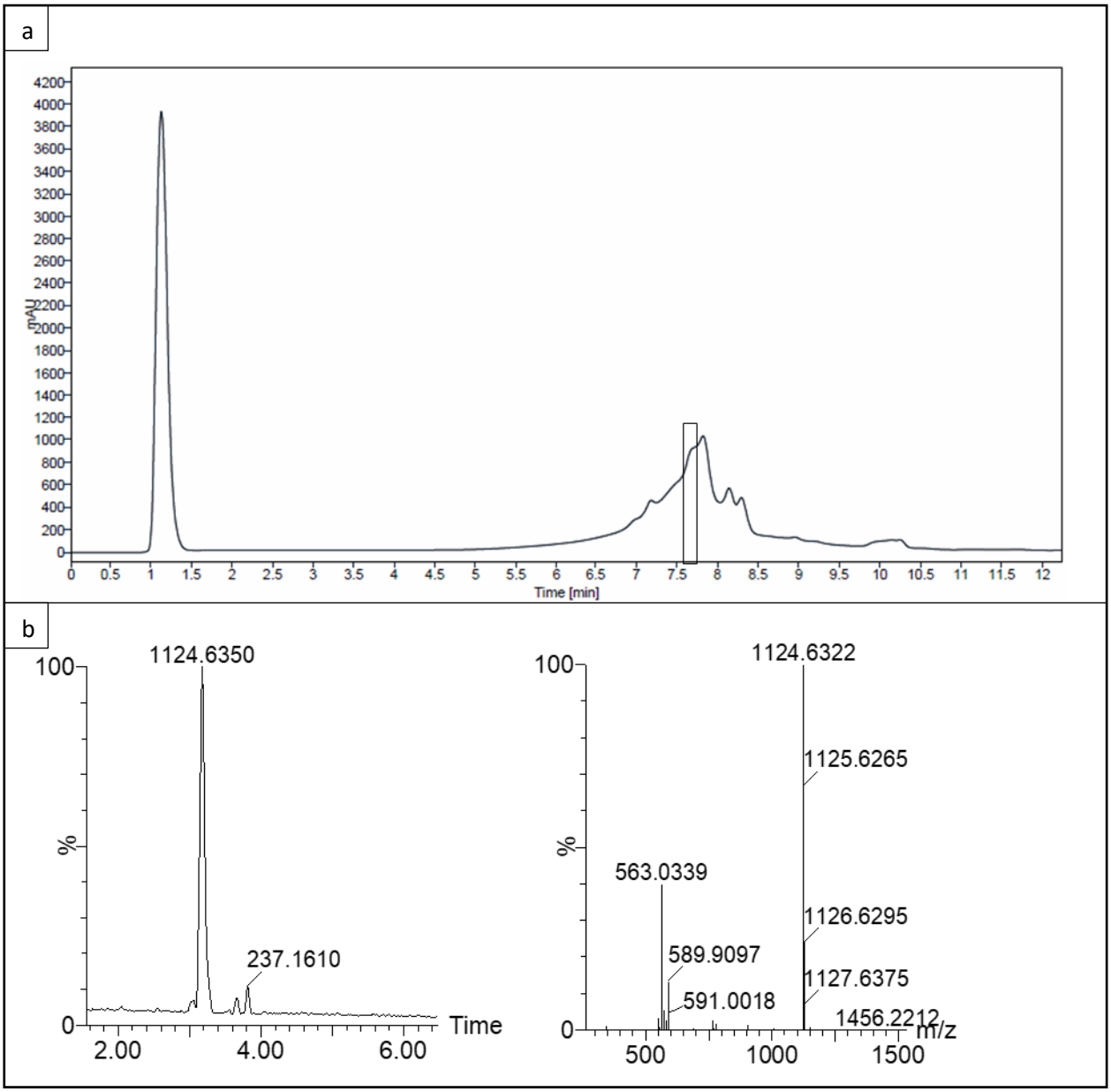

Figure S3: Purification of xenopep peak collected after first HPLC run. (a) Second purification HPLC chromatogram of peak containing xenopep. The peak containing xenopep (indicated with square) had a retention time of 7.6 minutes. (b) The UPLC-MS chromatograms of the peak containing xenopep collected at 7.6 min. (c) High resolution MS analysis of the peak containing xenopep

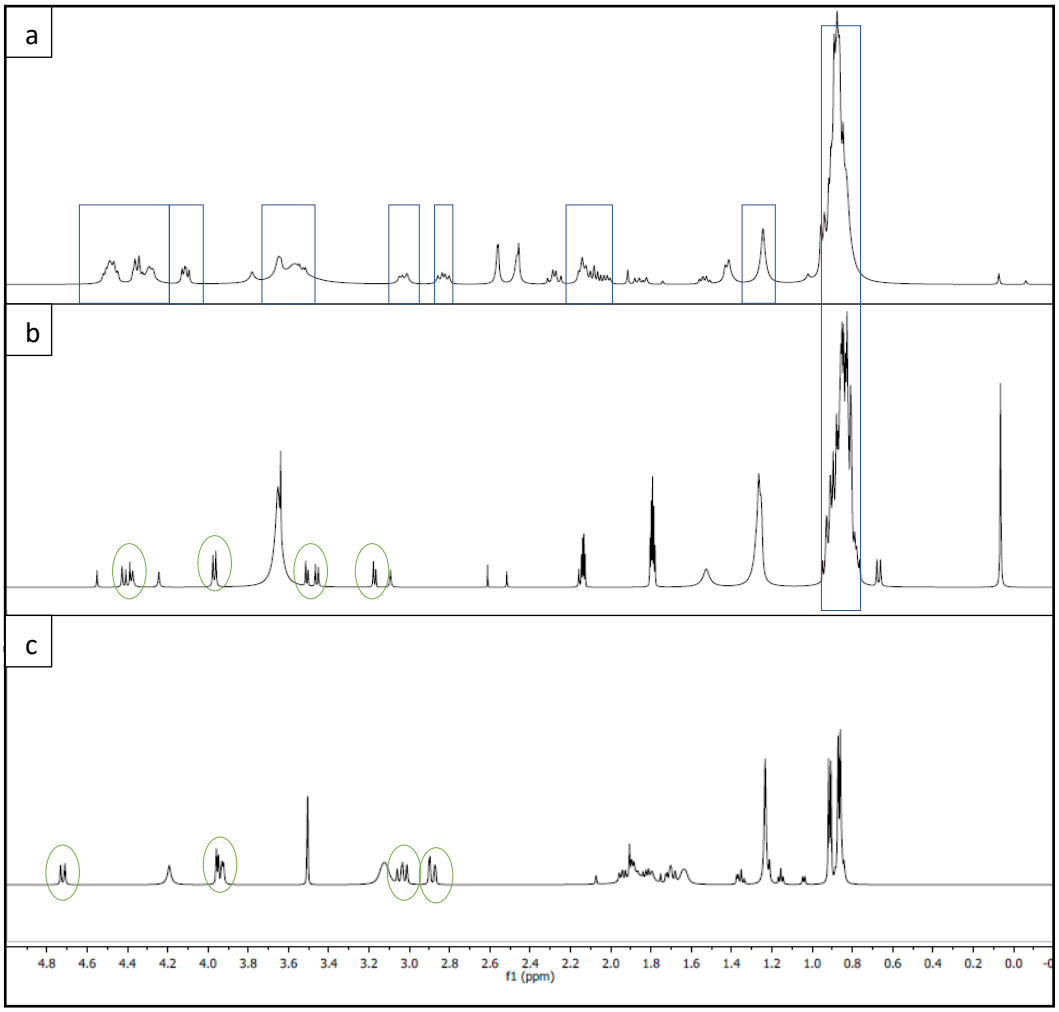

Figure S4: Comparison of Presat proton NMR of xenopep and rhabdin in the alpha protons (3-5 ppm) and aliphatic protons (0-3 ppm) region. (a) Xenopep dissolved in DMSO, (b) xenopep dissolved in 80% acetonitrile and (c) rhabdin dissolved in DMSO. The area indicated is from 5 ppm to 0 ppm. The blue squares in a indicates peak broadening and the green circles in b and c indicate aromatic amino acids.

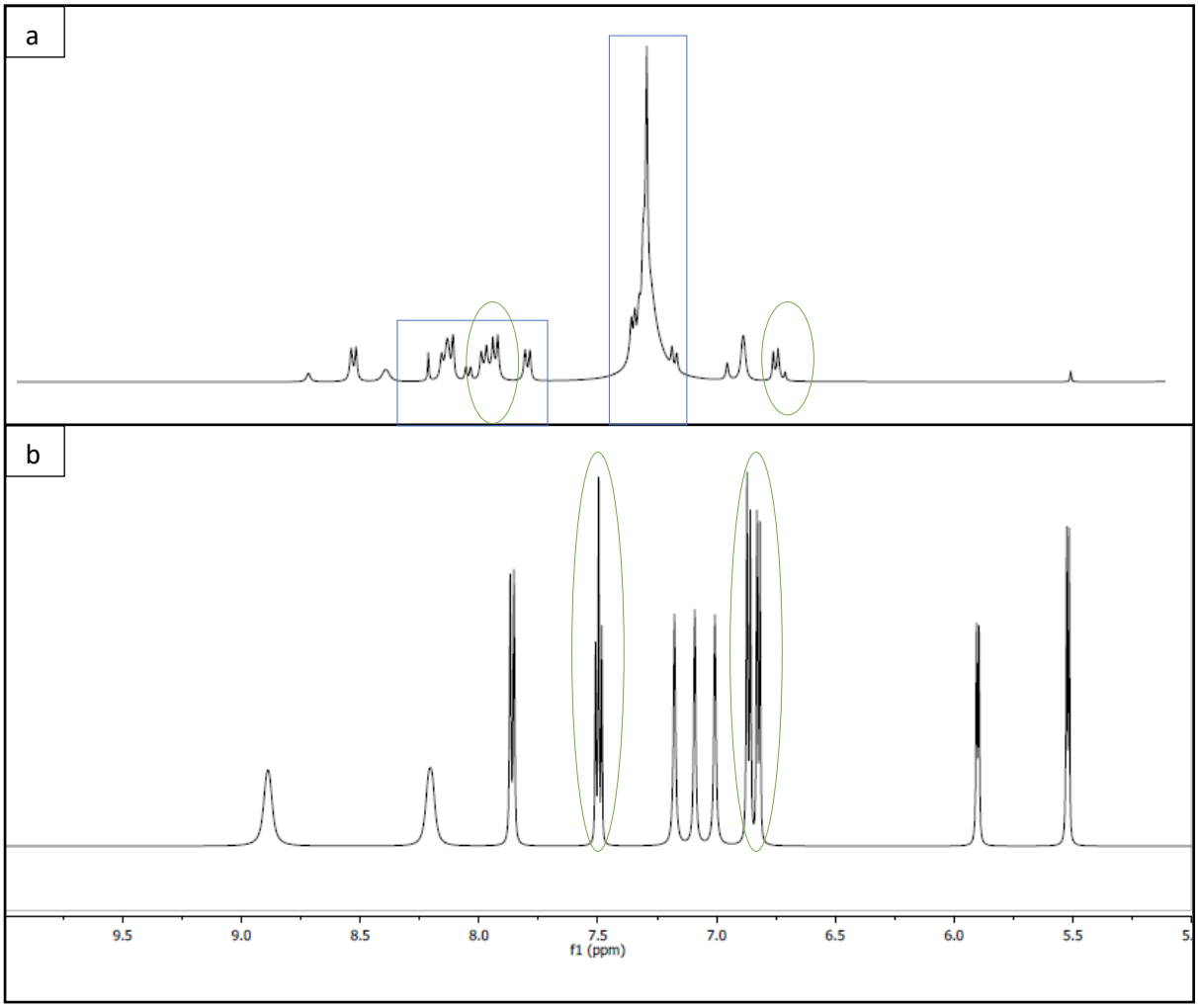

Figure S5: Comparison of Presat proton NMR of xenopep and rhabdin in the amide proton region between 6-9 ppm. (a) Xenopep dissolved in DMSO and (b) rhabdin dissolved in DMSO. The blue squares in a indicates peak broadening and the green circles in a and b indicate aromatic amino acids.

Table S1: Putative allocation of ^{1}H chemical shifts (ppm) of xenopep and rhabdin dissolved in DMSO (1:1, *v/v*) at 298K

AMINO ACID RESIDUE	AMIDE H (N-H)		ALPHA H (C-H)		BETA H, H' (H-C-H)	
	Xenopep	Rhabdin	Xenopep	Rhabdin	Xenopep	Rhabdin
Residue^{1x}	8.04	NA	3.30	NA	2.50	N/A
Residue^{1r}	N/A	7.27	N/A	3.17	N/A	1.96
Residue^{2}	8.26	8.21	-^{b}	-^{b}	3.62	3.61
Residue^{3}	-^{a}	-^{a}	4.32	4.33	-^{b}	2.49
Residue^{4}	-^{a}	-^{a}	4.20	4.22	-^{b}	-^{b}
Residue^{5}	7.97	7.98	4.15	4.17	2.51	2.50
Residue^{6}	7.82	7.85	4.18	4.19	-^{b}	1.75, 1.41
Residue^{7}	7.22	N/A	4.35	N/A	-^{b}	N/A
Residue^{8}	-^{a}	N/A	4.47	N/A	-^{b}	N/A
Residue^{9}	7.49	N/A	-^{b}	N/A	-^{b}	N/A

*N/A: Not applicable, -^{a}: Does not have an amide proton as internal residue, -^{b}: Not detected, Residue^{1X}: First residue in xenopep, Residue^{1R}: First residue in rhabdin

Table S2: Antimicrobial activity of xenopep at three different concentrations (15 µM, 30 µM and 45 µM) against 5 beneficial gut commensal bacteria i.e., *Lactobacillus plantarum* 423, *Lactobacillus rhamnosus* R11, *Lactobacillus reuteri* DSM 17938, *Lactobacillus casei* 106 and *Enterococcus mundtii* ST4SA.

	Erythromycin	15 µM	30 µM	45 µM
***L. plantarum* 423**	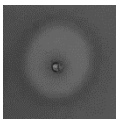	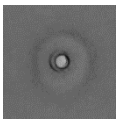	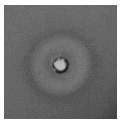	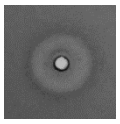
***L. rhamnosus* R11**	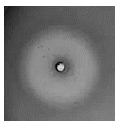	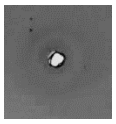	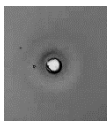	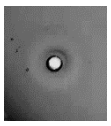
***L. reuteri* DSM 17938**	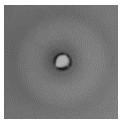	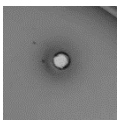	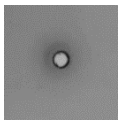	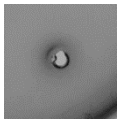
***L. casei* 106**	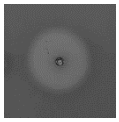	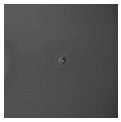	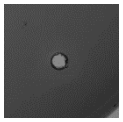	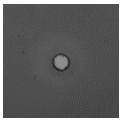
***E. mundtii* ST4SA**	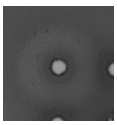	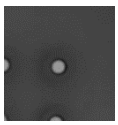	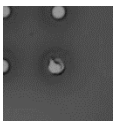	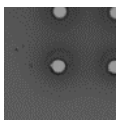

Table S3: Antimicrobial activity of xenopep and rhabdin after treating with various proteinases, exposing xenopep to different pH environments, heat treatment xenopep and rhabdin or storing xenopep in solution for 6 weeks. Untreated peptide was used as a positive control and nisin was used as a protease control.

Treatment	**Nisin**	**Xenopep**		**Rhabdin**
		Protease stability		
Concentration (µM)	10	20	15	12
Untreated				
Proteinase K				
Pepsin				
Trypsin				
		pH stability		
Concentration (µM)	10 mM Tris	30		N/A
pH 2				
pH 7				-
pH 12				
		Temperature stability		
Concentration (µM)	N/A	20	18	15	20	18	15
Untreated	-						
Boiling for 10 min @ 100°C							
		Long term stability in solution stability					
Concentration (µM)	N/A	20	18	15		N/A	
Untreated	-					-	
Storage for 6 weeks							

STELLENBOSCH UNIVERSITY

Chapter 5

General Discussion and Conclusions

General discussion and conclusions

The discovery and commercialisation of antibiotics, specifically penicillin and sulfonamides, revolutionised the early 1900's [1–6] and led to great advancements in the medical field. The use of antibiotics made complex surgeries such as organ transplants and open heart surgery possible [7, 8], unfortunately due to the reckless use of antibiotics we could soon find ourselves in a society without affective antibiotics [9]. Antibiotic resistance in bacteria is either intrinsic or acquired [10]. Intrinsic resistance refers to the natural resistance of a bacterium towards a specific antibiotic without the need for mutations or uptake of DNA from the environment [10, 11]. Acquired resistance is resistance acquired either via mutations or horizontal gene transfer of mobile DNA elements. Mutations (deletions, point mutations, inversions and insertions) occur due to repeated exposure to an antibiotic at sub-lethal concentrations [12]. Horizontal gene transfer entails the transfer of mobile genetic elements coding for genes that provide resistance to the micro-organism. These mobile genetic elements include prophages, transposons, resistance islands, integrons and self-replicating plasmids [10, 13]. In contrast to the development of antibiotic resistance the development of novel antibiotics has entered a slump and the need for novel classes of antibiotics is ever pressing.

The majority of antibiotics currently on the market were isolated from a select few genera [8], with many produced by Actinomycetes. This is due to the antibiotic boom the medical field experienced in the 1950's to 1970's. The complex lifestyle of filamentous bacteria contributes to their ability to produce a vast range of secondary metabolites [14].

In this study the secondary metabolites produced by *Xenorhabdus khoisanae* J194 was investigated. *X. khoisanae* J194 is an endosymbiont of *Steinernema jeffreyense* J194 [15]. *Xenorhabdus* spp. are known to produce various secondary metabolites (SM) with a wide range of bioactivities, including antibacterial, antifungal, insecticidal, anticancer, immunosuppressants, and proteases [16]. Even though *Xenorhabdus* spp. are widely known for their antimicrobial activity they are an unexploited niche for novel antibiotics. To date 23 classes of antimicrobial compounds have been isolated from various *Xenorhabdus* spp. [16, 17] of which the majority are produced via non-ribosomal peptide (NRP) synthetases or NRP hybrid synthetases. In contrast to NRP synthetases found in other bacteria, the NRP synthetases of *Xenorhabdus* generally do not incorporate non-proteinogenic as readily. This could be due to the isolated lifestyle these bacteria have, which may prevent horizontal gene transfer to the

same extent as other soil bacteria [18]. Antimicrobial peptides produced by *Xenorhabdus* are less diverse when looked at from an amino acid composition view point as only proteogenic amino acids are incorporated.

In this study *X. khoisanae* J194 produced three known *Xenorhabdus* antimicrobial compounds, PAX, xenocoumacins and xenoamicins. The biosynthetic gene clusters for these three compounds were also identified confirming their production by *X. khoisanae* J194. Three novel compounds were also isolated of which two are peptides, xenopep and rhabdin, synthesized via NRP synthetases. NRP are generally extremely unique and can include non-proteomic amino acids, D-amino acids, hydroxy acids or polyketides [19, 20]. Furthermore these peptides are known to have various tertiary structures including cyclic, branched-cyclic and linear structures [21]. These features lend the peptides a unique resistance to environmental stressors such as proteases, high temperatures and extreme pH [22].

Growth conditions is known to have a large impact on antibiotic production [23–26]. Similar observations were made for *X. khoisanae* J194. The known compounds, PAX, xenocoumacins and xenoamicins were only identified in the crude extracts of *X. khoisanae* J194 cultured in oxygen limiting conditions. PAX peptides are lysine rich cyclolipopeptides first isolated from *Xenorhabdus nematophilia* F1/1 [27]. Since then PAX peptides have been isolated from *Xenorhabdus bovienii* [28], *Xenorhabdus doucetiae* [29] and *X. khoisanae* [30, 31]. PAX7E was identified in the crude extract, with low signals for PAX 1, PAX 3 and PAX 5 also present. Xenocoumacins is one of the first antimicrobial compounds isolated from *Xenorhabdus* bacteria by McInerney *et al*. (1991) and is active against a broad spectrum of gram positive and gram negative bacteria [32]. Six xenocoumacins have been described [33], xenocoumacin II was identified in the crude extract of *X. khoisanae* J194. Xenoamicins are antiprotozoal non-ribosomal peptides first isolated from *Xenorhabdus mauleonii* by Zhou *et al*. (2013) [34]. The authors described eight variations of the peptide and showed that xenoamicin A is active against *Plasmodium falciparum* and *Trypanosoma brucei* rhodesiense. *X. khoisanae* J194 produced xenoamicin A, B, D and G with slight variations identified in xenoamicin B [31].

Both xenopep and rhabdin was produced on solid media, while only xenopep was produced in aerated broth. This indicates that oxygen availability has a big influence on the production of SM from *X. khoisanae* J194. The same was seen by Wang *et al*. (2008) who reported an increase in antimicrobial activity when oxygen levels were elevated [35]. Other research groups have also reported that salt [36], initial pH [37], temperature [38] and carbon and nitrogen

source [39, 40] can influence the production of SM by *Xenorhabdus* spp. Guo *et al*. (2017) also found that in an alkaline environment the production of xenocoumacin I by *Xenorhabdus nematophilia* YL001 was increased [41].

After analysing the whole genome of *X. khoisanae* J194 a putative operon was identified that encodes for both xenopep and rhabdin. This feature of *Xenorhabdus* spp. to produce multiple variations of a compound from a single operon is seen with PAX peptides [27], xenocoumacins [42, 43], xenoamicins [34], Xenocyloins [44], xenortides [45], rhabdopeptides [46], xentrivalpeptides [47], Taxlllaids [48] and fabclavines [49].

Khoicin, a novel tripeptide was also identified in the crude extract of *X. khoisanae* J194. High-resolution mass-spectrometry indicated that khoicin consists of two leucine or isoleucine residues and one arginine residue. Khoicin is mostly produced in oxygen limiting conditions and had the widest spectrum of activity, with activity recorded against *Staphylococcus aureus, Listeria monocytogenes, Staphylococcus epidermidis, Bacillus subtilis, Escherichia coli, Acinetobacter baumannii, Klebsiella pneumoniae, Salmonella typhimurium* and *Pseudomonas aeruginosa.* The only *Xenorhabdus* antimicrobial compounds with a broad spectrum of activity are xenocin [50], xenocoumacins [32] and fabclavines [49]. The narrow spectrum nature of *Xenorhabdus* compounds is most likely due the ability of *Xenorhabdus* spp. to produce multiple compounds at any given time.

Profiling the SM produced by *X. khoisanae* J194 under different conditions contributed to the knowledgebase of how the environment affects the SM produced by *Xenorhabdus* spp. This study also led to the discovery of three novel antimicrobial compounds produced by *X. khoisanae.* However, from the results in the first section of this study it is evident that further research is needed:

1. The effect of global regulators, incubation temperature, nutrients and media pH on the SM produced by *X. khoisanae* J194 needs to be evaluated. Many researchers have found that employing response surface methodology improves the results obtained in optimization of SM production [35, 39, 40]
2. Although high-resolution mass-spectrometry data indicated that khoicin is a tripeptide, more advanced structural analysis is needed to confirm the putative structure identified in this study. These analysis include nuclear magnetic resonance (NMR) spectroscopy and X-ray crystallography [51–53].

3. A putative operon for xenopep and rhabdin was identified in this study, but additional research is needed to functionally characterize the operon and to confirm the annotation of the genes. Heterologous expression of the operon and knock-out studies can be used in conjunction to functionally characterize the operon [42, 49, 54, 55]

High-resolution mass-spectrometry data indicated that xenopep could be a small proline rich peptide consisting of nine amino acids. The proline-rich antimicrobial peptide family was recently redefined by Welch *et al*. (2020)[56]. The authors proposed that for a peptide to be classified as proline rich it has to meet the following conditions: have ≥25% proline content, have antimicrobial activity, have intracellular targets (70s ribosome and/or DnaK) and have a net charge of ≥+1. Xenopep has a proline content of 33%, is active against Gram positive bacteria and has a net charge of +1 or O, depending on the final structure of xenopep. This indicates that xenopep could be a proline-rich peptide. Although rhabdin also has a proline content of 33% and is active against bacteria it has a net charge of 0. Similarities in the NMR proton spectrum of xenopep and rhabdin confirmed that these two peptides share a tetrapeptide sequence, HaaPPFI/L. This similarity was confirmed with the NMR proton spectra. Furthermore, the signals for two aromatic amino acids were also identified in the NMR spectra. These two peptides could be phenylalanine and a modified tryptophan. Broad peaks and weak resolution prevented us from completely elucidating the structure of xenopep and rhabdin. The preliminary structure of xenopep, Q/KHaaPPFL/IQPV, has proteinase K and trypsin cleavage sites, yet the peptide was not cleaved by either proteinase. This indicates that the peptide could have a unique side chain, D-amino acid or non-proteinogenic amino acid protecting it from cleavage by proteinases [57–61]. The tertiary structure of xenopep could also lend protection to proteases. Preliminary NMR analysis indicated that xenopep has a beta strand and might have a U shape. The formation of oligomers/aggregates, visible in the high-resolution mass spectrometry analysis, could contribute to xenopep's resistance to proteases. Xenopep is therefore unique, as many studies have focussed on increasing peptide resistance to proteases [60, 61].

Most antimicrobial peptides are active over a wide pH range [64], this characteristic was also seen with xenopep. Degradation was expected with high temperature exposure, but the activity of xenopep increased significantly after incubation at 100 °C for 10 minutes. This could indicate that xenopep is prone to unwanted aggregation, that may dissolve at high temperature to release active moieties. This tendency to aggregate was also seen in the proton NMR spectra. The significant loss in activity observed after storing xenopep in solution at 22°C for 60 days

also indicated that xenopep could be aggregating in solution. The formation of aggregates/oligomerisation is ubiquitous in the vast majority of AMP's, but the effect of aggregation/oligomerisation on activity varies greatly [65]. The term oligomerisation is used when ordered oligomeric structures retaining or changing functionality are formed, opposed to a disordered aggregate in which functionality is lost. Some peptides such as Alamethicin use oligomerisation to their advantage when forming pores in the cell membrane [66]. In another study by Remington *et al.* (2020) it was shown that aggregation of synergistic peptides enhances the synergistic properties [67]. Oligomerisation can also increase peptide selectivity as seen for the anticancer peptide KillerFLIP [68]. Aggregation, opposed to oligomerisation is an unwanted characteristic as seen with xenopep in this study. In another study the effect of aggregation on modified magainin II and cecropin A-melittin were evaluated by Zou *et al.* (2018) [69]. The authors showed that when cecropin A-melittin and modified magainin II aggregate, the energy cost to embed a peptide in the membrane increases ultimately lowering the antibacterial potency. Aggregation can thus act as a double-bladed sword, it could protect a peptide from the environment, but it could also cause a decrease in activity.

AMP's can be subdivided into different groups depending on various characteristics. One characteristic that is often used to classify and subdivide AMP's is the mode of action. AMP's can be either classified as membrane acting or non-membrane acting peptides. The majority of peptides are membrane acting and these peptides can be further subdivided depending on the specific model used to disrupt the membrane [57, 67, 69, 70]. Peptides associated with the toroidal model include arenicin, lacticin Q and magainin II. These peptides create pores in the membrane by embedding in the cell membrane, ultimately forming pores and causing cell leakage [71]. A variation of the toroidal model also exists, the disordered toroidal pore model. In this model peptides are present in the middle of the pore as well as at the edge of the pore. Although this model has only been observed in simulation, NMR studies has indicated that both pleurocidin [72] and Tp-10 [73] make use of this model. The barrel-stave model relies on the formation of aggregates to incur activity. The peptide aggregates penetrate the cell membrane forming channels and can also cause the cell membrane to collapse [74, 75]. The carpet-like model disintegrates the membrane in a similar way to how detergents cause membrane damage. The peptides form a carpet-like barrier around the bacterial cells. These types of peptides tend to have a higher minimum inhibitory concentration as a threshold concentration has to be reached before pores are formed [64, 76]. Various other less well-known models have also been described such as the non-lytic membrane depolarising model,

the anion carrier model, the oxidized phospholipid model, the non-bilayer intermediate model, the charged lipid clustering model and the membrane thinning/thickening model. [75]

As mentioned above xenopep is classified as a proline rich AMP. Many such proline-rich peptides inhibit protein synthesis by targeting the 70s ribosome and/or DnaK [77]. Xenopep does not seem to follow such a mode of action. The increase in PI-stained *L. monocytogenes* ATCC 7644 cells, decrease in membrane potential, loss of intracellular components (ATP leakage) and scanning electron microscopy (SEM) images reported in this study indicated that xenopep targets the cell membrane of its target organisms. Cell elongation and filamentation observed after treating *L. monocytogenes* with xenopep indicated that xenopep might also act as a penicillin binding protein 3 inhibitor, but more research is needed to confirm this. Although it is still unknown whether xenopep targets DnaK or the 70s ribosome it is not improbable and additional research is needed to confirm if xenopep does target protein synthesis and does indeed belong to the proline-rich antimicrobial peptide family. A reduction in cell-counts were observed within 180 min, suggesting that xenopep is fast acting. The generation time of *L. monocytogenes* ATCC 7644 is 90 minutes, thus indicating that xenopep can prevent a *L. monocytogenes* infection from spreading in the environment. Furthermore, a decrease in membrane potential was observed within three minutes indicating that xenopep forms membrane pores/lesions within minutes after its made contact with the cell membrane. This statement is also supported by the ATP release assay as external ATP was detected after two minutes. These results correlate with other membrane acting peptides such as melimine and Mel4 [78, 79]. A carpet/net covering was observed in the SEM images, the same structures were also observed when *Streptococcus pneumoniae* was treated with indolicidin and ranalexin hybrid peptides [80] and *P. aeruginosa* ATCC 27853 was treated with *Macropis fulvipes* venom [81]. According to Jindal *et al.* (2017) the carpet/net like structure observed is likely due to membrane destabilisation causing the leakage of intracellular components [80]. String like appendages was also observed, these appendages are likely bacterial nanotubes that are formed by dying cells due to a compromised cell wall or membrane [82].

The more selective an antibiotic is, the less likely it is for bacteria to develop resistance, this places xenopep in a unique position as it is an extremely selective antimicrobial peptide. This study showed that xenopep is active against *L. monocytogenes, S. epidermidis, Limosilactobacillus reuteri* DSM, *Enterococcus mundtii* and *Lacticaseibacillus casei*. This indicates that using xenopep to treat listeriosis will have less of a detrimental effect on the

microflora of a patient compared to the antibiotics, such as tetracycline, gentamycin, erythromycin, and ampicillin, currently used.

The characterisation of xenopep and rhabdin led to the discovery of two novel antilisterial peptides stable at both physiological and extreme conditions. The current study, therefore contributed to the database of known antimicrobial peptides produced by *Xenorhabdus* spp. and led to the discovery of novel antimicrobial peptides that could be used as antibiotics in the future. Although before xenopep and rhabdin can be considered as potential antibiotics, additional research is needed:

1. Although proton NMR spectral and high-resolution mass-spectrometry analysis indicated that both xenopep and rhabdin share a tetrapeptide sequence in their structure, 2-D NMR spectral analysis is needed to elucidate the final structure of the peptides. By using 2-NMR spectral analysis such as, correlation spectroscopy (COSY), total correlation spectroscopy (TOCSY) and rotating-frame nuclear overhauser effect spectroscopy (ROESY) the structure of xenopep and rhabdin can be elucidated 32, 49, 54].
2. Although the protease, temperature, pH and storage stability of xenopep was reported in this study, the pH and storage stability of rhabdin was not reported. Therefore, the pH and storage of rhabdin needs to be investigated.
3. The mode of action of rhabdin is still unknown and should be investigated. In addition to the assays used in this study (membrane depolarisation, PI uptake, ATP leakage and scanning electron microscopy) the effect of rhabdin on the intracellular components of its target pathogens should also be investigated. Additional proteomic studies is also needed to fully elucidate the mode of action of xenopep [83].
4. The immunomodulatory properties and cytotoxicity against human kidney, liver, neuron and epithelial cells of xenopep and rhabdin should also be investigated. *Ex vivo* tissue culturing techniques can be used to investigate the cytotoxicity [84, 85], while ELISA assays can be used to investigate the immunomodulatory properties of xenopep and rhabdin [86].

Final word

In conclusion oxygen availability had an impact on the SM produced by *X. khoisanae* J194 and three (khoicin, rhabdin and xenopep) novel antimicrobial compounds were identified in the crude extract of *X. khoisanae* J194. This contributes to the knowledgebase of *Xenorhabdus*

compounds research. Rhabdin and xenopep exhibited strong antilisterial activity. Although additional toxicity research is needed these peptides could be used to treat *L. monocytogenes* infections or as an antilisterial disinfectant in ready-to-eat process plants. Rhabdin and khoicin exhibited a broad-spectrum of activity and although additional cytotoxicity assays are needed, these compounds could have a potential as broad-spectrum antibiotics or disinfectants. Pore/lesion formation was identified in *L. monocytogenes* exposed to xenopep and although a more in-depth study is needed to determine the precise mode of action, this study did contribute to the knowledgebase of the mode of actions used by *Xenorhabdus* compounds. This is only the third study to report on the mode of action of *Xenorhabdus* compounds.

References

1. Hare R (1982) New light on the history of Penicillin. Med Hist 26:1–24
2. Zaffiri L, Gardner J, Toledo-Pereyra LH (2012) History of antibiotics. From salvarsan to cephalosporins. J Investig Surg 25:67–77
3. Chain E, Florey H, Gardber A, Heatly NG, Jennings MA, Orr-Ewing J, Sanders AG (1940) Penicillin as a chemotherapeutic agent. Lancet 236:226–228
4. Wainwright M, Kristiansen JE (2011) On the 75th anniversary of Prontosil. Dye pigment 88:231–234
5. Cohen LS, Cluff LE (1961) The sulfonamides. Am J Nurs 61:54–58
6. Comroe JH (1978) Pay Dirt: The story of streptomycin. Part 1. From Waksman to Waksman. Am Rev Respir Dis 117:773–781
7. Martínez JL, Baquero F (2014) Emergence and spread of antibiotic resistance: Setting a parameter space. Ups J Med Sci 119:68–77
8. Hutchings M, Truman AE, Wilkinson B (2019) Antibiotics: past, present and future. Curr Opin Microbiol 51:72–80
9. Fair RJ, Tor Y (2014) Antibiotics and bacterial resistance in the 21st century. Perspect Medicin Chem 6:25–64
10. Henriques Normark B, Normark S (2002) Evolution and spread of antibiotic resistance. J Intern Med 252:91–106
11. Cox G, Wright GD (2013) Intrinsic antibiotic resistance: Mechanisms, origins, challenges and solutions. Int J Med Microbiol 303:287–292
12. Andersson DI, Hughes D (2014) Microbiological effects of sublethal levels of antibiotics. Nat Rev Microbiol 12:465–478
13. Huddleston JR (2014) Horizontal gene transfer in the human gastrointestinal tract: Potential spread of antibiotic resistance genes. Infect Drug Resist 7:167–176
14. Mast Y, Stegmann E (2019) Actinomycetes: The antibiotic produces. Antibiotics 8:105–109

15. Dreyer J, Malan AP, Dicks LMT (2017) Three novel *Xenorhabdus* – *Steinernema* associations and evidence of strains of *X. khoisanae* switching between different clades. Curr Microbiol 74:938–942

16. Dreyer J, Malan AP, Dicks LMT (2018) Bacteria of the genus *Xenorhabdus*, a novel source of bioactive compounds. Front Microbiol 9:1–14

17. Booysen E, Dicks LMT (2020) Does the future of antibiotics lie in secondary metabolites produced by *Xenorhabdus* spp.? A Review. Probiotics Antimicrob. Proteins 12:1310–1320

18. Sajnaga E, Kazimierczak W (2020) Evolution and taxonomy of nematode-associated entomopathogenic bacteria of the genera *Xenorhabdus* and *Photorhabdus*: an overview. Symbiosis 80:1–13

19. Inoue M (2011) Total synthesis and functional analysis of non-ribosomal peptides. Chem Rec 11:284–294

20. Hancock REW, Chapple DS (1999) Peptide antibiotics. Antimicrob Agents Chemother 43:1317–1323

21. Martínez-Núñez MA, López VELY (2016) Non-ribosomal peptides synthetases and their applications in industry. Sustain Chem Process 4:13–20

22. Agrawal S, Adholeya A, Deshmukh SK (2016) The pharmacological potential of non-ribosomal peptides from marine sponge and tunicates. Front Pharmacol 7:333-352

23. Hassan MN, El-Naggar MY, Said WY (2001) Physiological factors affecting the production of an antimicrobial substance by *Streptomyces violatus* in batch cultures. Egypt J Biol 3:1–10

24. da Silva IR (2012) The effect of varying culture conditions on the production of antibiotics by *Streptomyces* spp., isolated from the Amazonian soil. Ferment Technol 01:1–5

25. Talluri VP (2017) Optimization of cultural parameters for the production of antimicrobial compound from *Lactobacillus fermentum* (MTCC No. 1745). J Bacteriol Mycol Open Access 4:154–157

26. Yang E, Fan L, Jiang Y, Doucette C, Fillmore S (2012) Antimicrobial activity of bacteriocin-producing lactic acid bacteria isolated from cheeses and yogurts. AMB Express 2:48-59

27. Gualtieri M, Aumelas A, Thaler JO (2009) Identification of a new antimicrobial lysine-rich cyclolipopeptide family from *Xenorhabdus nematophila*. J Antibiot 62:295–302

28. Watzel J, Hacker C, Duchardt-ferner E, Bode HB, Wöhnert J (2020) A new docking domain type in the peptide-antimicrobial-Xenorhabdus peptide producing non-ribosomal peptide synthetase from *Xenorhabdus bovienii*. ASC Chem Biol 15:982-989

29. Vo TD, Spahn C, Heilemann M, Bode HB (2021) Microbial cationic peptides as a natural defence mechanism against insect antimicrobial peptides. ACS Chem Biol 16:447-451

30. Dreyer J, Rautenbach M, Booysen E, van Staden AD, Deane SM, Dicks LMT (2019) *Xenorhabdus khoisanae* SB10 produces lys-rich PAX lipopeptides and a xenocoumacin in its antimicrobial complex. BMC Microbiol 19:1–11

31. Booysen E, Rautenbach M, Stander MA, Dicks LMT (2021) Profiling the production of antimicrobial secondary metabolites by *Xenorhabdus khoisanae* J194 under different culturing conditions. Front Chem 9:1–15

32. McInerney B V, Taylor WC, Lacey MJ, Akhurst RJ, Gregson, RP (1991) Biologically active metabolites from *Xenorhabdus* spp., Part 2. Benzopyran-1-one derivatives with gastroprotective activity. J Nat Prod 54:785–795

33. Reimer D, Pos KM, Thines M, Grün P, Bode HB (2011) A natural prodrug activation mechanism in non-ribosomal peptide synthesis. Nat Chem Biol 7:888–890

34. Zhou Q, Grundmann F, Kaiser M, Schiell M, Gaudriault S, Batzer, Kurz M, Bode HB (2013) Structure and biosynthesis of xenoamicins from entomopathogenic *Xenorhabdus*. Chem Eur J 19:16772–16779

35. Wang YH, Feng JT, Zhang Q, Zhang X (2008) Optimization of fermentation condition for antibiotic production by *Xenorhabdus nematophila* with response surface methodology. J Appl Microbiol 104:735–744

36. Crawford JM, Kontnik R, Clardy J (2010) Regulating alternative lifestyles in entomopathogenic bacteria. Curr Biol 20:69–74

37. Wang Y, Fang X, Cheng Y, Zhang X (2011) Manipulation of pH shift to enhance the growth and antibiotic activity of *Xenorhabdus nematophila*. J Biomed Biotechnol 2011:1–9

38. Chen G, Maxwell P, Dunphy GB, Webster JM (1996) Culture conditions for *Xenorhabdus* and *Photorhabdus* symbionts of entomopathogenic nematodes. Nematologica 42:127–130

39. Wang YH, Li YP, Zhang Q, Zhang X (2008) Enhanced antibiotic activity of *Xenorhabdus nematophila* by medium optimization. Bioresour Technol 99:1708–1715

40. Wang Y, Fang X, An F, Wang G, Zhang X (2011) Improvement of antibiotic activity of *Xenorhabdus bovienii* by medium optimization using response surface methodology. Microb Cell Fact 10:98

41. Guo S, Zhang S, Fang X, Liu Q, Gao J, Bilal M, Wang Y, Zhang X (2017) Regulation of antimicrobial activity and xenocoumacins biosynthesis by pH in *Xenorhabdus nematophila*. Microb Cell Fact 16:1–14

42. Reimer D, Luxenberger E, Brachmann AO, Bode HB (2009) A new type of pyrrolidine biosynthesis is involved in the late steps of xenocoumacin production in *Xenorhabdus nematophila*. ChemBioChem 10:1997–2001

43. Park D, Ciezki K, van der Hoeven R, Singh S, Reimer D, Bode HB, Forst S (2009) Genetic analysis of xenocoumacin antibiotic production in the mutualistic bacterium *Xenorhabdus nematophila*. Mol Microbiol 73:938–949

44. Proschak A, Zhou Q, Schöner T, Thanwisai A, Kresovic D, Dowling A, Ffrench-Constant R, Proschak E, Bode HB (2014) Biosynthesis of the insecticidal xenocyloins in *Xenorhabdus bovienii*. ChemBioChem 15:369–372

45. Reimer D, Nollmann FI, Schultz K, Kaiser M, Bode HB (2014) Xenortide biosynthesis by entomopathogenic *Xenorhabdus nematophilia* J Nat Prod 8:1976-1980

46. Zhao L, Kaiser M, Bode HB (2018) Rhabdopeptide/xenortide-like peptides from *Xenorhabdus innexi* with terminal amines showing potent antiprotozoal activity. Org Lett 20:5116–5120

47. Zhou Q, Dowling A, Heide H, Wöhnert, Brandt U, Baum J, Ffrench-constant R, Bode HB (2012) Xentrivalpeptides A − Q: Depsipeptide diversification in *Xenorhabdus*. J Nat Prod 75:1717–1722

48. Kronenwerth M, Bozhüyük KAJ, Kahnt AS, Steinhilber D, Gaudriault S, Kaiser M, Bode HB (2014) Characterisation of taxlllaids A – G; natural products from *Xenorhabdus indica*. Chem Eur J 20:17478–17487

49. Fuchs SW, Grundmann F, Kurz M, Kaiser M, Bode HB (2014) Fabclavines: Bioactive peptide–polyketide-polyamino hybrids from *Xenorhabdus*. Chembiochem 15:512–516

50. Singh J, Banerjee N (2008) Transcriptional analysis and functional characterization of a gene pair encoding iron-regulated xenocin and immunity proteins of *Xenorhabdus nematophila*. J Bacteriol 190:3877–3885

51. Yee AA, Savchenko A, Ignachenko A, Lukin J, Xu X, Skarina T, Evdokimova E, Liu CS, Semesi A, Guido V, Edwards AM, Arrowsmith CH (2005) NMR and X-ray crystallography, complementary tools in structural proteomics of small proteins. J Am Chem Soc 127:16512–16517

52. Fuchs SW, Proschak A, Jaskolla TW, Karas M, Bode HB (2011) Structure elucidation and biosynthesis of lysine-rich cyclic peptides in *Xenorhabdus namtophila*. Org Biomol Chem 9:3130–3132

53. Xi X, Lu X, Zhang X, Bi Y, Li X, Yu Z (2019) Two novel cyclic depsipeptides xenematides F and G from the entomopathogenic bacterium *Xenorhabdus budapestensis*. J Antibiot 72:736–743

54. Kronenwerth M, Bozhüyük KAJ, Kahnt AS, Steinhilber D, Gaudriault S, Kaiser M, Bode HB (2014) Characterisation of taxlllaids A-G; natural products from *Xenorhabdus indica*. Chem - A Eur J 20:17478–17487

55. Lucas J, Goetsch M, Fischer M, Forst S (2018) Characterization of the pixB gene in *Xenorhabdus nematophila* and discovery of a new gene family. Microbiology 164:483–494

56. Welch NG, Li W, Hossain MA, Separovic F, O'Brien-Simpson NM, Wade JD (2020) (Re)defining the proline-rich antimicrobial peptide family and the identification of putative new members. Front Chem 8:1–12

57. Zhong C, Zhu N, Zhu Y, Liu T, Gou S, Xie J, Yao J, Ni J (2020) Antimicrobial peptides conjugated with fatty acids on the side chain of D-amino acid promises antimicrobial potency against multidrug-resistant bacteria. Eur J Pharm Sci 141:105123

58. Patch JA, Barron AE (2002) Mimicry of bioactive peptides via non-natural, sequence-specific peptidomimetic oligomers. Curr Opin Chem Biol 6:872–877

59. Maurya IK, Thota CK, Sharma J, Tupe SG, Chaudhary P, Singj MK, Thakur IS, Deshpande M, Prasad R, Chauhan VS (2013) Mechanism of action of novel synthetic dodecapeptides against *Candida albicans*. Biochim Biophys Acta 1830:5193–5203

60. Hamamoto K, Kida Y, Zhang Y, Shimizu T, Kuwano K (2002) Antimicrobial activity and stability to proteolysis of small linear cationic peptides with D-amino acid substitutions. Microbiol Immunol 46:741–749

61. Meng H, Kumar K (2007) Antimicrobial activity and protease stability of peptides containing fluorinated amino acids. J Am Chem Soc 129:15615–15622

62. Lewies A, Wentzel JF, Jordaan A, Bezuidenhout C, Du Plessis LH (2017) Interactions of the antimicrobial peptide nisin Z with conventional antibiotics and the use of nanostructured lipid carriers to enhance antimicrobial activity. Int J Pharm 526:244–253

63. Nordström R, Andrén OCJ, Singh S, Malkoch M, Davoudi M, Schmidtchen A, Malmsten M (2019) Degradable dendritic nanogels as carriers for antimicrobial peptides. J Colloid Interface Sci 554:592–602

64. Huan Y, Kong Q, Mou H, Yi H (2020) Antimicrobial peptides: classification, design, application and research progress in multiple fields. Front Microbiol 11:1–21

65. Brown JS, Mohamed ZJ, Artim CM, Thornlow DN, Hassler JF, Rigogliosa VP, Daniel S, Alabi CH (2018) Antibacterial isoamphipathic oligomers highlight the importance of multimeric lipid aggregation for antibacterial potency. Commun Biol 1:220

66. Lipkin RB, Lazaridis T (2015) Implicit membrane investigation of the stability of antimicrobial peptide b-barrels and arcs. J Membr Biol 248:469–486

67. Remington JM, Liao C, Sharafi M, Ste.Marie EJ, Ferrel JB, Hondal RJ, Wargo MJ, Schneebeli ST, Li J (2020) Aggregation state of synergistic antimicrobial peptides. J Phys Chem Lett 9501–9506

68. Vaezi Z, Bortolotti A, Luca V, Perilli G, Mangoni ML, Khosravi-Far R, Bobone S, Stella L (2020) Aggregation determines the selectivity of membrane-active anticancer and antimicrobial peptides: The case of killerFLIP. Biochim Biophys Acta - Biomembr 1862:. https://doi.org/10.1016/j.bbamem.2019.183107

69. Zou R, Zhu X, Tu Y, Wu J, Landry M (2018) Activity of antimicrobial peptide aggregates decreases with increased cell membrane embedding free energy cost. Biochemistry 57:2606–2610.

70. Clark S, Jowitt TA, Harris LK, Knight CG, Dobson CB (2021) The lexicon of antimicrobial peptides: a complete set of arginine and tryptophan sequences. Commun Biol 4:1–14.

71. Matsuzaki K, Murase O, Fujii N, Miyajima K (1995) Translocation of a channel-forming antimicorbial peptide, magainin 2, across lipid bilayer by forming a pore. Biochemistry 34:6521–6526

72. Mason AJ, Marquette A, Bechinger B (2007) Zwitterionic phospholipids and sterols modulate antimicrobial peptide-induced membrane destabilization. Biophys J 93:4289–4299

73. Almeida PFF, Yandek LE, Pokorny A, Flore A (2007) Mechanism of the cell-penetrating peptide transportan 10 permeation of lipid bilayers. Biophys J 92:2434–2444

74. Lohner K, Prossnigg F (2009) Biological activity and structural aspects of PGLA interaction with membrane mimetic systems. Biochim Biophys Acta - Biomembr 1788:1656–1666

75. Nguyen LT, Haney EF, Vogel HJ (2011) The expanding scope of antimicrobial peptide structures and their modes of action. Trends Biotechnol 29:464–472

76. Oren Z, Shai Y (1998) Mode of action of linear amphipathic α-helical antimicrobial peptides. Biopolymers 47:451–463

77. Mattiuzzo M, Bandiera A, Gennaro R, Benrincasa M, Pacor S, Antcheva N, Scocchi M (2007) Role of the *Escherichia coli* SbmA in the antimicrobial activity of proline-rich peptides. Mol Microbiol 66:151–163

78. Yasir M, Dutta D, Willcox MDP (2019) Mode of action of the antimicrobial peptide Mel4 is independent of *Staphylococcus aureus* cell membrane permeability. PLoS One 14:1–22

79. Yasir M, Dutta D, Willcox MDP (2019) Comparative mode of action of antimicrobial peptide melimine and its derivative Mel4 against *Pseudomonas aeruginosa*. Sci Rep 9:1–12

80. Jindal HM, Zandi K, Ong KC, Velayuthan RD, Rasid SM, Raju CS, Sekaran SD (2017) Mechanisms of action and *in vivo* antibacterial efficacy assessment of five novel hybrid peptides derived from Indolicidin and Ranalexin against *Streptococcus pneumoniae*. PeerJ 5:e3387

81. Ko SJ, Kim MK, Bang JK, Seo CH, Luchian T, Park Y (2017) *Macropis fulvipes* Venom component macropin exerts its antibacterial and anti-biofilm properties by damaging the plasma membranes of drug resistant bacteria. Sci Rep 7:1–15

82. Pospíšil J, Vítovská D, Kofroňová O, Muchová K, Šanderovà H, Hubálek M, Šiková M, Modrák M, Benada O, Barák, Krásný L (2020) Bacterial nanotubes as a manifestation of cell death. Nat Commun 11:1–12

83. Senges CHR, Stepanek JJ, Wenzel M, Raatchen N, Ay Ü, Märtens Y, Prochnow P, Hernáandez MV, Yayci A, Schbert B, Janzing NBM, Warmuth HL, Kozik M, Bongard J, Alumasa JN, Albada B, Penkova M, Lukežič T, Sorto NA, Lorenz N, Miller RG, Zhu B, Benda M, Stülke J, Schäkermann S, Leichert LI, Scheinpflug K, Brötz-Oesterhelt H, Hertweck C, Shaw JT, Petković H, Brunel JM, Keiler KC, Metzler-Nolte N, Bandow JE (2021) Comparison of proteomic responses as global approach to antibiotic mechanism of action elucidation. Antimicrob Agents Chemother 65:e01373-20

84. Elmore E, Luc TT, Steele VE, Kelloff GJ, Redpath JL (2000) The human epithelial cell cytotoxicity assay for determining tissue specific toxicity. Methods Cell Sci 22:17–24.

85. Elmore E, Siddiqui S, Desai N, Moyer MP, Steele VE, Redpath JL (2002) The human epithelial cell cytotoxicity assay for determining tissue specific toxicity: method modifications. Methods Cell Sci 24:154-153

86. Kindrachuk J, Jenssen H, Elliott M, Nijnik A, Magrangeas-Janot L, Pasupuleti M, Thorson L, Ma S, Easton DM, Bains M, Finlay B, Breukink EJ, Georg-Sahl H, Hancock

REW (2013) Manipulation of innate immunity by a bacterial secreted peptide: Lantibiotic nisin Z is selectively immunomodulatory. Innate Immun 19:315–327